

# Mission assessment for hybrid-electric single aisle aircraft

**Aerospace Engineering Thesis**  
Assia Haddou



 **TU Delft**





# Mission assessment for hybrid-electric single aisle aircraft

## Aerospace Engineering Thesis

by

Assia Haddou

as part of the requirements for the degree of  
Master of Science in Aerospace Engineering  
at the Delft University of Technology

January 25, 2021

Student number:	4109961	
Date:	January 2021	
Thesis committee:	Dr. ir. M.F.M. Hoogreef Drs. W. Lammen Dr. ir. G. La Rocca Ir. P. Roling	Supervisor TU Delft Supervisor NLR Chair Examiner
Credits titel page picture:	Cameron Casey; Chicago, United States	



# Preface

This thesis report marks the end of my journey as a student at the faculty of Aerospace Engineering at Delft University of Technology. What a peculiar time to be arriving at such a milestone in my life. This marks the end and a new beginning at the same time, which feels strange. My graduation topic on hybrid-electric aircraft is part of the future and it motivates me to learn and explore the topic even more.

I am very grateful to have been given the opportunity to work alongside Wim Lammen at the NLR. He has provided me with many insights and showed me the way to tackle problems along the way. I would like to thank Wim for his patience and understanding attitude towards me. I would also like to thank Maurice Hoogreef for his guidance during my thesis project. The past year has been a challenge but my two supervisors helped me get through it. I also would like to emphasize my gratitude for their time and availability to guide me through this project.

I would like to thank Gianfranco La Rocca and Paul Roling in advance for being in my thesis committee and grading my work. I am also grateful to have met my fellow students Arnault-Quentin and Huy with whom I shared an office at NLR.

And lastly I want to thank my mom and my dad, who paved the way for me to be where I am now.

*Assia Haddou  
Delft, January 2021*



# Executive summary

The environmental impact of aviation is a well-known issue scientists all around the world are desperate to tackle. The population that can afford air travel is growing and this demand is likely to double within the next 20 years [28]. This increasing demand comes at a hefty price: the emissions of greenhouse gases cause climate change and local air pollution.

One of the main research topics at the moment to try to stagnate these consequences of air travel is the electrification of aircraft. Although all-electric aircraft might sound like a good idea for smaller aircraft, the current electric component technology level is still insufficient to propel larger aircraft. Currently more researchers are shifting their focus towards hybrid-electric propulsion systems. When a gas turbine is being supported by a battery, the core flow of the gas turbine can be scaled down due to the lower power requirements. This also leads to higher combustion temperatures which in turn can drastically increase  $NO_x$  production [9, 40].

The objective of this study was to add to the scientific knowledge about the performance of hybrid-electric aircraft by assessing changes in the mission of a hybrid-electric A320neo. A sensitivity study was performed on four mission variables in order to decrease the block fuel, energy consumption and emissions. In order to increase the propulsive efficiency and decrease the mass of the main engines, the engine core has been scaled down and the Bypass Ratio has been increased.

The four mission variables that this study focuses on are:

1. Adjusting the cruise altitude
2. Adjusting the take-off and climb flight velocities
3. Adjusting the range
4. Adjusting the degree of hybridization

For this purpose the aircraft performance tool Mission, Aircraft and Systems Simulation (MASS) has been used, which has been developed at Royal Netherlands Aerospace Centre (NLR). This tool assesses parallel hybrid-electric aircraft for a given mission. The reference aircraft which has been used for this purpose is the Airbus A320neo. The mission model had to be redesigned to be more efficient at automating the mission variation process.

The results showed that the cruise phase made the greatest impact on the fuel consumption, which led to an overall fuel reduction of 3.10% at an altitude of 37000ft, a cruise hybridization of  $\phi_{CR} = 0.1$ , a range of  $R = 1500km$  and 92% scaled engines. The energy reduction was 0.49% and the  $NO_x$  reduction was 1.12%. These results have been constrained by the Maximum Take-off Weight (MTOW), the Maximum Landing Weight (MLW) and the maximum turbine inlet temperature  $T_{t4,max}$ . Electrically assisting the take-off and the initial climb phases with a hybridization factor of  $\phi_{TO} = 0.07$  turned out to be necessary in order to lower the turbine inlet temperature of the down-scaled engines to match the reference aircraft's temperature.

The study shows that designing a new mission for hybrid-electric aircraft does impact the overall fuel consumption and emissions. However, the gains are very small for EIS2030 battery technology forecasts. Mission assessment is therefore a tool that has the potential to increase the performance of hybrid-electric aircraft, but it needs to work alongside other measures, such as hydrogen technology.





# Contents

<b>Executive summary</b>	<b>v</b>
<b>List of Figures</b>	<b>ix</b>
<b>List of Tables</b>	<b>xi</b>
<b>Abbreviations</b>	<b>xiii</b>
<b>Nomenclature</b>	<b>xvi</b>
<b>1 Introduction</b>	<b>1</b>
1.1 The underlying issue of environmental impact . . . . .	1
1.2 Electrification of aircraft . . . . .	2
1.3 Focus of the thesis . . . . .	4
1.3.1 Research objective . . . . .	5
1.3.2 Research questions . . . . .	5
1.4 Relevance and justification of the topic . . . . .	6
<b>2 Background and literature overview</b>	<b>9</b>
2.1 Aircraft emissions. . . . .	9
2.2 Hybrid-electric propulsion . . . . .	14
2.3 Power management . . . . .	16
2.4 Electric powertrain technology . . . . .	17
2.5 Mission literature . . . . .	18
2.6 Actors and stakeholders in the aviation industry . . . . .	23
2.7 Reference aircraft and engine . . . . .	25
<b>3 Methodology</b>	<b>29</b>
3.1 Introduction on the framework and methodology . . . . .	30
3.1.1 Framework and methodology . . . . .	30
3.1.2 Validation approach . . . . .	31
3.2 Aircraft performance and mission model . . . . .	31
3.2.1 Aircraft performance model MASS . . . . .	32
3.2.2 Mission model extension . . . . .	35
3.2.3 Engine sizing . . . . .	38
3.2.4 Electric component masses and sizing . . . . .	39
3.2.5 Aircraft sizing . . . . .	41
3.3 Reference mission and validation . . . . .	41
<b>4 Mission analysis results</b>	<b>47</b>
4.1 Effect of engine scaling and need for hybridization . . . . .	48
4.2 Electric component masses . . . . .	52
4.3 Sensitivity analysis of the flight phases . . . . .	54
4.3.1 Take-off phase analysis . . . . .	54
4.3.2 Climb phase analysis. . . . .	55
4.3.3 Cruise phase analysis . . . . .	61
4.3.4 Combined hybridization of different phases . . . . .	63
<b>5 Conclusion and recommendations</b>	<b>65</b>
<b>Bibliography</b>	<b>69</b>



# List of Figures

2.1	Future estimation of aircraft fuel consumption for different scenarios. Adapted from: ICAO, 2019 [30]	10
2.2	Combustion products and their atmospheric processes that influence Radiative Forcing agents. $NO_x$ has a negative influence on methane ( $CH_4$ ) which means that it reduces the methane concentrations. Based on information from: Wuebbles et al., 2007 [56] and Prather et al., 1999 [46]	11
2.3	Radiative Forcing (RF) components in 2005 from aviation. Adapted from: Lee et al., 2009 [38] and updated with Burkhardt and Kärcher, 2011 [12]	12
2.4	The influence of combustion temperature on the formation of $CO$ and $NO_x$ . Adapted from: Lefebvre and Dilip, 2010 [40]	13
2.5	Combustion products for gas turbine engines at different percentages of the takeoff power. Adapted from: Lefebvre and Dilip, 2010 [40]	13
2.6	The three main hybrid-electric propulsion architectures: (a) Series, (b) Parallel and (c) Series-parallel. Adapted from: Jansen et al., 2017 [33] and Tan, 2018 [48]	14
2.7	Example of a power management strategy. Adapted from: Lammen and Vankan, 2020 [37]	16
2.8	Specific power of different electric motors, piston engines and turbine engines. Adapted from: Hepperle, 2012 [24]	17
2.9	Specific power and specific energy forecast for electric motors, generators, power electronics and batteries. Adapted from: Tan, 2018 [48]	18
2.10	Specific energy forecast for batteries. Adapted from: Misra (NASA), 2018 [42]	19
2.11	An example of different optimum values for the cruise altitude for fuel consumption and $CO_2$ emissions. Adapted from Vos et al., 2017 [52]	21
2.12	Pareto multi-objective representation of the fuel consumption and the total energy consumption for different ranges of a A320. Adapted from Ang et al., 2018 [9]	22
2.13	Hybrid-electric commercial transport aircraft range for different battery specific energy densities and hybridization factors: a) $\phi = 0.125$ , b) $\phi = 0.25$ and c) $\phi = 0.50$ . Adapted from Wroblewski et al., 2019 [55]	23
2.14	Mass breakdown of the A320neo. The horizontal axis depicts the mass in $kg$ . Legend: Max. Take-Off Weight (MTOW), Operational Empty Weight (OEW), Max. Zero-Fuel Weight (MZFW), Max. Payload (MPL), Max. Fuel Load (MFL), Design Payload (DPL), Design Fuel Load (DFL). Data retrieved from: [7] [32] [35]	26
2.15	Dimensions of the A320neo [6]	26
2.16	CFM LEAP-1A26 engine data [19]	27
3.1	Research framework with four phases: (a) Preliminary research, (b) Conceptual model, (c) Results, (d) Conclusions and recommendations	30
3.2	MASS framework [37].	32
3.3	Free body diagram of an aircraft during steady level flight. Aircraft without forces retrieved from Airbus [7]	32
3.4	Former MASS mission model hybridization capabilities. [37]	34
3.5	Instantaneous cutback versus dynamic cutback. [34]	37
3.6	Reference flight velocity (CAS) input with dynamic cutback.	37
3.7	Typical efficiency of a turboprop, turbofan, electric and fuel cell drivetrain. Adapted from: Hepperle, 2012 [24]	40
3.8	Original reference flight from OpenAP without Gaussian noise.	42
3.9	Reference flight characteristics of an A320 mission from Airbus [4] (straight line), compared to the new mission based on data from OpenAP (dotted line). This figure shows the fuel flow, fuel burn, altitude and velocity. The reference flight range is 1500km.	44

3.10 Reference flight characteristics of an A320 mission from Airbus [4] (straight line), compared to the new mission based on data from OpenAP (dotted line). This figure shows turbine inlet temperature, the thrust, the flight path angle and the flight phase. The reference flight range is 1500km. . . . .	45
4.1 The effect of engine scaling alone on the block fuel without electric assistance. These results are not feasible without electric assistance due to the increased $T_{t4}$ . . . . .	48
4.2 The effect of engine scaling alone on the cruise SFC without electric assistance. These results are not feasible without electric assistance due to the increased $T_{t4}$ . . . . .	48
4.3 Reference flight engine scaling effect on $T_{t4}$ and SFC [ $g/N \cdot s$ ]. . . . .	49
4.4 1: Engine scaling effect on $T_{t4}$ and SFC [ $g/N \cdot s$ ]. Closeup of the take-off phase. . . . .	50
4.5 Engine scaling effect on the SFC. (2) Closeup of the beginning of the cruise phase. (3) Closeup of the beginning of the descent phase. . . . .	51
4.6 The effect of electrically assisting the take-off phase with $V_{TO} = 85m/s$ in order to decrease the turbine inlet temperature $T_{t4}$ of the scaled engine (92%). . . . .	52
4.7 The effect of hybridization on the electric equipment masses: the inverter, the electric motor and the battery mass. The battery mass is divided into the fixed offtakes part and the varying hybridization part. . . . .	53
4.8 Mass breakdown of the A320neo. The horizontal axis depicts the mass in $kg$ . Legend: Max. Take-Off Weight (MTOW), Operational Empty Weight (OEW), Max. Zero-Fuel Weight (MZFW), Max. Payload (MPL), Max. Fuel Load (MFL), Design Payload (DPL), Design Fuel Load (DFL). Data retrieved from: [7] [32] [35]. Repetition of Figure 2.14 . . . . .	53
4.9 Effect of the take-off velocity and $\phi_{TO}$ variations on the total block fuel of the entire mission. . . . .	54
4.10 Climb 1 and climb 2 phases. . . . .	55
4.11 Effect of the climb1 velocity (CAS) and $\phi_{CL1}$ variations on the block fuel. With take-off hybridization $\phi_{TO} = 0.06$ and Engine Scale is 92%. . . . .	56
4.12 Effect of the climb1 velocity and $\phi_{CL1}$ variations on the total energy consumption. With take-off hybridization $\phi_{TO} = 0.06$ and Engine Scale is 92%. . . . .	57
4.13 Effect of the climb1 velocity and $\phi_{CL1}$ variations on the $T_{t4}$ peak and the emissions. With take-off hybridization $\phi_{TO} = 0.06$ and Engine Scale is 92%. . . . .	57
4.14 Effect of the climb2 velocity and $\phi_{CL2}$ variations on the block fuel. With take-off hybridization $\phi_{TO} = 0.06$ and Engine Scale is 92%. . . . .	59
4.15 Effect of the climb2 velocity and $\phi_{CL2}$ variations on the total energy consumption. With take-off hybridization $\phi_{TO} = 0.06$ and Engine Scale is 92%. . . . .	59
4.16 Effect of the climb2 velocity and $\phi_{CL2}$ variations on the $T_{t4}$ peak. With take-off hybridization $\phi_{TO} = 0.06$ and Engine Scale is 92%. . . . .	60
4.17 Effect of the climb2 velocity and $\phi_{CL2}$ variations on the $NO_x$ emissions. With take-off hybridization $\phi_{TO} = 0.06$ and Engine Scale is 92%. . . . .	60
4.18 Effect of the cruise altitude and $\phi_{CR}$ variations on the total block fuel and energy consumption. With take-off hybridization $\phi_{TO} = 0.07$ and Engine Scale is 92%. . . . .	61
4.19 Effect of the cruise altitude and $\phi_{CR}$ variations on the $T_{t4}$ and the $NO_x$ emissions. With take-off hybridization $\phi_{TO} = 0.07$ and Engine Scale is 92%. . . . .	61
4.20 Effect of the range and $\phi_{cruise}$ variations on the total block fuel. With take-off hybridization $\phi_{TO} = 0.07$ and Engine Scale is 92%. . . . .	63
4.21 Sensitivity analysis summary. . . . .	63

# List of Tables

2.1	Flightpath 2050 and CleanSky2 emission reduction goals relative to EIS2000 aircraft per passenger kilometer [1] . . . . .	10
2.2	The main advantages and disadvantages of hybrid-electric architectures . . . . .	15
2.3	Battery pack current and theoretical specific energy densities (Wh/kg) and their main challenges [42, 48] . . . . .	17
2.4	Air traffic industry stakeholders and some examples. Adapted from ATAG, 2018 [21] . .	24
2.5	Characteristics of the A320neo [5, 6, 19, 32] . . . . .	25
3.1	Summary of the mission model modifications compared to the former model. . . . .	36
3.2	Reference mission characteristics . . . . .	43



# Abbreviations

- BLI** Boundary Layer Ingestion. 7
- CeRAS** Central Reference Aircraft data System. 34
- CORSIA** Carbon Offsetting and Reduction Scheme for International Aviation. 2
- EAPS** Electrically Assisted Propulsion System. 3, 14, 15
- EIS** Entry Into Service. 7, 10, 40
- END** Environmental Noise Directive. 2
- eVTOL** electric Vertical Take-off and Landing. 24
- GSP** Gas turbine Simulation Program. 30, 34
- HEP** Hybrid Electric Propulsion. 4, 30, 32, 34, 38
- IATA** International Air Transport Association. 1, 9
- ICAO** International Civil Aviation Organization. 2, 10
- ICCT** International Council on Clean Transportation. 9
- ICE** Internal Combustion Engine. 2–5, 14–16, 19–21, 25
- MASS** Mission, Aircraft and Systems Simulation. v, ix, 5, 29–32, 34, 35, 38, 41–43, 47, 65
- MLW** Maximum Landing Weight. v, 31, 40, 41, 52–54, 62, 63
- MTOW** Maximum Take-off Weight. v, 41, 62, 63
- NLR** Royal Netherlands Aerospace Centre. v, 29–32, 65
- OEI** One Engine Inoperative. 25
- OEW** Operational Empty Weight. 52
- OpenAP** Open-source Aircraft Performance model. 5, 18, 19, 29, 31, 36, 41–43, 47
- OpenVSP** Open-source Vehicle Sketch Pad. 33
- OPR** Overall Pressure Ratio. 25
- RF** Radiative Forcing. 6, 11, 12
- SFC** Specific Fuel Consumption. 51
- SR** Specific Range. 20
- UAV** Unmanned Aerial Vehicle. 16
- VLM** Vortex Lattice Method. 33





# Nomenclature

## Greek symbols

$\alpha$	Angle of attack	rad
$\delta$	Dimensionless pressure	-
$\dot{\gamma}$	Flight path angular velocity	rad s <sup>-1</sup>
$\eta_{el}$	Electric components efficiency	-
$\eta_{ice}$	Gas turbine thermal efficiency	-
$\eta_{int}$	Component integration efficiency	-
$\eta_{prop}$	Propulsive efficiency	-
$\gamma$	Flight path angle	rad
$\mu$	Friction coefficient	-
$\phi$	Hybridization factor	-
$\rho$	Density	kg m <sup>-3</sup>
$\theta$	Dimensionless temperature	-
$\xi$	Throttle setting	-

## Roman symbols

$\dot{h}$	Vertical velocity	m s <sup>-1</sup>
$\dot{m}_{core}$	Engine core mass flow	kg s <sup>-1</sup>
$C_D$	Drag coefficient	-
$C_{D0}$	Zero lift drag coefficient	-
$C_{Dflaps}$	Flaps drag coefficient	-
$C_{Dgear}$	Landing gear drag coefficient	-
$C_{Dmach}$	Drag coefficient due to compressibility effects	-
$C_L$	Lift coefficient	-
$C_{L0}$	Lift coefficient at zero angle of attack	-
$D$	Drag force	N
$D_{core}$	Engine core diameter	m
$D_{ground}$	Friction drag from wheels	N
$e_{bat}$	Battery specific energy	W h kg <sup>-1</sup>
$e_{fuel}$	Fuel specific energy	W h kg <sup>-1</sup>
$E_{miss}$	Total mission energy (fuel + battery)	J

$F_{TO}$	Take-off thrust	N
$g$	Gravitational constant	$\text{m s}^{-2}$
$k$	Induced drag coefficient	-
$L$	Lift force	N
$L_{den}$	Day, evening, night average noise level	dB
$L_{night}$	Night average noise level	dB
$m$	Aircraft mass	kg
$M_{cr}$	Cruise mach number	-
$M_{mo}$	Maximum operating mach number	-
$M_{MR}$	Maximum range mach number	-
$N$	Normal force	N
$P_{el}$	Electric power	W
$P_{ice}$	Gas turbine power	W
$p_m$	Electric motor specific power	$\text{kg}^{-1}$
$R$	Range	m
$R_{bat}$	Breguet range for battery powered aircraft	m
$R_{fuel}$	Breguet range for fuel powered aircraft	m
$S$	Wing planform area	$\text{m}^2$
$T$	Thrust	N
$T_{t4}$	Turbine inlet temperature	K
$V$	True Air Speed	$\text{m s}^{-1}$
$V_1$	Decision speed	kn OR $\text{m s}^{-1}$
$V_2$	Take-off climb speed	kn OR $\text{m s}^{-1}$
$V_{EF}$	Engine failure speed	kn OR $\text{m s}^{-1}$
$V_{LOF}$	Lift-off speed	kn OR $\text{m s}^{-1}$
$V_{mo}$	Maximum operating speed	$\text{m s}^{-1}$
$V_R$	Rotation speed	kn OR $\text{m s}^{-1}$
$W_{bat}$	Battery weight	kg
$W_{engine}$	Engine weight	kg
$W_{fuel}$	Fuel weight	kg
$W_{PL}$	Payload weight	kg
$W_{TO}$	Take-off gross weight	kg

# Introduction

More than half of the global population is currently living in middle or upper class families and the rate of growth of this population is increasing each year [36]. This leads to an increasing population that can afford air travel. In fact, the rapidly growing demand for air travel is mainly caused by the increase in middle class households. The International Air Transport Association (IATA) expects that this demand will be twice as high in the next 20 years [28]. This increase in air travel leads to an increase in many environmental complications such as:

- Climate change
- Local air pollution
- Noise pollution

This chapter provides a brief introduction into these topics, the impact that electrification of aircraft can provide and an overview of the stakeholders in the aviation industry. Furthermore the focus and main research aim and questions of this thesis will be provided.

## **1.1. The underlying issue of environmental impact**

Today marks a crossroad in the attempts to combat climate change. In various industries people are trying to come up with solutions to overcome these challenges. The aviation industry is one of the contributors to these environmental challenges of today. Even though the fuel efficiency of aircraft has increased over the past decades, the environmental impact of this industry is still growing each year. This is mainly due to the globally increasing demand for air travel which is one of the most affordable

means of travel of this day. There are several reasons for this competitive spot in the transport market, but the main cause still remains the increasing demand for fast transport options.

Aircraft produce emissions from burning fossil fuels in the Internal Combustion Engine (ICE) to produce thrust. These emissions mainly consist out of carbon dioxide ( $CO_2$ ), carbon monoxide ( $CO$ ), nitrogen oxide ( $NO_x$ ), water vapor ( $H_2O$ ), sulphur oxide ( $SO_x$ ), unburnt hydrocarbons ( $HC$ ) and particulate matter ( $SOOT$ ). These emissions all have a different impact on the environment.  $CO_2$  for example is independent of the location of emission which means that its contribution to global warming is only dependent on the amount of  $CO_2$  in the atmosphere.  $NO_x$  is very dependent on the location of the emission. During cruise,  $NO_x$  is emitted directly into the tropopause which causes global warming. Closer to the ground, at take-off for example,  $NO_x$  can contribute to local air pollution around the airport. Decreasing the local air quality has negative health consequences for the local population [40]. The impact of aviation on global warming tends to be higher than expected due to the pollutants being directly emitted at high altitudes. In the transport sector, an aircraft is also one of the highest producers of emissions per person. According to data gathered from International Civil Aviation Organization (ICAO) and The World Bank, one person on a round trip from London to New York generates about three times more  $CO_2$  than an average citizen in Tanzania emits in a year [10, 29]. In order to tackle the challenge of emissions, ICAO developed the globally operating Carbon Offsetting and Reduction Scheme for International Aviation (CORSIA) program to lower aircraft emissions. The main goal is to stagnate the yearly growth of emissions to the values of 2019 and 2020. The program is intended to start in 2021.

Noise pollution is the production of substantial noise which has a significant impact on the ecosystem. It is usually man-made noise originating from heavy traffic, industrial sources or aircraft. Regulations surrounding noise pollution in the European Union are imposed by the Environmental Noise Directive (END). The most recent plan from END dates from 2018 and entails measures like restrictions for aircraft taking off or landing during nighttime but also providing funding for the local population to insulate their homes [2]. The scope of this report does not include noise assessment.

## 1.2. Electrification of aircraft

In order to tackle the environmental problems of aviation there is a need for new technologies that do not include the combustion of fossil fuels or lower the use of these fuels significantly. One of the main research topics at the moment is the electrification of aircraft. Electrification is a measure with many advantages. The first advantage is the decrease of emissions which in turn decreases the environmental impact of air travel. Electrification leads to lower fuel consumption which also means that the industry is less dependent on fossil fuels, which is a finite energy source.

There are three major categories within this research area, which are:

- More-electric aircraft
- Electrically Assisted Propulsion Systems
- All-electric aircraft

Currently there is a trend towards 'more-electric' aircraft. This entails the electrification of several aircraft components such as the environmental control systems and hydraulics in order to decouple them from the combustion engine. Pneumatic power from bleed air and hydraulic power from a pumping system can be exchanged with electrical systems. This is often seen as the first step in making several aircraft systems independent from the jet engine. The environmental control systems usually utilize bleed air from the engine to pressurize the cabin which is not very efficient as the over-pressurized air has to be cooled first before it can be introduced to the cabin. Replacing this system with electric compressors specifically designed for cabin pressurization could prevent pressure loss and the possible occurrence of a fume event, which is when the cabin air gets contaminated with chemicals from engine oil or fuel. More-electric aircraft systems will make it easier to make the transition to hybrid-electric or all-electric aircraft on the long run.

According to NASA, Electrically Assisted Propulsion System (EAPS) are propulsion configurations where the ICE is partly supported by an electric energy source [33]. NASA distinguishes two main categories, which are: turbo-electric and hybrid-electric propulsion systems. Turbo-electric configurations usually consist out of a turbofan or turboshaft which drives a generator to generate power. Hybrid-electric propulsion systems consist out of two power sources which are the turbofan or turboshaft combined with an energy storage device such as a battery or a hydrogen tank [33]. The main advantage of Electrically Assisted Propulsion Systems is the potential to reduce fuel consumption due to the partially electrically provided energy. In Section 2.2, a more detailed description of these systems is provided.

All-electric aircraft are fully powered by an electric energy source such as a battery. There is no ICE present in these configurations which means that there is no combustion and hence no fuel consumption. All-electric aircraft face a couple of challenges out of which the main three are: energy storage mass, energy storage cost and certification and safety. [43] The development of all-electric aircraft sounds very promising but for large passenger aircraft it will not be feasible in the near future due to the current low battery energy density. Jet fuel has an energy density of more than 60 times<sup>1</sup> that of a current lithium-ion battery (Dever et al., 2015 [18]). This means that batteries need to be very heavy to accommodate for the energy consumption of large passenger aircraft. The batteries will also take up a lot of volume which means that the aircraft will have to be redesigned to prevent possible drag penalties. Also the charging time of batteries can impose a problem. Refuelling a single aisle aircraft

---

<sup>1</sup>Jet fuel has an energy density of approximately 12000 Wh/kg and a current lithium-ion battery 200 Wh/kg. Although there are other batteries that have a higher energy density such as lithium-sulfur and lithium-oxygen, there are downsides to these batteries such as the generally shorter service life [18]

such as an A320 takes approximately 15 to 20 minutes while supercharging a car can take more than an hour.

### 1.3. Focus of the thesis

Many studies nowadays focus on new all-electric or hybrid-electric propulsion architectures that could provide an insight in the feasibility of electrification of aircraft in the near future. These new architectures however change many aircraft and flight characteristics when compared to contemporary aircraft. Applying this new propulsion system can for example have an impact on aircraft sizing parameters and a possible drag penalty. For this research only mass sizing will be accounted for. Geometry sizing is out of scope.

For hybrid-electric propulsion systems also the mass of the aircraft increases significantly due to the added battery weight. The difference between the take-off mass and the landing mass will also be lower due to the anticipated lower fuel burn for this configuration. Several mission variables are dependent on the mass of the aircraft. The studies that have been performed on mission profiles primarily entail energy management strategies and currently unattainable battery specific energy densities rather than mission alterations such as cruise altitude and velocity variations. In some studies parallel Hybrid Electric Propulsion (HEP) systems show some promising results with the mission profiles of ICE aircraft [17]. These studies mainly account for smaller aircraft. It could be worthwhile to investigate the effects of changing the mission profile for the hybrid-electric architecture instead. De Vries et al. for example states that hybrid-electric aircraft have a higher wing loading which may lead to a lower optimal cruise altitude than for the ICE aircraft. [16] It is interesting to investigate the effects of engine sizing as well as variations of the mission profile for the hybrid-electric powertrain. More on the literature of the possible effects of the mass on the mission profile can be found in section 2.5.

This research project's main goal is to investigate the effects of varying the mission profile for parallel hybrid-electric aircraft in order to minimize fuel and energy consumption and emissions. This has the potential to help explore the mission differences between hybrid-electric aircraft and contemporary ICE aircraft. The main focus of this thesis is to determine whether the following adjustments to the mission have the potential to decrease fuel consumption and emissions for hybrid-electric aircraft:

1. Adjusting the cruise altitude
2. Adjusting the take-off and climb flight velocities
3. Adjusting the take-off, climb and cruise degree of hybridization
4. Adjusting the flight range
5. Adjusting the ICE scale

### 1.3.1. Research objective

The research objective for this thesis project has been formulated and it is divided into sub-goals. The main research objective of this thesis is:

*"The research objective is to analyze the feasibility and assess the deployment of parallel hybrid-electric powertrain systems for single aisle aircraft by establishing a model to determine the effects of different mission profiles on the overall energy/fuel consumption and emissions."*

In order to achieve this project goal, the following sub-goals have been established. First a literature study has been performed on the state-of-the-art of hybrid-electric propulsion, mission profiles and the environmental impact. The next step was the gathering of the required theory about gas turbines, electrical components and aircraft performance models. The collected information has been documented in a literature review report [22]. The next step was to perform a sensitivity analysis on several missions to evaluate the performance of parallel hybrid-electric single aisle aircraft. For this purpose an existing aircraft performance model called MASS has been used. A description of MASS can be found in Section 3.2.1. To perform the mission analysis, this model needed to be extended with an enhanced mission assessment model. Once the proper working of this mission model is validated, Open-source Aircraft Performance model (OpenAP) [47] data will be used to construct a typical mission of the reference aircraft (Airbus A320neo). The extended model was then validated against OpenAP performance data for this mission. With this extended MASS model the mission design space will be explored to examine the combinations of various mission profile variables to achieve the lowest energy consumption, fuel consumption and emissions. The results will be compared against the reference ICE aircraft and subsequently conclusions will be drawn. A detailed description of this methodology can be found in Chapter 3.

### 1.3.2. Research questions

The main question for the thesis project is:

*"What are the differences in mission profile for parallel hybrid-electric single aisle aircraft compared to ICE aircraft in order to achieve the highest overall energy and fuel efficiency and the lowest emissions?"*

This main research question is divided into three parts:

1. To what extent does the performance of the hybrid-electric aircraft fit in with the mission requirements of the A320neo?
2. What is the best combination of hybrid-electric architecture and mission profile that leads to the minimization of overall energy/fuel consumption and emission?
  - (a) Sensitivity analysis of engine scaling

- (b) Sensitivity analysis of climb and cruise power management (hybridization)
  - (c) Sensitivity analysis of cruise altitude
  - (d) Sensitivity analysis of climb velocities
  - (e) Sensitivity analysis of range
3. What recommendations can be made based on the outcomes of this research project?

## 1.4. Relevance and justification of the topic

Aircraft that are solely powered by fossil fuels as we know them now are not sustainable in the future, as mentioned in the introduction in Chapter 1 and in the literature survey. This calls for a drastic change in design and the development of different types of more sustainable propulsion methods. In this field there are several different solutions and options that are being researched at the moment. This section provides a brief overview of the main research areas and a justification of the chosen research topic for this literature study and thesis project. The overview is presented in the way of critical questions that one can have in relation to the chosen topic.

### 1. *Is it possible to construct a world without air travel at all?*

For the first time in history people around the world are connected with each other and the demand for fast travel options is growing. As mentioned in the introduction in Chapter 1, this increasing demand is mainly caused by the growth of middle class households. This is a positive trend as an increasing amount of people are getting out of extreme poverty. Globalization has a positive effect on political, cultural and economical aspects. Working together on a global scale has the potential to increase the efficiency of gathering and sharing knowledge. But is air travel necessary to connect us all?

There are several different options to satisfy the global need for fast travel options. One of which is the Hyperloop concept which was first introduced by E. Musk in 2012. This concept consists out of very low pressure tubes that makes it possible to transport a train capsule with high velocities. However, concepts like the Hyperloop ask for the development of new infrastructures which is a very costly affair. This is also not a short term solution for the current environmental state. Sustainable air travel does not require new infrastructures and therefore is a more suitable short term solution.

### 2. *Why are fuel cell powered aircraft not taken into account?*

Fuel cell technology consist out of hydrogen cells which use reverse electrolysis to generate electricity. The main advantage of fuel cell systems is the decrease of several Radiative Forcing (RF) agents. The only emission product that remains is water vapor. Although hydrogen fuelled fuel cells are relatively light weight compared to batteries providing the same power, hydrogen poses several challenges out of which the main disadvantages are the cost to produce hydrogen and the need for a new infrastructure for distribution.



However, fuel cell technology can be implemented in the proposed configuration of this thesis. This makes the hybrid-electric research topic even more relevant as changing the used fuels at a later stadium when the technology is advanced is always possible to decrease the emissions even further.

3. *Why are other ways to increase fuel efficiency besides mission optimization not relevant for this thesis?*

There are several other ways to increase fuel efficiency. The most obvious one is to optimize the design of the turbofan. For example Rolls-Royce is working on a propulsion system by introducing a power gearbox to increase the propulsion efficiency of their turbofan. They claim a fuel reduction of 25% for aircraft Entry Into Service (EIS) before 2030 [2]. However, this is not a long term solution. This engine will still be depending on fossil fuels and there is a ceiling as to how far one can go by optimizing the existing turbofan design.

Another relevant research area is the development of distributed propulsion systems which increases the performance of aircraft. This calls for a redesign of the entire aircraft and is not suited for retrofitting onto already existing aircraft.

Open rotor technology is also a hot topic when it comes to increasing efficiency as it decreases both fuel consumption and noise. It can also be a great addition to the hybrid-electric or all-electric configurations. However, due to the lack of a nacelle it is a challenge to get it certified for blade loss. For this thesis it is also important that the results can be compared to a reference aircraft which is hard to find when one wants to analyze the efficiency of an open rotor aircraft. This is also the case for Boundary Layer Ingestion (BLI) which can be an addition to the hybrid-electric or all-electric configurations.

4. *Why are sustainable fuels not taken into account?*

As mentioned before in question 2 of this section, sustainable fuels can be used together with the parallel hybrid-electric configuration, but for the matter of comparing and analysing the results of this research project, jet-A fuel will be used.

5. *Why is a parallel-hybrid configuration chosen instead of a series-hybrid or turbo-electric propulsion system?*

The series-hybrid and turbo-electric configurations have the advantage of being suitable for introducing distributed propulsion as they allow for separating the fans from the main engine. However, they are not easily retrofitted onto existing turbofans as they call for a complete redesign of the engine.

6. *Why is the current battery technology not feasible?*

Although it is difficult to assess up front where battery technology is headed, for this thesis an assumed battery technology of 2030 is used. It is evident that assuming higher battery energy densities result in a higher range of an aircraft. However, the EIS2030 aircraft are being designed now so this technology level can be assumed. The first simulations also yielded that lower battery specific energy densities

do not result in lower fuel consumption for hybrid-electric aircraft compared to the reference due to the high battery mass.

# 2

## Background and literature overview

In the previous chapter some main topics required for this report have been introduced. In this chapter these topics will be elaborated on to provide the reader with the prior knowledge needed for better comprehension of the research performed. Also a literature overview will be provided in this chapter. The topics that will be addressed are:

- Aircraft emissions
- Hybrid-electric propulsion
- Electric powertrain technology
- Mission literature
- Reference aircraft and engine
- Actors and stakeholders in the aviation industry

### 2.1. Aircraft emissions

The demand for air travel is increasing worldwide. The IATA expects that this demand will be twice as high in the next 20 years [28]. This increase in air travel leads to many environmental complications. According to the International Council on Clean Transportation (ICCT),  $CO_2$  emissions from commercial aviation have increased by one third in between 2013 and 2017 and now account for 2.4% of the annual  $CO_2$  emissions from combustion of fossil fuels. The majority of these emissions (81%) stem from passenger operations [20].

But  $CO_2$  is not the sole problem; the aviation industry has impacted the environment in many other ways such as noise pollution and the emission of other greenhouse gases. Approximately 3.6% of

Table 2.1: Flightpath 2050 and CleanSky2 emission reduction goals relative to EIS2000 aircraft per passenger kilometer [1]

Flightpath 2050 goal:	
$CO_2$	75% reduction
$NO_x$	90% reduction
Noise	65% reduction

the total European greenhouse gas emissions are caused by aviation [2]. To put this into perspective, aviation is accountable for 13.4% of the total emissions from transport and is therefore the second largest polluting transport sector [2]. In order to lower the total environmental impact every sector has to play its part. While other sectors are showing a steady decrease in emissions, the aviation sector is one of the few where emissions are continuing to grow [3]. This is probably partly due to the long service life of aircraft.

Table 2.1 shows the European Commissions emission reduction goals for EIS2050 aircraft compared to aircraft from 2000. Within a time frame of 50 years the objective is to lower man-made emissions from aviation drastically. There are several ways to lower the environmental impact of aviation to meet these Flightpath 2050 goals. Progression in aircraft design and combustion engine technology have been the main contributors in reducing fuel consumption since the sixties [30]. Figure 2.1 shows the ICAO fuel consumption forecast for different technological development scenarios. It is clear that a technological advancement in the form of optimization of the already existing aircraft designs will not be enough to meet the environmental goals. Therefore, current research approaches focus more on sustainable fuels and electric aviation. According to ICAO these two approaches could potentially stop the increase in emissions.

Environmental impact from emissions stem from the difference between incoming radiation from the sun of which a part is being absorbed by particles in the earth's atmosphere and a part is being reflected

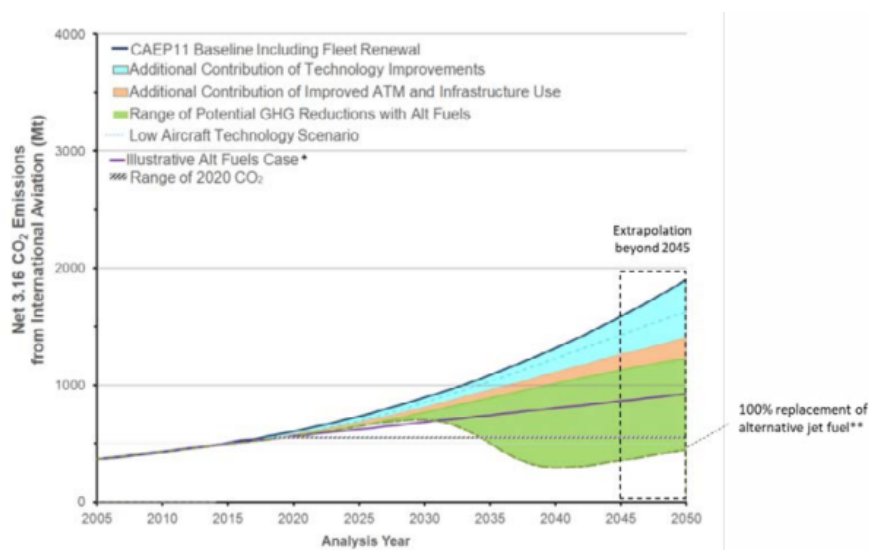


Figure 2.1: Future estimation of aircraft fuel consumption for different scenarios. Adapted from: ICAO, 2019 [30]

back into space. This difference between absorbed and reflected radiation is called RF and the particles which absorb the radiation are called RF agents. The higher the concentration of RF agents in the atmosphere, the higher the total energy that will be absorbed and this is the main cause of climate change.

Figure 2.2 depicts the typical combustion products of a jet engine which for the most part consist out of carbon dioxide ( $CO_2$ ), carbon monoxide ( $CO$ ), nitrogen oxide ( $NO_x$ ), water vapor ( $H_2O$ ), sulphur oxide ( $SO_x$ ), unburned hydrocarbons ( $HC$ ) and particulate matter ( $SOOT$ ) [46, 56]. From these combustion products only  $CO_2$  and  $H_2O$  are directly emitted RF agents. The other products either influence the concentrations of RF agents or they are responsible for cloud, aerosol and contrail formation [45].  $NO_x$  is an example of a product that influences the concentration of other RF agents when it reacts with sunlight to produce ozone ( $O_3$ ).  $H_2O$ ,  $SO_x$ ,  $HC$  and  $SOOT$  undergo micro-physical processes to produce the RF agents aerosol and contrails which in turn cause the formation of clouds. [2]

Lee et al. made an overview of the RF from aviation in 2005 which is depicted in Figure 2.3 [38]. In his study Lee made an estimation of the RF of cirrus so this value is updated using the paper of Burkhardt and Kärcher [12]. Important to notice from this figure is the cooling effect that  $NO_x$  has on the atmosphere because of the reduction of methane ( $CH_4$ ) [14]. However, this cooling effect is less significant than the warming effect it has due to the production of ozone ( $O_3$ ).

From the RF agents in Figure 2.3 it is clear that  $CO_2$ ,  $NO_x$  and contrail forming from particulate matter are the most potent forcing agents. This is why these agents are mainly targeted in emission reduction measures. Although the contribution of aviation to the total emission of  $NO_x$  is relatively low, this  $NO_x$

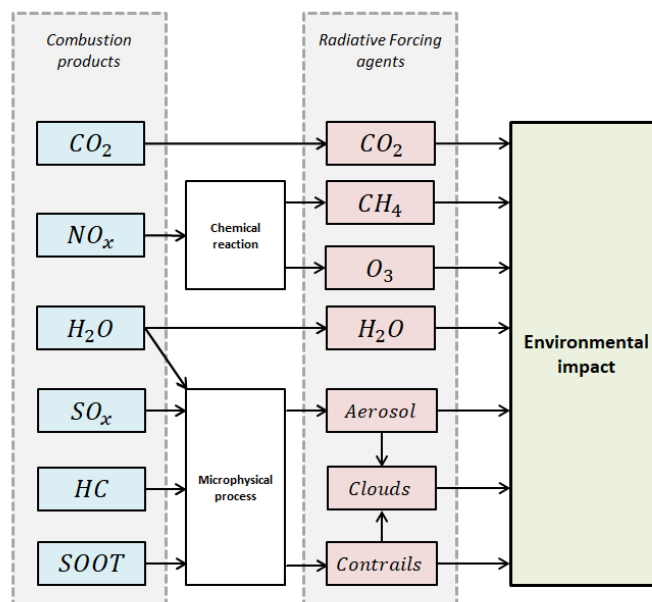


Figure 2.2: Combustion products and their atmospheric processes that influence Radiative Forcing agents.  $NO_x$  has a negative influence on methane ( $CH_4$ ) which means that it reduces the methane concentrations. Based on information from: Wuebbles et al., 2007 [56] and Prather et al., 1999 [46]

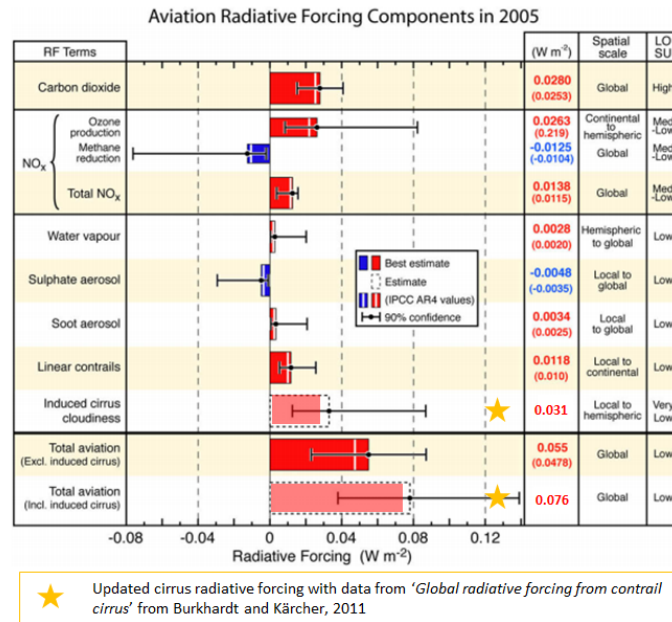


Figure 2.3: Radiative Forcing (RF) components in 2005 from aviation. Adapted from: Lee et al., 2009 [38] and updated with Burkhardt and Kärcher, 2011 [12]

is directly emitted in the upper troposphere and lower stratosphere where it has a strong effect on the production of  $O_3$ . Lower in the atmosphere the production of  $O_3$  can cause respiratory complications on humans because of its highly corrosive property [2].  $CO_2$  on the other hand has a very long lifetime and its contribution to climate change is independent of the location in the atmosphere of the emission [54].  $CO_2$  is directly related to fuel burn so as fuel efficiency of aircraft increases, its automatically will result in a decreasing emission of  $CO_2$ . Contrail formation contributes to the total amount of clouds in the atmosphere and they cover approximately 0.1% of the global surface [54]. Clouds prevent part of the earth's radiation from being emitted back into space but they also prevent part of the sun's incoming radiation from entering the atmosphere. However, they do not cancel each other out because the effect of contrails and higher clouds are different when they are emitted higher up in the atmosphere, which leads to a positive net RF.

Hybrid-electric propulsion has the potential to lower emissions through the reduction of the combustion products that are emitted during flight due to lower fuel burn. The part of the energy that will be provided by the battery or fuel cell will not contribute to the emission of greenhouse gases during flight. A hydrogen fuel cell uses reverse electrolysis to generate electricity from hydrogen. Its only emission is water vapor but hydrogen nowadays is more expensive than fossil fuels and needs a redesign of the distribution infrastructure [14]. However, hybrid-electric propulsion allows for the down-scaling of the gas turbine which can lead to a higher required combustion temperature (for example in the case of an electrical/battery system failure).

Figure 2.4 depicts the formation of  $CO$  and  $NO_x$  against the combustion temperature [40]. With increasing combustion temperature both the formation of  $CO$  and  $NO_x$  will start to increase.  $CO$  (and

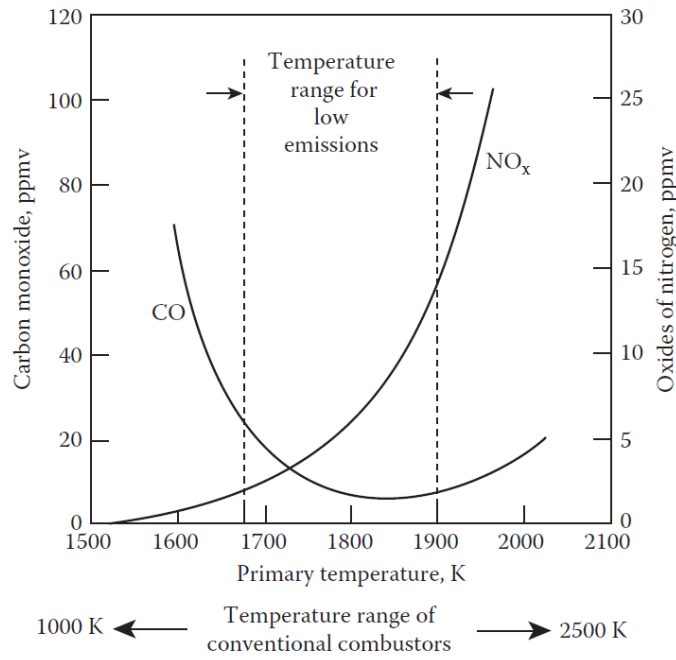


Figure 2.4: The influence of combustion temperature on the formation of  $CO$  and  $NO_x$ . Adapted from: Lefebvre and Dilip, 2010 [40]

$CO_2$ ) emissions will still be relatively low beyond 2000K but  $NO_x$  starts to increase rapidly beyond 1900K. From an emissions point of view the optimal temperature range in the first stage of combustion sits approximately between 1650K and 1900K. For this thesis project it is important to keep track of the combustion temperature when down-scaling of the engine is applied.

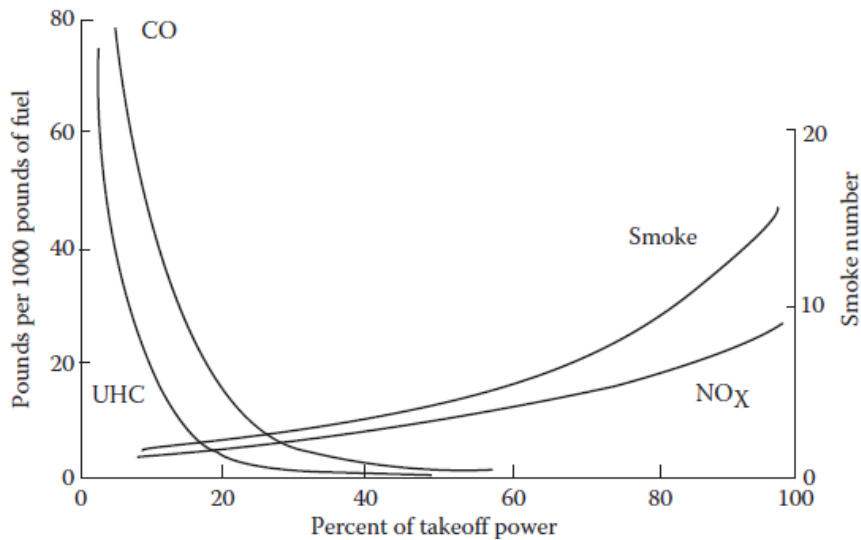


Figure 2.5: Combustion products for gas turbine engines at different percentages of the takeoff power. Adapted from: Lefebvre and Dilip, 2010 [40]

Figure 2.5 shows the amount of combustion products produced by the gas turbine as a function

of the percentage of the take-off power. When this power setting is low it results in a low equivalence ratio<sup>1</sup> which means that there is excess of air during the combustion process (lean burn). Therefore the combustor is operating at lower peak temperatures. At low temperatures the formation of  $CO$  and  $HC$  are highest. On the contrary, when the engine power setting is higher, the equivalence ratio is closer to one so there is more complete combustion taking place. The peak combustion temperatures are higher and therefore the formation of  $NO_x$  and smoke are highest at this point [40].

For parallel hybrid-electric aircraft the take-off power required from the ICE is lower due to the added electrical power originating from the batteries. This has the potential to reduce the  $NO_x$  emissions. However, one should keep in mind that down-scaling the gas turbine also influences the combustion temperature as stated before.

## 2.2. Hybrid-electric propulsion

In the previous chapter a brief introduction has been given about the electrification trend of aircraft. EAPS can serve as a steppingstone to all-electric aircraft. There are many different EAPS configurations but the two main categories are: turbo-electric systems and hybrid-electric systems[33]. When the words "hybrid-electric" are used in this report, turbo-electric systems are excluded from this category, according to the EAPS classification of NASA [33]. Turbo-electric systems use a generator as the power source that is driven by a turbofan or turbo-shaft and they do not use an energy storage device like a battery. Hybrid-electric systems use a battery and an ICE as a combined source of energy (Jansen et al., 2017 [33]).

The three main hybrid-electric powertrain architectures are the series, parallel and the series-parallel architectures. Figure 2.6 shows a schematic drawing of these three configurations (Jansen et al., 2017 [33] and Tan, 2018 [48]).

In the series configuration (Figure 2.6a) a turbo-shaft drives a generator. The electrical energy from the generator is used to drive one or more electric motors that are used to drive the fan(s). The additional electric energy can be stored in a battery for usage later on. In the parallel configuration (Figure 2.6b) the battery delivers extra power to the shaft of a turbofan through an electric motor. In the series-parallel configuration (Figure 2.6c) a part of the ICE energy drives a turbofan and another part

<sup>1</sup>A low equivalence ratio relates to a low fuel to air ratio during combustion.

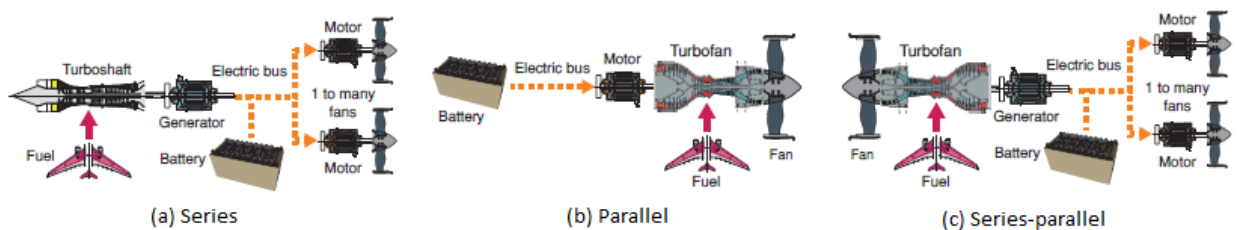


Figure 2.6: The three main hybrid-electric propulsion architectures: (a) Series, (b) Parallel and (c) Series-parallel. Adapted from: Jansen et al., 2017 [33] and Tan, 2018 [48])



Table 2.2: The main advantages and disadvantages of hybrid-electric architectures

	<b>Advantages</b>	<b>Disadvantages</b>
<b>Series</b>	<ul style="list-style-type: none"> <li>+ The ICE is not coupled to the fan which allows for distributed propulsion</li> <li>+ The ICE can operate at an optimal rotational speed due to the decoupled ice and fan</li> </ul>	<ul style="list-style-type: none"> <li>- Weight penalty due to the need for a generator</li> <li>- Low efficiency: large energy losses due to the amount of energy conversions</li> <li>- Not suitable for retrofitting onto existing aircraft</li> </ul>
<b>Parallel</b>	<ul style="list-style-type: none"> <li>+ Lower weight penalty (no generator)</li> <li>+ Lower energy losses due to the low amount of energy conversions</li> <li>+ Better suitable for retrofitting</li> </ul>	<ul style="list-style-type: none"> <li>- Due to the mechanical coupling between the ICE and the fan, the ICE cannot operate at an optimal RPM</li> <li>- Weight penalty due to high battery mass</li> </ul>
<b>Series-parallel</b>	<ul style="list-style-type: none"> <li>+ Allows for distributed propulsion</li> </ul>	<ul style="list-style-type: none"> <li>- Weight penalty due to the need for a generator</li> <li>- Low efficiency: large energy losses due to the amount of energy conversions</li> </ul>

can be stored in batteries to drive electric motors which in turn can drive other fans.

The articles of Hung and Gonzalez [27] and Harmon et al. [23] provide an overview of the conceptual design of hybrid-electric systems for small aircraft. They also discuss the main (dis)advantages of the hybrid-electric configurations. A summary of their statements and some additions are provided in Table 2.2 which shows that the parallel configuration is most suited for retrofitting onto existing aircraft because it does not necessarily need a redesign of the aircraft. However, a big disadvantage is the mechanical coupling between the ICE and the fan which limits the efficiency of the engine. Another major disadvantage of hybrid-electric propulsion is the weight that is associated with the battery and/or generator. In contrast to jet fuel which reduces in mass during the flight, a battery is dead weight that stays constant.

In the article of Brejle and Martins [11] the writers provide a summary of manned EAPS from 2003 till 2017 that have been built and flown. One of the aspects that stand out are the fact that all aircraft are relatively small (up to 4 seats) and that the ranges are limited. Another aspect is that current studies mostly focus on future battery technology in order to avoid very low ranges [17, 55]. This is due to one of the main challenges of hybrid-electric aircraft which is the high mass penalty due to the size of the battery and/or generator. One of the ways to decrease this weight is to either utilize a turbo-electric powertrain or to decrease the size of the batteries needed, which is the case for a parallel hybrid-electric architecture [16]. Other challenges of hybrid-electric propulsion are the low battery specific power, the increased powertrain complexity and the high costs associated with the implementation.

Based on work that has been done on several hybrid-electric configurations, the parallel architecture could be a suitable next step for aircraft. One of the main advantages of this configuration is the

possibility to retrofit it onto existing aircraft testbanks, which makes the implementation less invasive. One study shows a reduction in fuel consumption of approximately 7.5% compared to the conventional ICE of a single aisle aircraft (Ang et al., 2018 [9]). Another study carried out by Harmon et al. [23] compared a parallel hybrid-electric Unmanned Aerial Vehicle (UAV) with a gasoline powered UAV and they found significant energy savings for three hour missions.

### 2.3. Power management

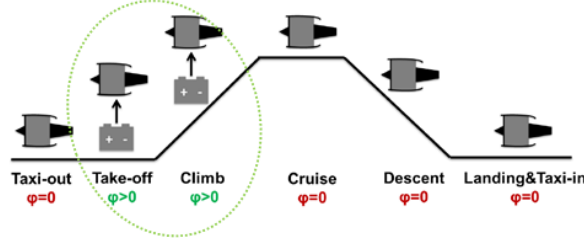


Figure 2.7: Example of a power management strategy. Adapted from: Lammen and Vankan, 2020 [37]

Power management describes the choice for availability of electrical power to assist the turbofan, per flight phase [8]. The higher the demand for electrical power, the higher the battery weight will be. For the parallel hybrid-electric aircraft the power split or hybridization factor ( $\phi$ ) indicates the share of power that is delivered by the electric energy carrier [15, 16, 41, 57]. The power management strategy is a design choice that determines the part of the total required power per flight phase that is being provided by an electric energy carrier such as a battery. The percentage of the power delivered by an electric energy source is defined by Equation 2.1.

$$\phi = \frac{P_{el}}{P_{el} + P_{ice}} \quad (2.1)$$

If the hybridization factor  $\phi = 0$  then the thrust required by the mission is fully provided by the ICE and if  $-1 < \phi < 0$  then the battery is charging (negative power) [15]. At  $\phi = 1$  the aircraft is all-electric. A commonly seen power management strategy is to utilize the battery during the taxi phase in order to provide better local air quality around airports. Another strategy is to make the hybridization factor variable within one flight phase.

Figure 2.7 shows a power management strategy where the battery is only utilized during take-off and climb. This is a common strategy in the literature due to the highest thrust requirement usually occurring in these flight phases. This allows for the core mass flow of the ICE to be scaled down as it does not have to be sized for maximum thrust requirements. However, there is a trade-off between the increasing weight of the battery with higher hybridization and the benefits of downsizing the ICE.

There are several limiting factors to downsizing the ICE when the hybridization is low, meaning more power has to be delivered by the ICE. In this case, downsizing the engine may lead to a higher turbine inlet temperature ( $T_{t4}$ ) which contributes to a rapid increase in  $NO_x$  production [8][40]. Moreover, due

to material properties of engine, this turbine inlet temperature needs to be monitored to stay below a reference value. In Section 3.2.3 this reference value will be determined and the topic of engine scaling will be elaborated on.

## 2.4. Electric powertrain technology

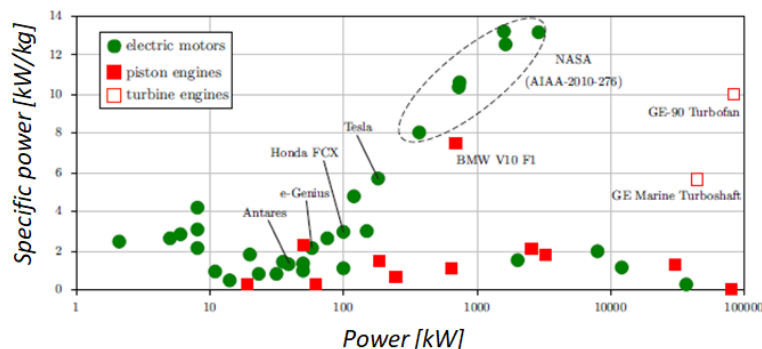


Figure 2.8: Specific power of different electric motors, piston engines and turbine engines. Adapted from: Hepperle, 2012 [24]

The parallel hybrid-electric powertrain typically consists out of the following components: a gas turbine, an electric motor and an electric energy carrier such as a battery or a fuel cell. For the purposes of this thesis a battery has been used. A battery is an energy carrier which converts the stored chemical energy into electrical energy in order to provide power. In this section a review of the current electric powertrain technology will be provided.

The specific energy density is the amount of energy that can be stored in an energy carrier per unit mass. This is used to determine the amount of energy that can be stored in for example a battery ( $e_{bat}$ ), fossil fuel ( $e_{fuel}$ ) or fuel cell of a particular mass. The specific power is the amount of power that an electric motor can deliver per unit mass ( $p_m$ ).

Jet-A fuel has a specific energy of 11900 Wh/kg so that is approximately 50 times the specific energy of a current Lithium-ion battery. Table 2.3 provides the current battery pack specific energy densities of four different batteries. The energy loss between the cell efficiency and the battery pack efficiency is approximately 30-40% [42]. Lithium-Sulphur and Lithium-Air batteries are the most promising battery

Table 2.3: Battery pack current and theoretical specific energy densities (Wh/kg) and their main challenges [42, 48]

	<i>Specific energy 2020:</i>	<i>Theoretical specific energy:</i>	<i>Challenges:</i>
<i>Li-ion</i>	250 Wh/kg	400 Wh/kg	- Low theoretical energy density
<i>Li-metal</i>	300 Wh/kg	750 Wh/kg	- Low cycle life - Low long term life
<i>Li-sulphur</i>	350 Wh/kg	2600 Wh/kg	- Low cycle life (<300) - High self discharge rate
<i>Li-air</i>	400-500 Wh/kg	3500 Wh/kg	- Low cycle life - Complex

technologies in the current state of the art. However, flying a 737 type hybrid-electric aircraft with a range of at least 900 miles requires a battery pack specific energy density of at least 750 Wh/kg<sup>2</sup> according to NASA. Other requirements are a specific power of at least 1000 W/kg and a battery cycle life of at least 1000 cycles [42]. In order to successfully operate a hybrid-electric aircraft one must also consider the discharge rate (C-rate), charging time and life cycle.

Figure 2.8 shows the specific power of different electric motors, piston engines and turbine engines. The current specific power of electric motors that are used for aircraft propulsion is around 4 kW/kg.

Figure 2.9 shows the specific power and specific energy forecast of electric motors, generators, power electronics and batteries according to a literature review of Tan, 2018 [48]. This forecast predicts a battery specific energy density of 750 kWh/kg and an electric motor specific power of approximately 12.5 kW/kg for EIS 2030 aircraft. This is however a rather optimistic extrapolation of the current trend in battery technology.

Figure 2.10 shows the NASA forecast which assumes a battery cell specific energy increase of 8% per year. With the current cell-to-pack loss of 32% this adds up to about 450 Wh/kg for EIS 2030 batteries. For the more advanced cell-to-pack loss of 15%, a specific energy of almost 600 Wh/kg can be achieved.

## 2.5. Mission literature

A typical mission profile consists out of several flight phases each having different thrust, power, velocity and altitude requirements. Typically the mission will be divided in the following phases: taxi, take-off, climb, cruise, descent and approach. For this report, a reference mission of the A320 has been used which is obtained from data in OpenAP. This open-source aircraft performance tool also contains

<sup>2</sup>On cell level the energy density has to be around 1000 Wh/kg

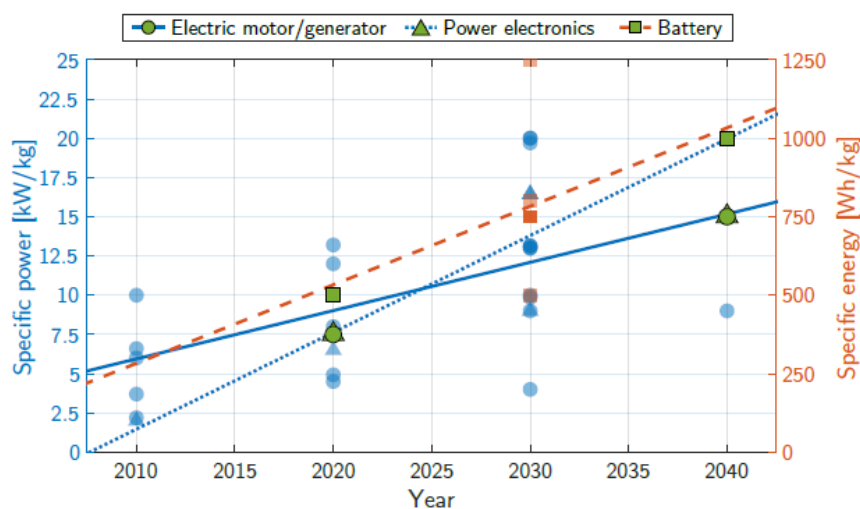


Figure 2.9: Specific power and specific energy forecast for electric motors, generators, power electronics and batteries. Adapted from: Tan, 2018 [48]

performance data on these missions. The reference mission is based on the average of the missions in the database of OpenAP.

The minimum fuel required for a specific mission is achieved by flying at maximum  $L/D$ , which is an indicator for the aerodynamic efficiency of the aircraft. Due to fuel consumption, the weight of the aircraft changes which in turn changes the lift. As the weight decreases, the lift decreases ( $L = W = 0.5\rho V^2 S C_L$ ) so in order to keep the  $C_L$  constant  $\rho$  has to decrease too. In order to keep the lift coefficient  $C_L$  constant, the air density has to decrease, which is accomplished by flying at a higher altitude. The best way to keep the  $L/D$  constant is by continuously increasing the altitude during cruise, but due to air traffic control regulations this is not common practice. Instead a step climb is used during long haul flights in order to approximate the maximum  $L/D$  flight.

In the literature there are some studies on (hybrid-)electric propulsion which tend to show promising fuel savings. However, the studies usually consider very low range missions or take into account far future battery technology. The aircraft's mission is usually provided as a top-level requirement. Also the mission flown by the hybrid-electric aircraft is usually the same as the reference aircraft's mission. Each of the flight phases mentioned before is usually hybridized with a constant hybridization factor.

One study compared the range performances of parallel and series powertrains and concluded that the parallel configuration had a higher range than the series configuration for the same battery energy density (Dean et al., 2018 [17]). This is linked to the high weight penalty for the series and series-parallel configurations. In another paper on the analysis of hybrid-electric propulsion systems it was found that one fourth of the mass of a hybrid-electric propulsion system consists out of battery mass which makes the hybrid powertrain more than three times heavier than a conventional powertrain [25].

Wroblewski and Ansell state that parallel architectures' weight reduction is partly caused by the advantage of the combined power supply which allows both the ICE and the electric motor to be smaller, while for series and series-parallel propulsion the ICE and the electric motor have to be sized for maximum power requirements (Wroblewski and Ansell, 2019 [55]). Wroblewski and Ansell compared different mission ranges with varying hybridization factors and battery energy densities to

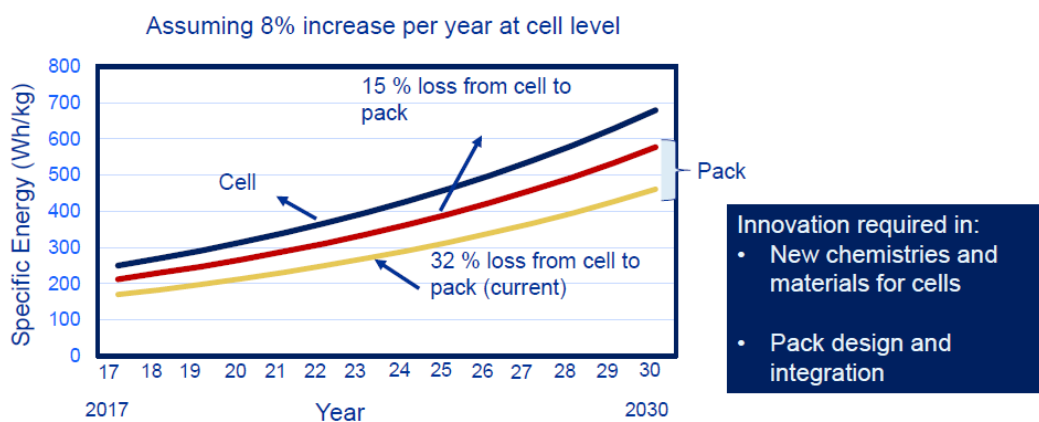


Figure 2.10: Specific energy forecast for batteries. Adapted from: Misra (NASA), 2018 [42]

the conventional turbofan engine of a reference single aisle aircraft and concluded that with the current battery technology the range would still be too small for the parallel hybrid configuration.

However, a recent study suggests that when comparing hybrid-electric configurations one should evaluate each concept at its optimum cruise altitude, instead of keeping the cruise altitude the same for both the reference and the hybrid-electric aircraft (de Vries et al., 2019 [16]). The outcomes for both Dean and Wroblewski could probably be more realistic (taking into account near future battery technology) if the optimal cruise altitude had been considered instead of the cruise altitude of the reference aircraft. Climbing to cruise altitude costs energy so that has to be compensated by the energy that is saved by flying at a higher altitude. According to de Vries et al. the optimal cruise altitude for hybrid-electric aircraft seems to be lower than for conventional ICE aircraft. De Vries et al. states that hybrid-electric aircraft have a higher wing loading which leads to a lower optimal cruise altitude than for the ICE aircraft (de Vries et al., 2019 [16]).

This thesis investigates these possible mission alterations needed for hybrid-electric aircraft and their impact on fuel, energy and emissions. There are several mission variables which influence the performance of the hybrid-electric aircraft. These mission variables are:

1. *Velocity*
2. *Cruise altitude*
3. *Hybridization factor*
4. *Range*

#### 1. *Velocity*

The first mission variable is the velocity. The cruise velocity at which the mission range is maximized is called the maximum range mach number ( $M_{MR}$ ). This Mach number stands for the speed at which the specific fuel consumption is at its minimum for a given constant altitude (hence the highest range). The lower the weight of the aircraft becomes, the lower the optimum Mach number  $M_{MR}$  because of the increased Specific Range (SR). So for a conventional turbojet aircraft at constant cruise altitude, the optimal Mach number decreases during the flight because of the weight reduction caused by the fuel burn [4]. For hybrid-electric aircraft this weight reduction is significantly lower due to the fixed battery and electric component mass so the difference between the  $M_{MR}$  at the beginning and the end of the cruise phase is lower. Usually the cruise speed is chosen to be constant during flight so that means that a hybrid-electric aircraft can operate closer to its optimal speed during the whole cruise phase while the conventional aircraft has a greater difference to its optimum.

Another thing to consider is the fact that the peak efficiency of an electric motor usually is at low speed. For example the Tesla model S can reach its maximum range for one charging cycle at a constant speed of around 40 km/h. The faster the speed, the more drag the vehicle exhibits which requires more power from the electric motor. In the end for the same range, a faster travelling vehicle will have consumed more energy than a slower one. However, the faster driving vehicle has a shorter

travel time so there is an optimum to be found. Whether this also applies to hybrid-electric aircraft engines has to be determined.

## 2. Cruise altitude

The second mission variable is the cruise altitude. For a given constant cruise Mach number the optimum cruise altitude increases with decreasing weight. So as the aircraft burns fuel during the cruise flight phase, the optimum altitude becomes higher. As mentioned before, this optimum altitude is the altitude at which the aircraft is operated at its optimum lift to drag ratio  $L/D$  [4]. Due to the battery weight, a hybrid-electric powertrain is much heavier than a conventional turbofan [26]. This means that the optimum  $L/D$  of a hybrid-electric aircraft probably lays at a lower altitude than a conventional ICE aircraft. On top of that, there is also a lower weight reduction during the flight due to the constant battery mass and the lower fuel burn. This higher wing loading of hybrid aircraft has the potential to lower the optimum cruise altitude.

Vos et al., researched the effects of different fuel types with different energy densities on the optimal cruise altitude of single aisle aircraft [52]. They confirmed that fuel type had an influence on the optimal cruise altitude of an aircraft. Of more importance to this research project is the note that the optimal altitude for minimum fuel consumption can be quite different from the optimal altitude for minimum emissions. An example of this difference can be found in Figure 2.11 which originated from the cruise altitude sensitivity study from Vos et al.

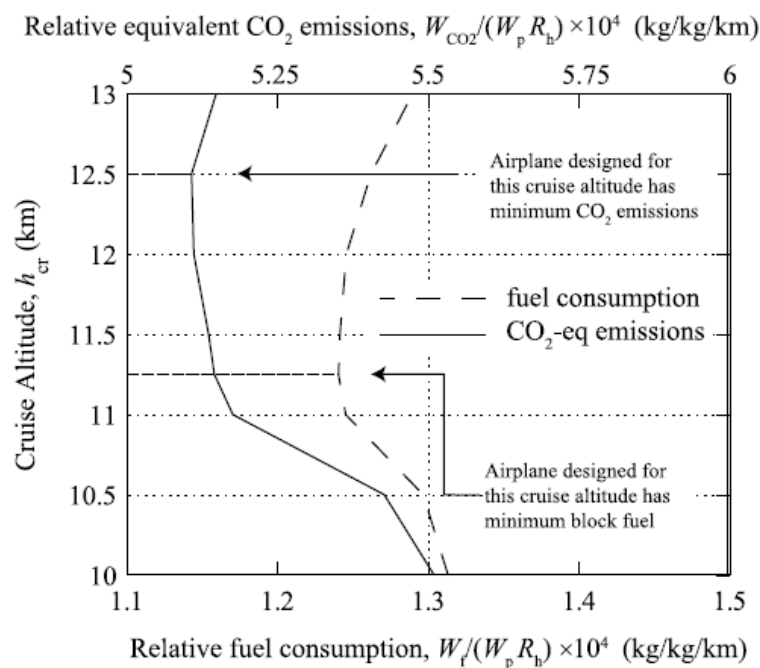


Figure 2.11: An example of different optimum values for the cruise altitude for fuel consumption and  $CO_2$  emissions. Adapted from Vos et al., 2017 [52]

### 3. Hybridization factor

The third mission variable is the hybridization factor. This factor determines the partial power that is provided by the electrical system. The higher the chosen power split, the higher the battery mass will become. This increase in weight should not compromise the overall performance of the combined powertrain when the main engines are scaled down. As the core mass flow of the scaled engine decreases, the turbine inlet temperature increases. It is assumed that the scaled engine has the same ceiling temperature as the unscaled engine. In the study of Ang et al., a 90% scaled engine with a take-off power split of 24.9% and a climb power split of 13.6% resulted in a overall fuel consumption for an A320 of 7.5% [8].

### 4. Range

The fourth mission variable is the range which shows a strong correlation to the mission objective which is to minimize fuel consumption, total energy and emissions.

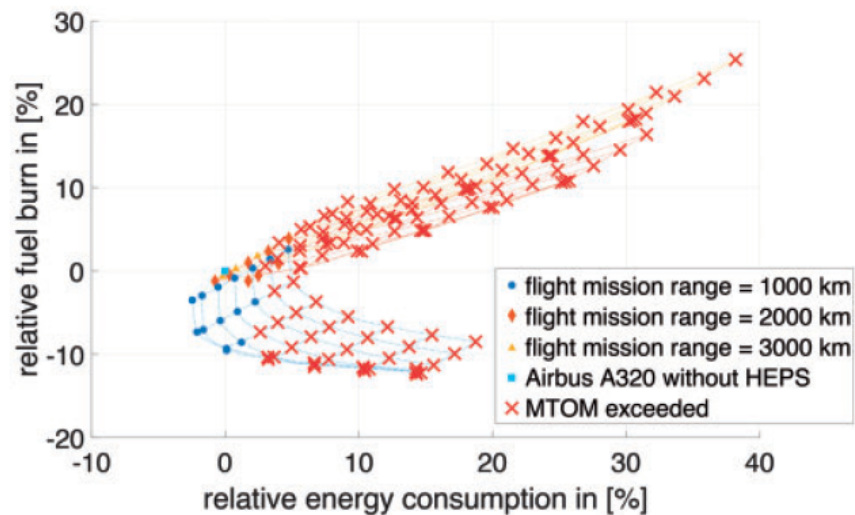


Figure 2.12: Pareto multi-objective representation of the fuel consumption and the total energy consumption for different ranges of a A320. Adapted from Ang et al., 2018 [9]

Figure 2.12 shows a Pareto front optimization for different mission ranges of a hybrid-electric aircraft based on the A320 [9]. The figure shows that according to this study, the only feasible range that results in a reduction in fuel consumption and total energy is 1000 km. Higher ranges result in the same or even a higher fuel and energy consumption that for the reference aircraft without a hybrid configuration.

Wroblewski et al. conducted a study to compare the ranges of different battery specific energy densities and hybridization factors. Figure 2.13 shows the results of the range calculations for a hybrid-electric aircraft based on the Boeing 737-700. This study shows that in order to achieve higher ranges, the battery specific energy density needs to be much higher than the current technology allows. A current Lithium-ion battery allows for a battery specific energy density of 250 Wh/kg. A proposal for a better solution would be to also vary the cruise altitude and speed. This could possibly lead to more



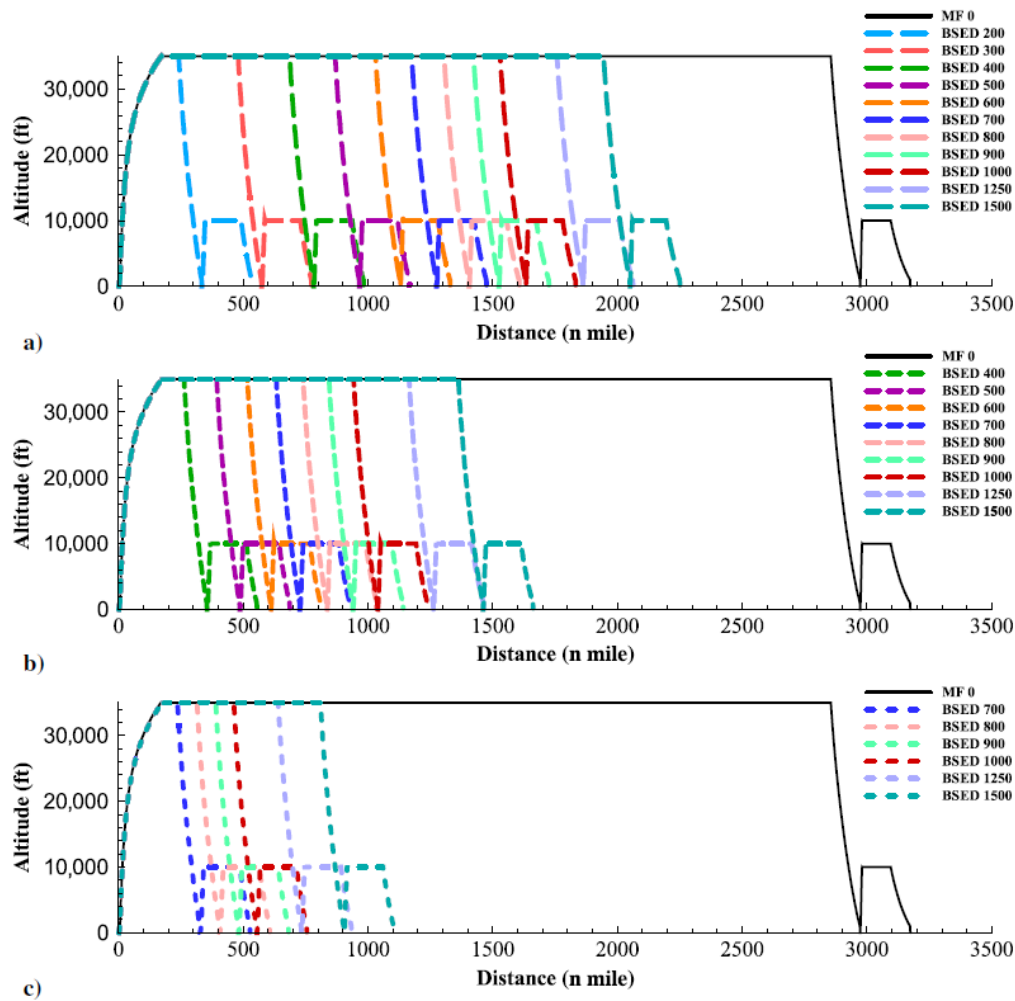


Figure 2.13: Hybrid-electric commercial transport aircraft range for different battery specific energy densities and hybridization factors: a)  $\phi = 0.125$ , b)  $\phi = 0.25$  and c)  $\phi = 0.50$ . Adapted from Wroblewski et al., 2019 [55]

reasonable battery energy densities.

Figure 2.13 also shows that when the hybridization factor is increased, the range decreases rapidly. This is caused by the increased energy demanded from the electric motor which therefore requires a bigger battery and hence a higher weight. Both studies (Ang et al. and Wroblewski et al.) consider similar single aisle aircraft with approximately the same cruise altitude.

## 2.6. Actors and stakeholders in the aviation industry

The challenges concerning the environmental impact of aviation asks for a global approach. In order to tackle a problem of this magnitude it is important to map the actors and certain groups who have an interest in the matter. These groups are called the stakeholders. Because all these stakeholders have shared interest in the aviation sector, they all need to be part of the solution. This makes the implementation of changes in bigger industries very complex. The first step in identifying the stakeholders is to determine people and authorities of interest by answering the following questions:

- Who or what creates the problem?
- Who are the users of air travel?
- Who is affected by the consequences of air travel?
- Who has a financial interest?
- Who influences the public opinion?
- Who can help to tackle the problem?
- Who has the power to change regulations?

Table 2.4: Air traffic industry stakeholders and some examples. Adapted from ATAG, 2018 [21]

<b>Stakeholder:</b>	<b>Examples:</b>
Airline suppliers	<i>Fuel suppliers, ground handlers, maintenance and repair</i>
Aircraft manufacturers	<i>Tier 1 and 2 suppliers, engine manufacturers, airframers</i>
Sales channels	<i>Travel agencies</i>
Cross-industry representative groups	<i>Air transport associations, flight safety foundation</i>
Aircraft financing	<i>Insurers, banks, lessors</i>
Unions	<i>Employee unions</i>
Air Navigation Service Providers	<i>Eurocontrol</i>
Airports	<i>Airport operators, airport associations</i>
Airlines and airspace users	<i>IATA, business and general aviation operators</i>
Tourism	<i>Tour operators, hotels, car rental companies</i>
Governments	<i>Civil Aviation Authority, ICAO, EU, national governments</i>
Passengers	<i>Safety and rights organizations</i>
Education and training institutions	<i>Universities, flight training facilities, research institutes</i>
Media	<i>Regional and global media outlets</i>
Business community	<i>International Chamber of Commerce, World Economic Forum</i>
Non-governmental organisations	<i>Environmental organizations, local groups, NGOs</i>

Table 2.4 depicts an overview of the main branches of stakeholders in the aviation sector and some examples of authorities within these branches. Each of these stakeholders has a specific interest and provides an answer to one or more of the previously mentioned questions. This means that these stakeholders all share the responsibility to make a difference in the field of aviation. But what are they contributing to the answer on in the present day? Well, many of the stakeholders are already working on different projects in the electrification field. Big airframer Airbus teamed up with engine manufacturer Rolls-Royce to work on their 2 megawatt series hybrid-electric 'E-Fan X' which was initially supposed to fly in 2020. After postponing the project to 2021, it currently has been cancelled [2, 53]. Airframer Boeing is involved with the development of the all-electric 'Pegasus' electric Vertical Take-off and Landing (eVTOL) flight demonstrator [53]. Besides these big airframers there are also a lot of startups in the field of electric flying as this new field creates opportunities for new players to enter the up to now closed market. Most of these startups consider small aircraft up to 6 seats, but there are some exceptions such as Zero-Avias hydrogen powered electric passenger aircraft designed to have

19 seats which is scheduled to fly in 2022 and Wright Electric which is developing a 180 seats short haul electric aircraft for EasyJet which is scheduled to fly around 2030 [53].

## 2.7. Reference aircraft and engine

For this thesis project the reference aircraft that will be used is the Airbus A320neo. This aircraft entered service in 2016 and is part of the Airbus A320 family. The twin-jet A320neo stands for the 'new engine option' version of the previous A320. Since the introduction of the 'neo' in 2016, the former A320 has been renamed A320ceo, where 'ceo' stands for 'current engine option'. The aircraft features CFM LEAP-1A high-bypass turbofan engines and additional sharklets on the wings which increase the total wingspan of the A320neo with 1.7m compared to the A320ceo.

Table 2.5 features the characteristics of the A320neo which are mainly adapted from Jane's all the world's aircraft [32]. Figure 2.14 shows the mass breakdown of the A320neo. On the website of Airbus [7] they state that the design payload of the A320neo is 2 tonnes more than that of its predecessor A320ceo. Jenkinson et al. [35] states that the design payload of the A320ceo is 14250kg, so the DPL of the A320neo would then approximately be 16250kg. The mass breakdown of the parallel hybrid-electric architecture will be slightly different from the one of the A320neo. The ICE will be scaled down and there will be less fuel load but instead there will be added weight due to the electric motor and the battery [15]. Also the battery weight does not change during flight so the difference between the take-off weight and the landing weight will be smaller.

Figure 2.15 shows the dimensions of the A320neo with the main difference between the A320ceo and neo being the increased wing span and the winglets.

The engine that will be used for modelling the hybrid-electric aircraft based on the A320neo is the CFM LEAP-1A26, which is a twin spool high bypass turbofan from the CFM-international engine manufacturer. It is the new engine option for the A320 since 2016. It features a higher Overall Pressure Ratio (OPR) than the CFM56 and a lean burn (lower temperature) combustor.

Figure 2.16 shows the engine data retrieved from the EASA type certificate sheet. The thrust for take-off is designed to be used for not more than 5 minutes on end. An exception is made for the case of One Engine Inoperative (OEI). In that situation the take-off thrust can be used for 10 minutes [19].

Table 2.5: Characteristics of the A320neo [5, 6, 19, 32]

<b>Wings</b>	Span	35.80m	<b>Speed</b>	$V_{mo}$	350kts
	Root chord	6.10m		$M_{mo}$	0.82
	Aspect ratio	9.5		$M_{cr}$	0.78
	Area	122.4m <sup>2</sup>		Rate of climb	2,500ft/min
<b>Weight</b>	Max. Zero-Fuel	62,800kg	<b>Altitude</b>	Cruise	37,000ft
	Max. Take-Off	79,000kg		Service ceiling	39,800ft
	Max. Landing	67,400kg			
	Max. Fuel	24,240kg			
	Max. Payload	20,400kg			

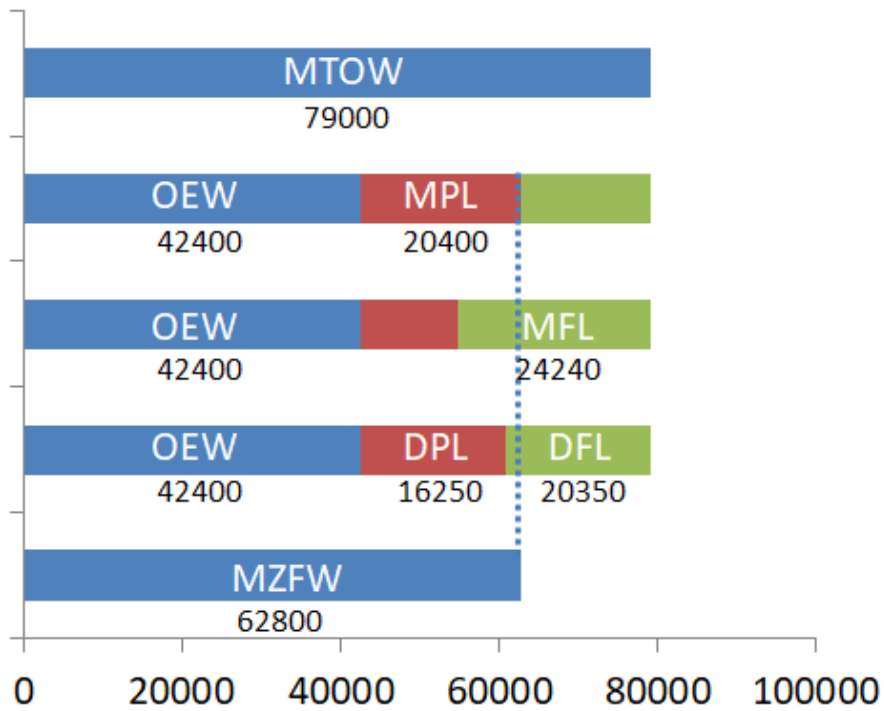


Figure 2.14: Mass breakdown of the A320neo. The horizontal axis depicts the mass in  $kg$ . Legend: Max. Take-Off Weight (MTOW), Operational Empty Weight (OEW), Max. Zero-Fuel Weight (MZFW), Max. Payload (MPL), Max. Fuel Load (MFL), Design Payload (DPL), Design Fuel Load (DFL). Data retrieved from: [7] [32] [35]

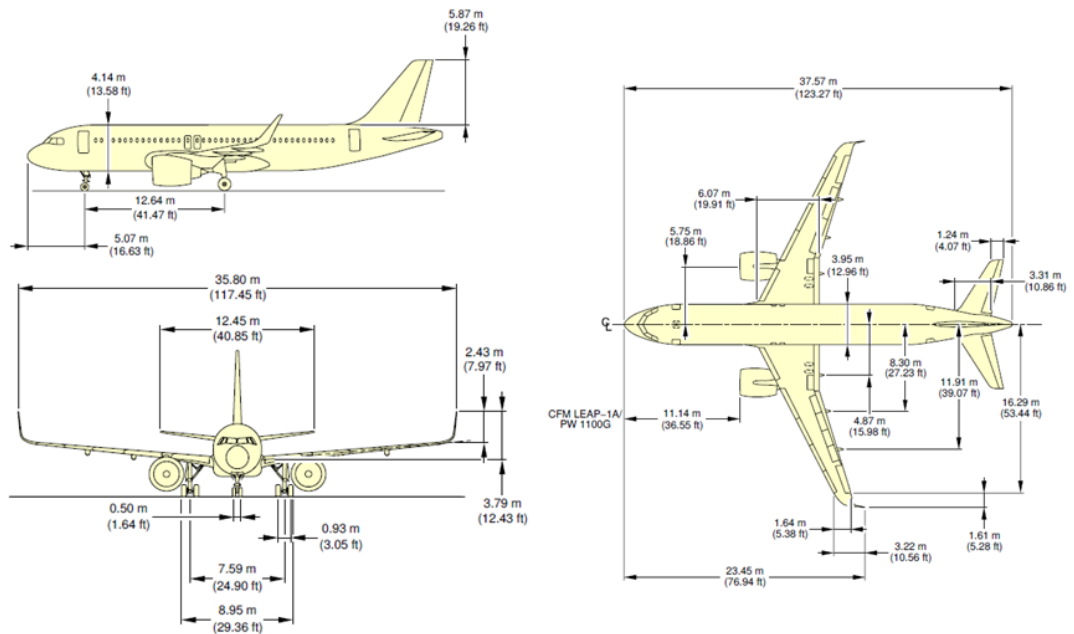


Figure 2.15: Dimensions of the A320neo [6]

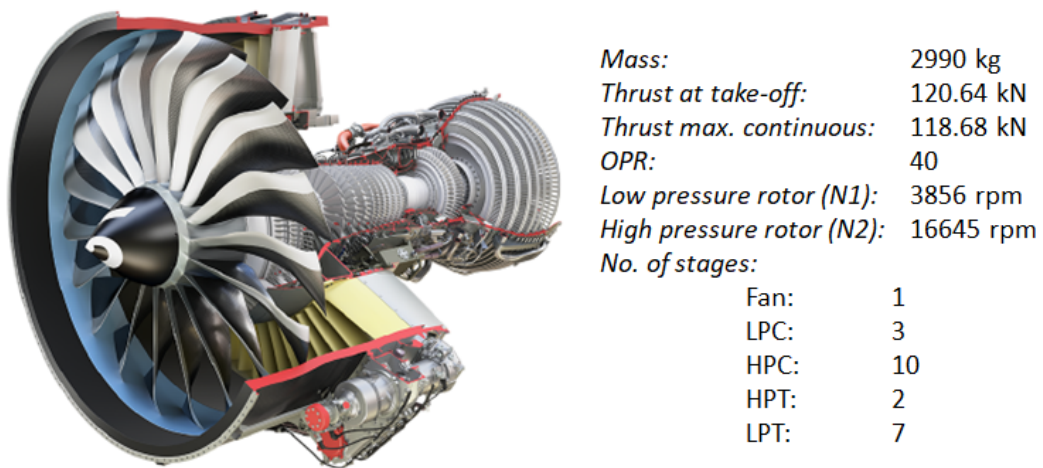


Figure 2.16: CFM LEAP-1A26 engine data [19]



# 3

## Methodology

In the previous chapter the background information and literature overview required for this report have been stated. In this chapter the methodology of the research project will be explained. The goal of this thesis is to assess different missions of a hybrid-electric single aisle aircraft in order to reduce fuel, energy and emissions. The mission variables of interest are the altitude, velocity, hybridization and the range. For this purpose a reference mission has been chosen which is based on data derived from an open source aircraft performance tool called OpenAP [47]. The missions are assessed using MASS which is a hybrid-electric aircraft simulation tool developed at NLR. For the purpose of this thesis, the MASS tool was extended with a new mission analysis segment which allows for a more efficient mission design process.

The topics that will be addressed in this chapter are:

- A brief overview of the research framework
- The aircraft performance model MASS
- The mission model extension
- Engine sizing
- Electric components
- Aircraft sizing
- Validation of the model
- The reference mission

### 3.1. Introduction on the framework and methodology

The method that has been chosen as a research strategy is the computer simulation experiment. This is due to the fact that the goal is to compare the fuel and energy consumption and emissions of parallel hybrid-electric aircraft with a conventional jet engine aircraft. Currently there are no hybrid-electric large passenger aircraft so all studies performed on this topic are studies based on simulations. The resources to perform this experiment are available at the TU Delft and NLR where this project has been executed. Moreover, NLR developed a parallel hybrid-electric aircraft simulation in Matlab which is available to perform the assessments with.

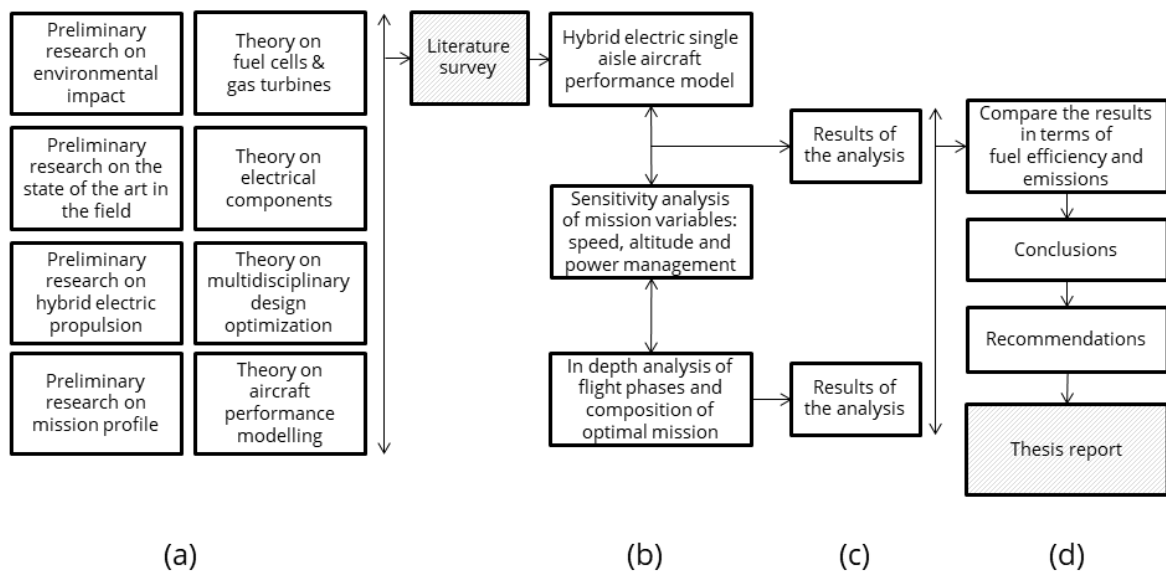


Figure 3.1: Research framework with four phases: (a) Preliminary research, (b) Conceptual model, (c) Results, (d) Conclusions and recommendations

#### 3.1.1. Framework and methodology

In order to meet the research objectives discussed in Section 1.3.1, a research framework has been defined in Figure 3.1. This project consists out of four phases (Figure 3.1a, b, c and d). The research questions will be a guide through the framework stated in this section. The first phase (Figure 3.1a) was the conducting of a literature study on the state-of-the-art in the field of HEP, the technical details of HEP and mission profiles [22].

The second phase of the project (Figure 3.1b) is the phase where the conceptual model for the simulation studies has been defined and built. This study entails a computer based simulation experiment with an aircraft flight performance model built in Matlab called MASS which evaluates hybrid-electric aircraft configurations [37]. The gas turbine model used in MASS is based on data gathered from Gas turbine Simulation Program (GSP). The MASS model has been validated by doing benchmark tests to



compare the results from the literature with the results of the model. The default mission in the MASS tool is based on mission data for an Airbus A320 gathered from *Getting grips with aircraft performance* (Airbus, 2002 [4]). This mission will be shown in Section 3.2.2. The textbooks of Torenbeek contain the flight performance methodology (Torenbeek, 1982 and 2013 [49, 50]).

Next a module has been added that varies the mission profile by using the hybridization factor, cruise altitude and mission velocities as design variables. In order to design the mission for minimum fuel consumption and emissions, a sensitivity analysis has been carried out in order to map the design space. There will be several constraining factors for the design variables such as the aircraft's MLW, engine characteristics and the service ceiling.

In the third phase (Figure 3.1c) the results of the different analyses on the conceptual model have been gathered. The performance results of the analysis of a baseline conventional aircraft without hybrid-electric propulsion will be compared to results of a hybrid-electric version of the same aircraft. The data that have been collected are the fuel and energy consumption and the emissions.

The last phase (Figure 3.1d) is the evaluation phase where conclusions will be drawn from the results of the experiment. This phase will be finished with a thesis report and presentation.

### 3.1.2. Validation approach

In order to reduce the likelihood of false assumptions, it is important to validate the model that will be used during the experiment. To do this, benchmark tests will be performed to compare the model results against available data. This is a critical step in data analysis in order to validate whether the gathered data makes sense. For this thesis OpenAP and MASS will be used for validation [47]. More details on this topic can be found in Section 3.3.

## 3.2. Aircraft performance and mission model

In order to evaluate different missions of the hybrid-electric aircraft, a model has to be developed which assesses hybrid-electric aircraft. The aircraft performance model that has been used for this purpose is the MASS framework, which is a tool developed at NLR. In Section 3.2.1 the characteristics and workings of this tool will be elaborated on.

In order to sample the mission design space efficiently, there is a need for a mission model of which the mission variables can be altered with the lowest set of data points possible. This allows the process of designing a mission to be automated instead of it being a manual process. The current mission model in MASS does not allow for fast and easy changes in mission. Therefore it requires a new mission evaluation model in order to efficiently sample the design space. This new mission model extension will be explained in Section 3.2.2.

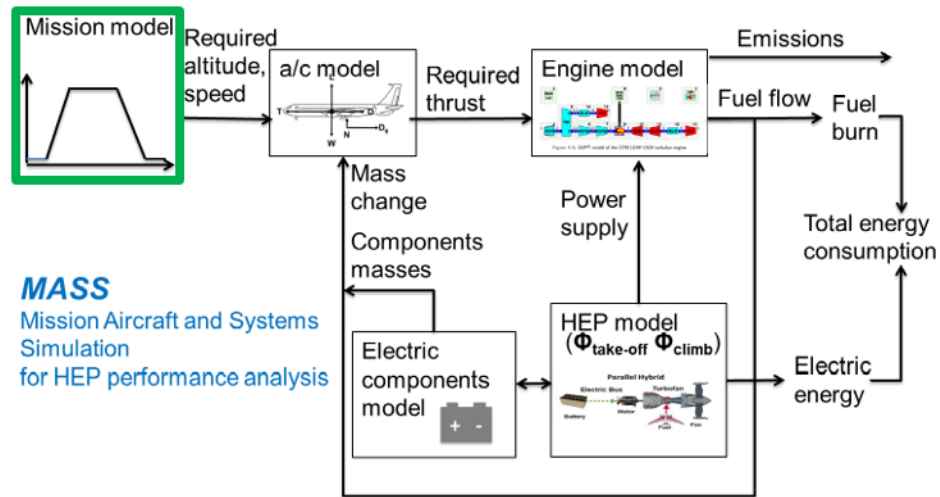


Figure 3.2: MASS framework [37].

### 3.2.1. Aircraft performance model MASS

The scope of this paper is the mission assessment of parallel HEP aircraft. For this purpose the MASS framework has been used [37]. This tool chain is developed by NLR and allows for the performance analysis of an aircraft with and without a parallel hybrid-electric propulsion system.

Figure 3.2 depicts the MASS framework. MASS consists of a mission input consisting out of six flight phases, where the mission input variables have to be defined for several points during the flight. The input variables are: horizontal distance  $d$ , altitude  $h$ , velocity  $V$ , flight phase, flap angle, gear status and the flight path angle  $\gamma$ . These mission variables are then interpolated to obtain the mission information per time step. Next  $\dot{V}$  and  $\dot{\gamma}$  are determined by taking the time derivative of the velocity and flight path angle arrays.

The mission information is used to simulate the flight path and determine the required thrust during the mission using an aerodynamic point mass model. The aircraft aerodynamic model is a performance model based on a straight flight path without roll or yawing movements [37]. This reduces the order of complexity of the flight path which allows for better comparison with other studies. Only forward flight

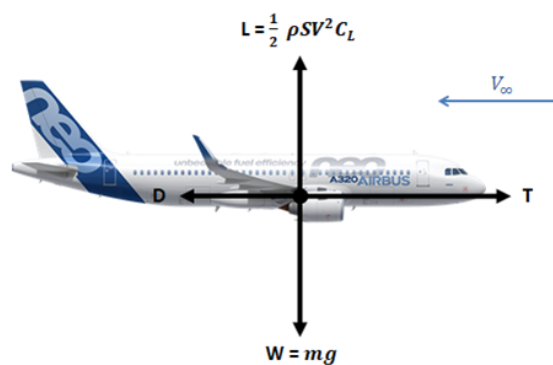


Figure 3.3: Free body diagram of an aircraft during steady level flight. Aircraft without forces retrieved from Airbus [7]

and pitch are being considered. Figure 3.3 shows the point mass representation of the forces acting on the aircraft during flight. The drag force  $D$  is calculated through:

$$D = \frac{1}{2}\rho V^2 S C_D \quad (3.1)$$

where  $\rho$  is the air density,  $V$  is the true air speed (TAS),  $S$  is the wing area and  $C_D$  is the drag coefficient.

In the weight-on-wheels case the aircraft has a normal force  $N$  pointing upwards and an additional drag component  $D_{ground}$  acting between the wheels and the ground surface:

$$D_{ground} = \mu \cdot N \quad (3.2)$$

$$N = mg - \frac{1}{2}\rho V^2 S C_{L_0} \quad (3.3)$$

where  $\mu$  is the friction coefficient,  $m$  is the mass of the aircraft,  $g$  is the gravity constant and  $C_{L_0}$  is the lift coefficient at the angle of attack  $\alpha = 0$ .

The total lift of the aircraft is defined by:

$$L = \dot{\gamma}mV + (mg - N) \cos(\gamma) \quad (3.4)$$

where  $\gamma$  is the flight path angle and  $\dot{\gamma}$  is the flight path angular velocity.

The drag coefficient  $C_D$  is determined using the following equation [51]:

$$C_D = C_{D_{ind}} + C_{D_{par}} + C_{D_{inter}} + C_{D_{wave}} \quad (3.5)$$

where  $C_{D_{ind}}$  is the lift induced drag coefficient,  $C_{D_{par}}$  is the parasite drag,  $C_{D_{inter}}$  is the interference drag and  $C_{D_{wave}}$  is the wave drag component. In the following section the methods will be stated briefly, for the detailed equations there will be references stated.

The induced drag coefficient  $C_{D_{ind}}$  and the lift coefficient  $C_L$  are calculated using a Vortex Lattice Method (VLM) which is employed by Open-source Vehicle Sketch Pad (OpenVSP). OpenVSP is an open-source parametric aircraft geometry model developed by NASA, which contains an aerodynamic tool called VSPAERO to evaluate the coefficients based on the aircraft geometry, center of gravity and Mach number [44] [51]. The parasite drag  $C_{D_{par}}$  is a summation of the parasite drag of the different aircraft components, also calculated using the wetted area approximation in OpenVSP, the aircraft geometry, the Mach number, the altitude, the interference coefficient and the skin friction coefficient [51]. The interference drag  $C_{D_{inter}}$  is calculated using a relation which is based on CFD evaluations [51]. The wave drag  $C_{D_{wave}}$  is determined where the free stream mach number is higher than the critical mach number  $M_{crit}$ . For this study this is only applied to the wing surfaces [51].

The thrust of the aircraft  $T$  now becomes:

$$T = m\dot{V} + D + D_{ground} + mg\sin(\gamma) \quad (3.6)$$

$$\sin(\gamma) = \frac{\dot{h}}{V} \quad (3.7)$$

where  $\dot{h}$  is the vertical velocity of the aircraft. More information on this flight performance methodology used in the MASS tool can be found in Lammen et al., 2020 [37].

The engine model requires this thrust information and the ambient conditions from the former models and is based on a CFM-LEAP-1a26 of which the corresponding engine data is retrieved from a neural network. This neural network is based on gas turbine data from the GSP which provides simulated engine data for all gas turbine stages as well as information on fuel flow and emissions. The emission data from GSP is based on interpolated engine emission measurements from the ICAO Aircraft Engine Emissions Databank [31][37]. Compared to the GSP simulation, the neural network in MASS has a prediction error between 1% and 2% [37], but in return it increases the computation speed significantly.

In the case of a simulation of an aircraft configuration with HEP, the HEP model is responsible for providing the gas turbine with a portion of the shaft power that is needed for the required thrust. This portion of the power which is generated by an electric energy source is defined by the hybridization factor  $\phi$  and is illustrated in Figure 3.4.

The electric component masses that have been added by the hybrid engine configuration are determined by the electric components model and are fed back to the aircraft model. The battery mass is divided into two parts, a small part of which is reserved for the shaft power off-takes which is fixed for this aircraft at  $52kW$  per engine. This assumption is retrieved from the Central Reference Aircraft data System (CeRAS) [13]. The remaining large portion of the battery is used for the chosen hybridization portion of the shaft power in the specified flight phase. How the hybridization part of the battery mass is determined can be found in Section 3.2.5. The increasing battery mass due to increasing hybridization forms a constraining factor at high  $\phi$  when the total mass of the aircraft exceeds the Maximum Landing Weight.

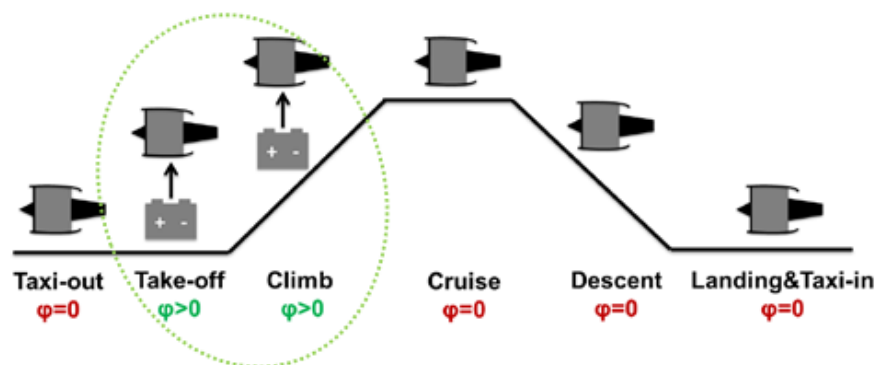


Figure 3.4: Former MASS mission model hybridization capabilities. [37]

### 3.2.2. Mission model extension

The purpose of this research project is to provide insight in the performance of a HEP single aisle aircraft with varying mission parameters and hybridization factors. The mission model of the MASS tool chain described in the previous section is highlighted by a green square in Figure 3.2. The model requires an input file with mission data. This file has to specify the following mission data for several points along the flight:

- Horizontal distance
- Altitude
- Flight velocity
- Flight phase
- Flap angle
- Landing gear status (up/down)

Therefore this mission model of the MASS tool chain requires manual mission alterations due to the many input points. Moreover the mission consists out of six flight phases (taxi, take-off, climb, cruise, descent and landing) which limits the HEP model.

To make the MASS model more suitable for mission assessment, the hybrid-electric aircraft performance tool was extended with a different mission model which allows for automation of the mission alterations. It also allows for more flexibility by permitting a varying hybridization in the previously defined flight phases. The main goals of this updated mission model are:

1. Increase the number of flight phases.
2. Allow for separate hybridization in each phase for a more refined hybridization throughout the mission.
3. Allow for efficient analysis of different missions by decreasing the amount of input data needed to simulate a complete mission.

The input file was reduced to the least required data points for the whole mission, while increasing the refinement of hybridization. This resulted in twelve flight phases instead of six. The first mission model consisted out of fewer flight phases, but it contained more data points for each phase. So even though the number of phases has been increased, the total number of data point have been decreased. For every phase the hybridization factor can be altered. Also a vertical speed  $V_{vert}$  was introduced instead of the horizontal distance parameter  $d_{hor}$ . This allows the cruise length to be adjusted in accordance with the desired range  $R$ .

Table 3.1 shows a summary of the main mission input changes of the new model compared to the former model. Although the mission input data is reduced by a third for the new model, it performs better in terms of thrust peaks compared to the former model. This is due to the addition of dynamic cutback to the new model, which will be elaborated on in the next section.

Table 3.1: Summary of the mission model modifications compared to the former model.

	Former mission model:	New mission model:
<i>Number of data points:</i>	33	12
<i>Number of flight phases:</i>	6	12
<i>Input variables:</i>	$h, V_{flight}, d_{hor}$	$h, V_{flight}, V_{vert}$
<i>Dynamic cutback:</i>	No	Yes

The mission input file has been reduced to the least amount of data points necessary in order to provide a simulation of an A320neo mission. These points correspond to the minimum required flight phases to construct a realistic A320 mission. This information is retrieved from the flight data provided by OpenAP [47], which in its raw data state is not suitable for efficient mission assessments due to the great amount of data points. The updated mission input model consists out of the following twelve flight phases:

- Taxi
- Take-off
- Initial climb
- Climb (3 phases: 2 phases with constant CAS, 1 phase with constant Mach)
- Cruise
- Descent (3 phases: 1 phase with constant Mach, 2 phases with constant CAS)
- Approach
- Landing

### Dynamic cutback

The downside of the great reduction of the amount of data points is the reduction of the fidelity of the mission, which results in sharper rate changes of the mission variables at the transition points between two phases. This leads to unrealistic mission inputs with sudden changes in rate of the flight altitudes and velocities at these locations. In a realistic mission the engine needs time to spool down and therefore the transitions are more gradual. When this time is not taken into account the engine has to instantly provide the increase in velocity which leads to high thrust peaks.

OpenAP smooths these transitions by adding artificial noise to the mission altitudes and True Air Speeds. The noise model which the tool uses is based on a Gaussian (normal) amplitude distribution and is retrieved from ADS-B data (versions 1 and 2) [47]. This added noise also makes the mission more realistic. However, the noise also decreases the computational speed, which is not desired for fast mission modelling. In terms of fuel consumption, the mission with noise does perform similarly to the mission without added noise. The main difference between the two is the lack of smooth transition points in the mission without noise, which leaves the unrealistic thrust peaks.

In order to tackle this problem and smooth out these transition points without having to add Gaussian noise, a dynamic cutback approach has been used. A dynamic cutback simulates the time needed for

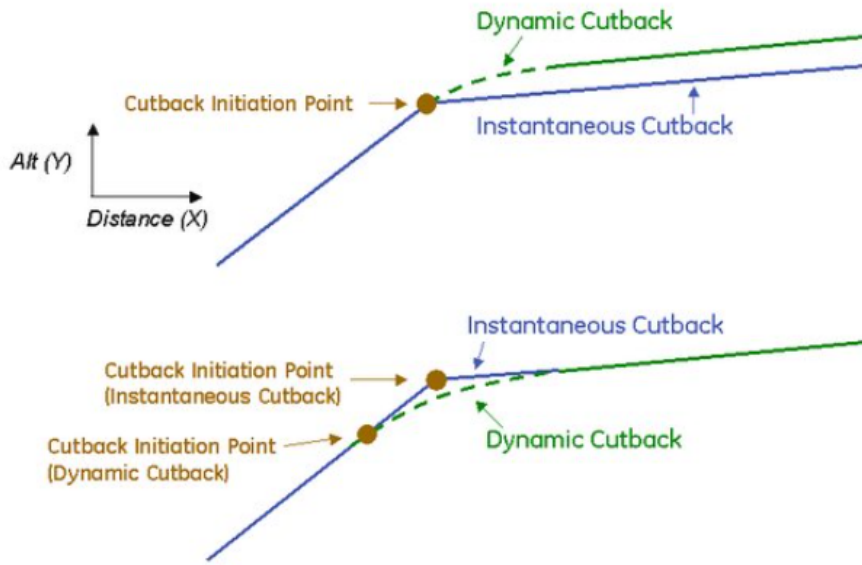


Figure 3.5: Instantaneous cutback versus dynamic cutback. [34]

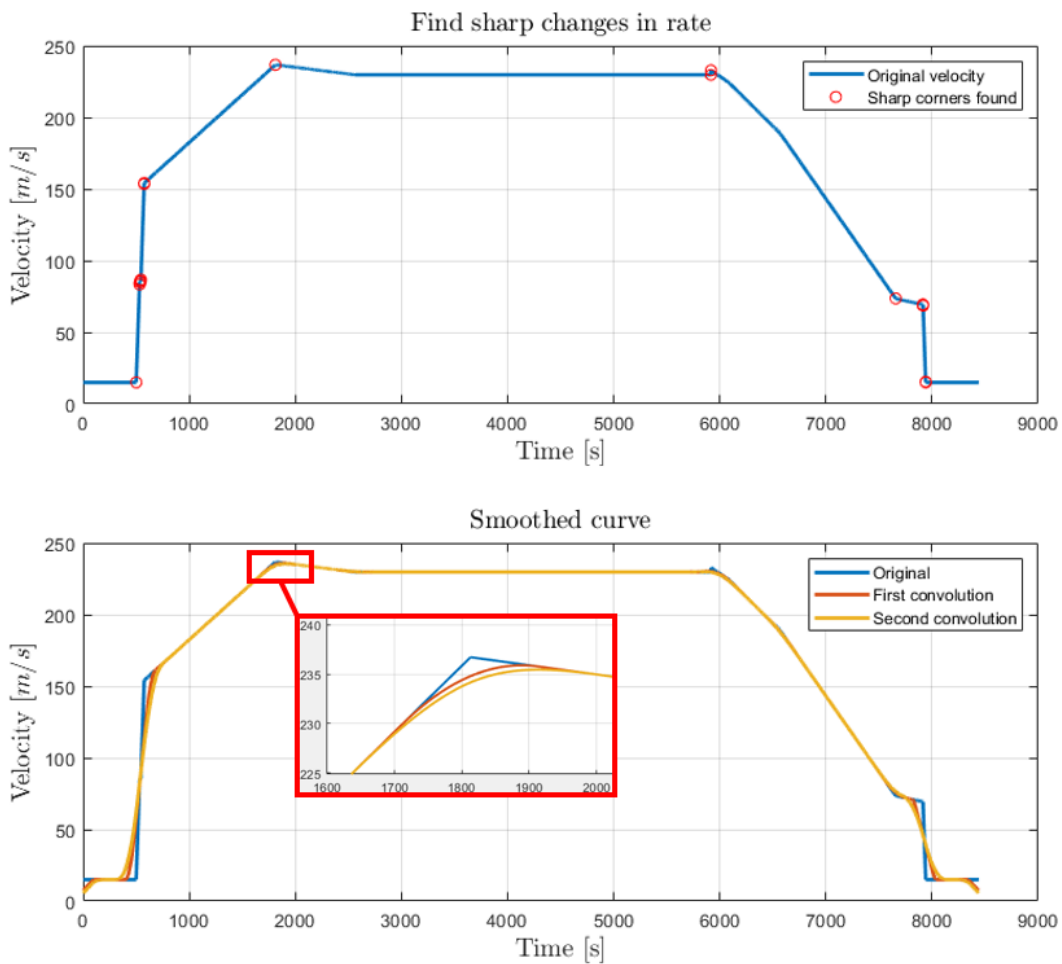


Figure 3.6: Reference flight velocity (CAS) input with dynamic cutback.

engine spool down instead of the instant change in rate. Figure 3.5 shows an example of the two main forms of dynamic cutback for a sudden altitude change. In the first case the dynamic cutback starts at the same location as the instantaneous cutback would. This results in a delay and therefore a slightly higher altitude for this example. In the second case the cutback is initiated before the instantaneous cutback location and this allows it to follow the mission as prescribed. This second form has been implemented in the new mission model for MASS because it does not change the initial mission provided, but only provides a more gradual change from one velocity to the other.

Figure 3.6 shows the velocity versus time plot of the reference A320neo flight. The upper plot depicts the velocity as prescribed by the new input file with twelve flight phases. The locations where a sharp change of rate occurs are shown by a red circle. These are the locations where the second derivative of the mission function is high.

Next a convolution integral is performed twice between the velocity data and a box filter in order to change the shape of the original velocity function. The result of this can be seen in the second plot of Figure 3.6. This approach eliminates the sharp changes in rate of the velocity and flight path angle and therefore it reduces the thrust peaks in the simulation.

### 3.2.3. Engine sizing

An important part of the HEP aircraft configuration is the down scaling of the gas turbines. This is done by scaling down the core mass flow while keeping the fan diameter constant. As a consequence the Bypass Ratio increases. The amount of thrust generated by the engine is determined by the total change in momentum of the air that flows through the engine. Although the bypass flow increases the velocity to a lesser degree than the core flow, the volume of the air through the bypass is much larger for a high bypass engine. The propulsive efficiency of an engine is defined by the part of the mechanical power output that is converted into thrust and is shown in the following equations:

$$\eta_{prop} = \frac{FV_0}{\Delta KE} \quad (3.8)$$

$$F = \dot{m} (V_{exhaust} - V_0) \quad (3.9)$$

$$\Delta KE = \frac{1}{2} \dot{m} (V_{exhaust} - V_0)^2 \quad (3.10)$$

This leads to the following equation for the propulsive efficiency:

$$\eta_{prop} = \frac{2}{1 + \frac{V_{exhaust}}{V_0}} \quad (3.11)$$

An increased Bypass Ratio increases the propulsive efficiency of the engines due to the larger mass flow which bypasses the core of the engine. The equation shows that it is more efficient to



slightly accelerate a larger mass flow instead of a small mass flow that is accelerated more by the core. Downscaling the core and increasing the Bypass Ratio improves the SFC and decreases the mass of the main engines because of the reduced core size.

To scale down the core mass flow, the mass flow and shaft speed scaling parameters  $c_{\dot{m}}$  and  $c_{V_{shaft}}$  from Equation 3.12 and Equation 3.13 are used [37].

$$c_{\dot{m}} = \frac{\dot{m}_{core}\sqrt{\theta}}{D_{core}^2\delta} \quad (3.12)$$

$$c_{V_{shaft}} = \frac{D_{core}^2 N}{\sqrt{\theta}} \quad (3.13)$$

In these equations  $\theta$  is the dimensionless temperature and  $\delta$  is the dimensionless pressure normalized with the ambient sea level temperature and pressure. With the core mass flow  $\dot{m}_{core}$  in  $kg/s$  and the core diameter  $D_{core}$  in  $m$ .

The reduction of the core mass flow results in an increase in shaft speed  $V_{shaft}$  and turbine inlet temperature  $T_{t4}$ . This is due to the smaller engine diameter having to provide a higher rotational velocity in order to achieve the required speed of the blade tips. To allow for the engine to withstand these higher velocities, heavier disks can be used.

The down scaling of the engine is still limited by the  $T_{t4}$ . This temperature constraint originates from material properties of the engines which do not allow for much higher temperatures during edge cases such as take-off in hot climates. However, a fixed  $T_{t4}$  limit has not been found in the literature. Therefore for the purpose of this study it is assumed that the  $T_{t4}$  of the downscaled engine has to be monitored to stay on or below the value of the reference unscaled engines. To prevent the engine from experiencing these higher temperatures, the engine needs to be assisted electrically during the most demanding flight phases.

### 3.2.4. Electric component masses and sizing

For the purpose of this study the electric energy carrier of choice is a battery, which converts stored chemical energy into electrical energy in order to provide power. In hybrid-electric aircraft this energy carrier can be used to provide extra power to the shaft. The specific energy density is the amount of energy that can be stored in an energy carrier per unit mass. This is used to determine the amount of energy that can be stored in for example a battery ( $e_{bat}$ ), fossil fuel ( $e_{fuel}$ ) or fuel cell of a particular mass. The specific power is the amount of power that an electric motor can deliver per unit mass ( $p_m$ ).

In a typical electric powertrain there are several energy conversions that take place. A battery converts chemical energy into electrical energy and an electric motor converts electrical energy into mechanical power. The efficiency of a complete powertrain system decreases with every energy conversion [24].

Figure 3.7 shows an example of a typical turboprop, turbofan, electric and fuel cell drivetrain combined

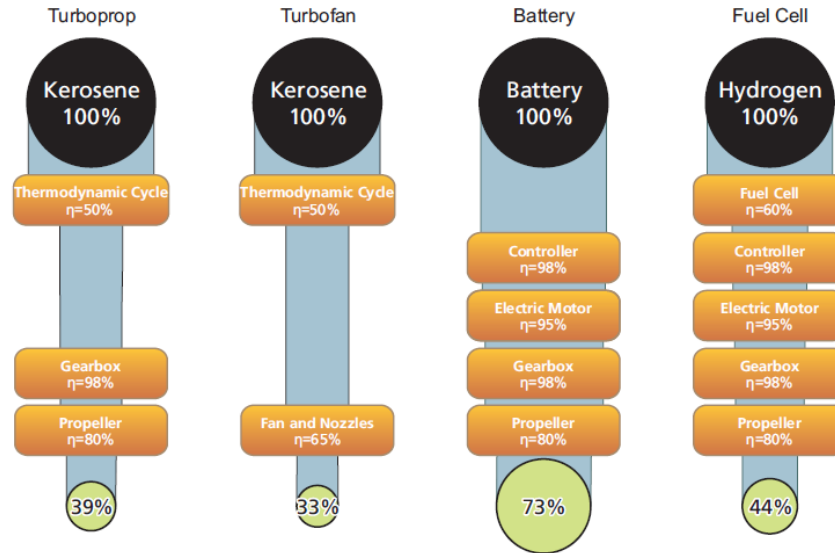


Figure 3.7: Typical efficiency of a turboprop, turbofan, electric and fuel cell drivetrain. Adapted from: Hepperle, 2012 [24]

efficiency. An electric motor has a much higher efficiency than a combustion cycle. However, due to the very low specific energy, batteries tend to become extremely heavy which counteracts the benefit of the high electric system efficiency.

In order to study the relation between the mass of the added electric powertrain and the hybridization factor  $\phi$ , the electric equipment scenario that has been used is the technology level of EIS2030. This translates to a battery specific energy of  $500Wh/kg$ . The specific power of the electric motor and the power inverter is  $7.5kW/kg$ . A separate cable mass is neglected in this study because it is assumed that this is included in the specific power values of the electric motors and power electronics. Furthermore the following equipment efficiencies have been used.

$$\eta_{EM} = \eta_{Inv} = 0.95 \quad \text{and:} \quad \eta_{Bat} = 0.925 \quad (3.14)$$

As mentioned in the previous chapter, the battery mass is divided into two parts, a of which a small part is reserved for the shaft power off-takes. This portion of the battery is fixed for this aircraft at  $52kW$  per engine [13]. The other bigger part of the battery is used for the chosen hybridization portion of the shaft power in the specified flight phase. The hybridization part of the battery mass is determined by the following equation:

$$m_{bat,\phi} = \frac{E_{shaft}\phi}{e_{bat}} \quad (3.15)$$

Here  $E_{shaft}$  is the shaft energy,  $\phi$  is the hybridization factor and  $e_{bat}$  is the battery specific energy. The increasing battery mass with increasing hybridization forms a constraining factor at high  $\phi$  when the total mass of the aircraft exceeds the MLW.

For the sizing of the electric equipment first the peak power and energy are determined in MASS

during a reference run. This is done for the reference aircraft without hybridization. Based on this data the sizing of the electric equipment was determined by calculating the portion of the power that has to be delivered by the battery according to the hybridization factor that was chosen for the different flight phases. This in turn increases the mass of the aircraft. The hybrid-electric aircraft is then reevaluated in the aircraft and engine model and provides a new power requirement. MASS uses an iterative model until the aircraft operating empty mass change is negligible.

### 3.2.5. Aircraft sizing

Figure 2.14 in Section 2.7 shows the mass breakdown of the reference A320neo. In this study the Design Payload is based on a flight with 150 passengers which contribute  $106kg$  of weight each<sup>1</sup>. For the hybrid-electric A320neo there will be weight added by the battery and the necessary electric equipment such as the electric motor and power electronics. Due to hybridization the fuel weight will be decreased compared to the reference. However, the operating empty mass of the aircraft will increase because the increase in battery mass is significantly higher than the fuel reduction due to hybridization. Because the aircraft will not be redesigned in this study, the MTOW and MLW are hard constraints due to the engine characteristics and the load restrictions. This means that an increased hybridization will be at the cost of the Payload.

## 3.3. Reference mission and validation

As mentioned before in Section 3.2.2, the choice was made to change the reference mission originally present in MASS. In this section three different missions will be discussed:

- The original mission from MASS based on an Airbus document containing general mission parameters. This mission is assessed using MASS [4]
- The mission from OpenAP which is used as a basis for the new reference mission. This mission is assessed using OpenAP [47]
- The new reference mission based on the mission from OpenAP including dynamic cutback which is discussed in Section 3.2.2. This mission will be used as a reference for this thesis report. The mission is assessed using MASS

The simulations for the A320neo in this study are based on a reference mission retrieved from the OpenAP [47]. OpenAP is an open-source aircraft performance tool which contains aircraft surveillance data for the A320. The available data consists out of upper and lower limits for the various velocities, altitudes and ranges out of which the average has been used as a basis of the reference mission. The main differences between the mission from Airbus and the mission from OpenAP are:

---

<sup>1</sup>A conservative passenger weight estimation based on an average passenger of  $91kg$  [13] and  $15kg$  of hand and hold luggage.

- The OpenAP mission contains information on altitude, velocity and the flight path angle. The Airbus mission contains information on altitude, velocity and range.
- The OpenAP mission is based on a realistic A320 flight whereas the Airbus mission is based on general Airbus mission characteristics.

For this thesis the choice was made to change the original mission. There are three main reasons for this change. The first reason is that it is preferred to utilize a mission which is closest to a real mission flown by an A320. The second reason is that the original mission contained the range as an input for every flight data point. This was not desired as it needed to be reevaluated for every point when the velocities would be changed during the assessments. This leads to the third reason which is the fact that the mission input file was too extensive to utilize for fast assessments. Therefore the choice has been made to change the original mission.

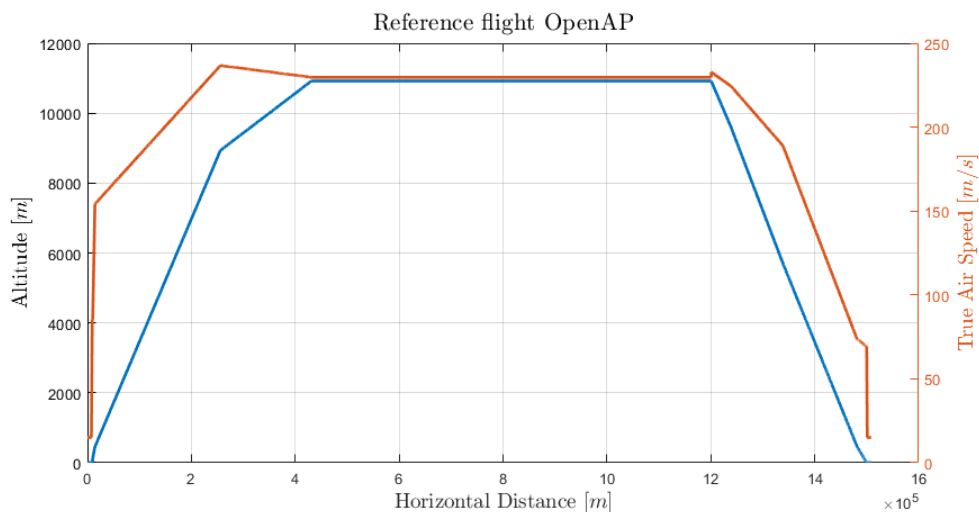


Figure 3.8: Original reference flight from OpenAP without Gaussian noise.

Figure 3.8 shows the reference flight retrieved from the data in OpenAP. This mission has a range of  $1500\text{km}$  and a cruise altitude of  $35827\text{ft}$ . The mission data also consists out of twelve main flight phases. The velocity plot shows the sharp changes in rate discussed in Section 3.2.2. OpenAP deals with these sharp changes by adding artificial Gaussian noise to the whole mission. Although this is also a good way to simulate a more realistic mission, it will increase the computation time. This is not desired for mission assessment when a big part of the mission parameters have to be sampled.

Therefore, in Section 3.2.2 the choice has been made to add dynamic cutback to the OpenAP mission shown in Figure 3.8. The original OpenAP mission and the new mission containing dynamic cutback have been compared. The original mission was evaluated using OpenAP and the new mission was evaluated using MASS. OpenAP is based on the CFM56-5B4 engine and MASS is based on the LEAP engine.

To validate the new mission and to show the differences between the original and the new mission model, a comparison has been made. The results are shown in Figure 3.9 and 3.10. The straight lines

Table 3.2: Reference mission characteristics

		<b>MASS new:</b>	<b>OpenAP orig.:</b>	<b>MASS orig.:</b>
Maximum turbine inlet temperature:	$T_{t4,max}$	1851K	-	1771K
Total fuel burn:	$W_{fuel}$	4998kg	-	4703kg
Thrust peak:	$F_{max,TO}$	196.9kN	200.8kN	171.7kN
Fuel flow at cruise:	$FF_{cruise}$	0.594kg/s	0.594kg/s	0.608kg/s
Specific Fuel Consumption at cruise:	$SFC_{cruise}$	0.0154g/N · s	-	0.0155g/N · s

depict the original mission characteristics and the dotted lines show the new mission model which is based on an A320 mission from OpenAP. The range of both missions is 1500km. The new mission is used as a starting point for the mission assessment in this thesis report. One of the main differences between the two missions is the length of the cruise phase. This phase is shorter for the new mission. Another difference is the effect that the dynamic cutback has on the mission performance. In Figure 3.9 the fuel flow shows no jumps in the new mission compared to the original one. Also in Figure 3.10 one can observe from the thrust plot that the new mission simulates engine spool down while the original mission shows instant changes in thrust. The same can be observed in the flight path angle plot.

A couple of important mission characteristics corresponding to the three missions are shown in Table 3.2. For the value of the thrust peak at take-off there is a small difference between the evaluation in OpenAP and MASS. The fuel flow at cruise is the same for the new mission and the OpenAP mission, which is surprising as the two models are based on different engines. For the Specific Fuel Consumption during cruise the original mission and the new mission in MASS are very close. The values also lay within the typical range for the LEAP engine found in the literature, which is between 0.0150g/N · s and 0.0159g/N · s [39].

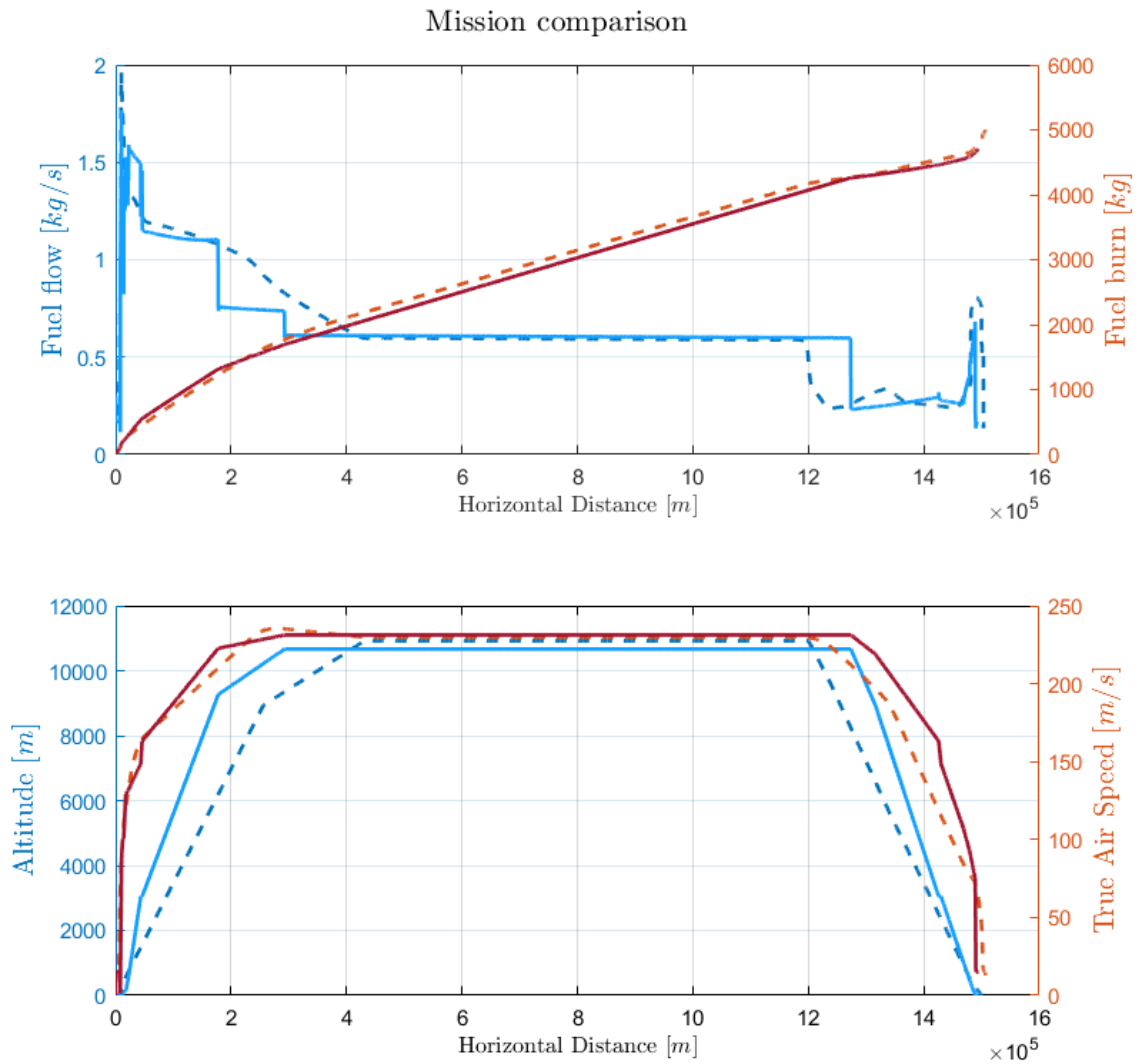


Figure 3.9: Reference flight characteristics of an A320 mission from Airbus [4] (straight line), compared to the new mission based on data from OpenAP (dotted line). This figure shows the fuel flow, fuel burn, altitude and velocity. The reference flight range is 1500km.

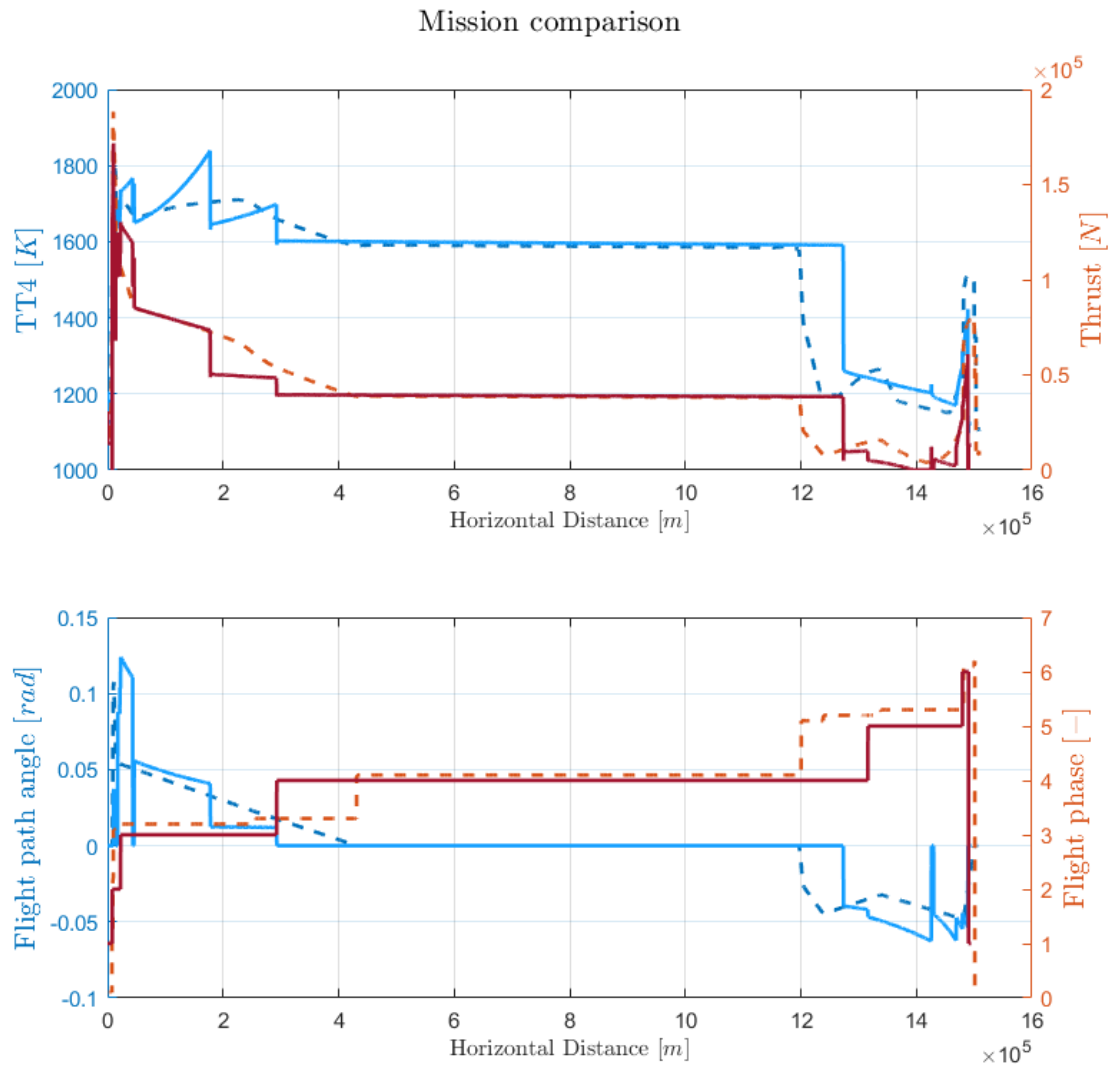


Figure 3.10: Reference flight characteristics of an A320 mission from Airbus [4] (straight line), compared to the new mission based on data from OpenAP (dotted line). This figure shows turbine inlet temperature, the thrust, the flight path angle and the flight phase. The reference flight range is 1500km.





# 4

## Mission analysis results

In the previous chapter the methodology of this research project has been stated. This chapter provides the results of the mission assessment. These results are obtained by changing the previously stated mission variables: altitude, velocities, hybridization and range. The analyses in this report focus on the take-off phase, the three climb phases and the cruise phase. The objective is obtain knowledge about the mission which best suits a hybrid-electric single aisle aircraft. All results found in this section have been assessed in MASS, extended with the new mission model. The new mission provided in Figures 3.9 and 3.10 (dotted line) has been used as a reference and starting point. This mission is based on mission data retrieved from OpenAP [47]. As mentioned in the previous chapter, hybridization  $\phi$  is used to electrically provide part of the shaft power during a specified flight phase. During the take-off phase,  $\phi_{TO}$  is mainly used to regulate the main engine's temperature due to engine core and Bypass scaling. Furthermore, this chapter will provide information on varying the initial climb hybridization  $\phi_{IC}$ , the climb hybridization  $\phi_{cl1}$  and  $\phi_{cl2}$  for respectively the first and second main climb phases and  $\phi_{CR}$  for the cruise phase. For the purpose of this study, only the previously mentioned flight phases will be analyzed. The descent phase will be disregarded due to it mostly being operated at idle. Regulations prohibit turning off the engines during any phase in flight.

The results that will be addressed in this chapter are:

- The effect of engine scaling and the need for electrically assisting the engine
- The distribution of the electric component masses
- A sensitivity analysis of the take-off phase, the climb phases and the cruise phase

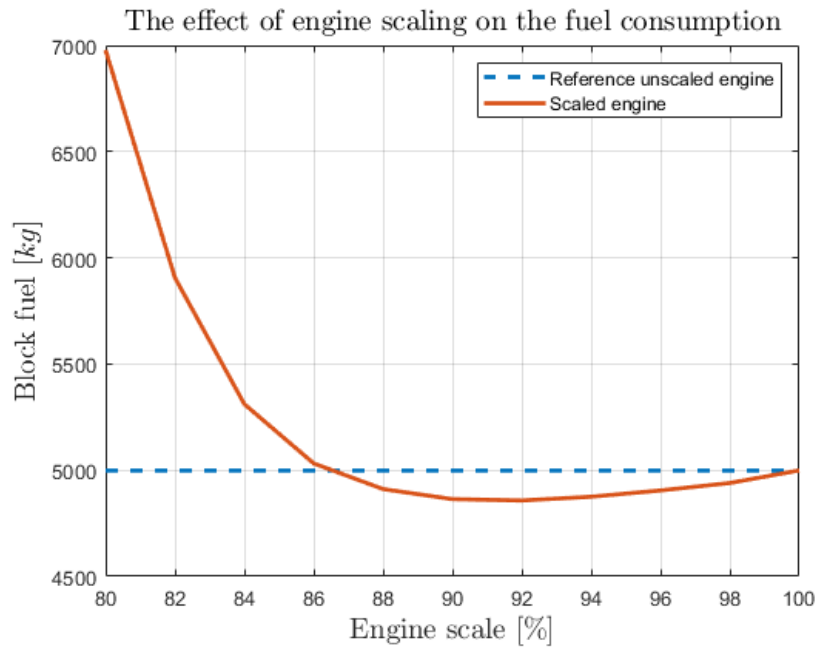


Figure 4.1: The effect of engine scaling alone on the block fuel without electric assistance. These results are not feasible without electric assistance due to the increased  $T_{t4}$

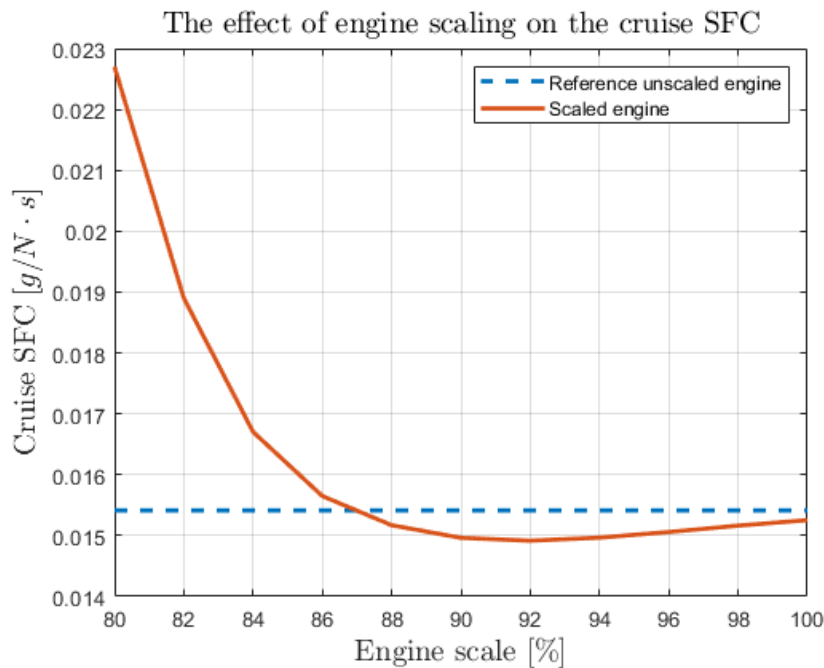


Figure 4.2: The effect of engine scaling alone on the cruise SFC without electric assistance. These results are not feasible without electric assistance due to the increased  $T_{t4}$

## 4.1. Effect of engine scaling and need for hybridization

As mentioned in Section 3.2.3, down scaling of the core of the main internal combustion engines and increasing the Bypass Ratio improves the propulsive efficiency of the engines. In this section the down scaling of the core and the increase in Bypass Ratio will be referred to as 'down scaling'. Figures 4.1

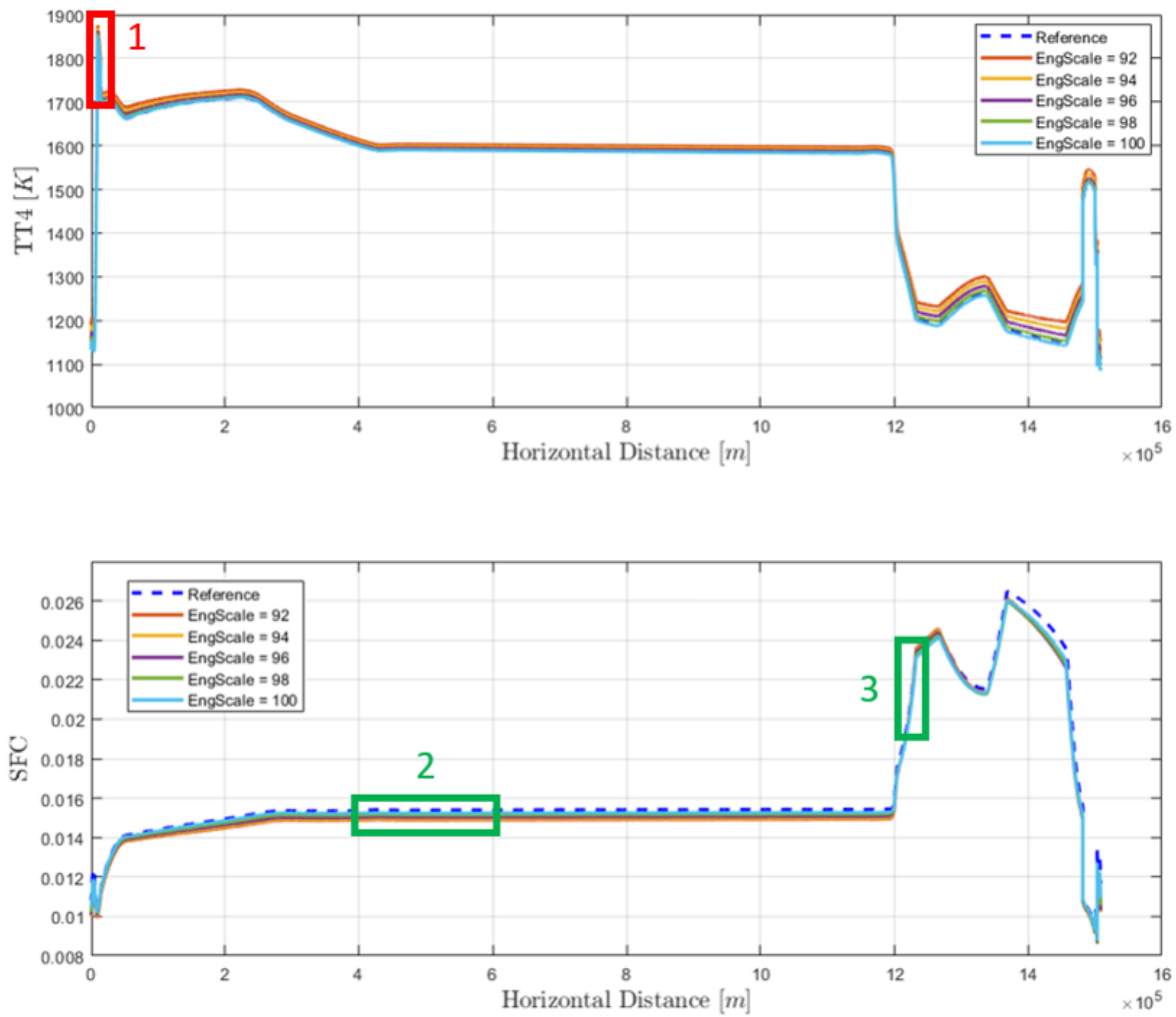


Figure 4.3: Reference flight engine scaling effect on  $T_{t4}$  and SFC [ $g/N \cdot s$ ].

and 4.2 show the effect of engine scaling alone on the block fuel and the cruise SFC without electric assistance. For the reference mission, scaling down the core of the engines to approximately 92% reduces the block fuel by 2.8%. This corresponds to an increased Bypass Ratio of 12.1. When the engine size is reduced further the fuel consumption starts to increase rapidly and the engine becomes very inefficient.

Reducing the size of the core of the main engines has an impact on the turbine inlet temperature as mentioned in Section 3.2.3. Therefore these results are not feasible without electrically assisting the engines. In the case of the reference A320 mission depicted in Figure 3.10, it is determined that the highest thrust requirement is during take-off. This is also where the turbine inlet temperature  $T_{t4}$  peaks at  $T_{t4,max} = 1851K$ . A fixed  $T_{t4}$  limit has not been found in the literature for the LEAP engine, so as mentioned before in Section 3.2.3, for the purpose of this study it is assumed that the  $T_{t4}$  of the down scaled engine must stay on or below the value of the reference unscaled engines.

The effects of engine scaling on the turbine inlet temperature without hybridization is shown in Figure 4.3 for the whole mission. A closeup of the parts marked by the squares can be found in Figures 4.4

and 4.5. Figure 4.4 depicts a closeup of the take-off phase. The figure shows the reference  $T_{t4}$  which is 1851K. For the engine scale of 100% the model does not exactly match the reference aircraft's  $T_{t4}$  and SFC due to the addition of an initial battery mass to provide electric energy for the power off-takes. The figure shows that the  $T_{t4,max}$  increases with decreased engine scale. This means that the electric assistance of the take-off phase is always necessary when scaling the main gas turbines down, in order to decrease the turbine inlet temperature to match the reference peak temperature. The SFC during take-off shows an increase in efficiency when the engines are scaled down, which is as expected due to the increased propulsive efficiency explained in the previous chapter.

Figure 4.5 shows a closeup of the beginning of the cruise phase (2) and the beginning of the descent phase (3). During cruise the efficiency of the engines show the same trend as seen before at the take-off

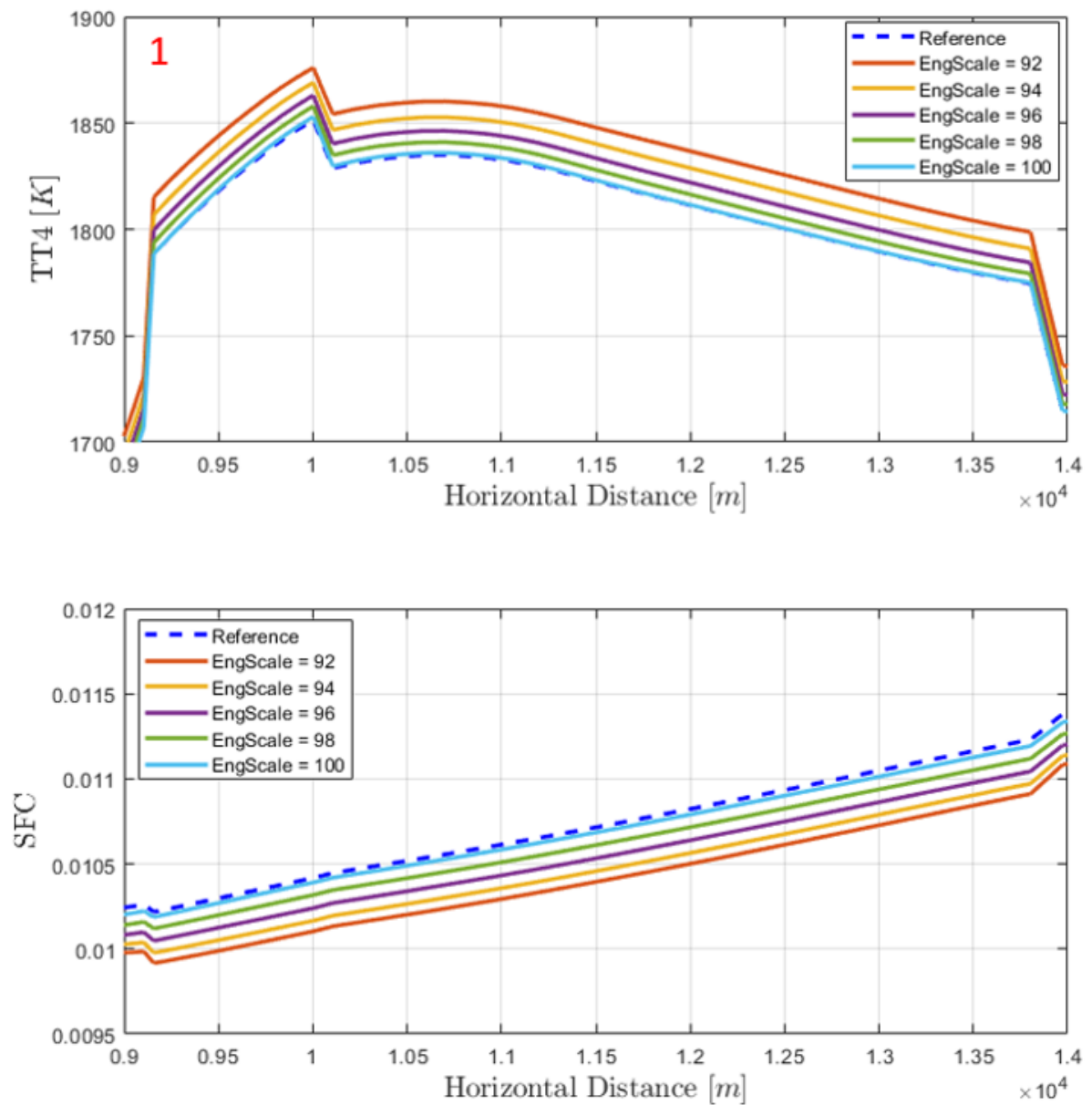


Figure 4.4: 1: Engine scaling effect on  $T_{t4}$  and SFC [ $g/N \cdot s$ ]. Closeup of the take-off phase.

phase, a decrease of SFC for smaller engines. However, this is not the case for the whole flight. During descent this trend flips and the smallest engine scale of 92% becomes the least efficient. This means that when the engine is idling, a downsized engine is less efficient than a full size engine. This is due to the low mass flow that passes through the core when the engine is at idle thrust. Therefore it is harder for the downsized engine to provide the shaft power required to drive the fan.

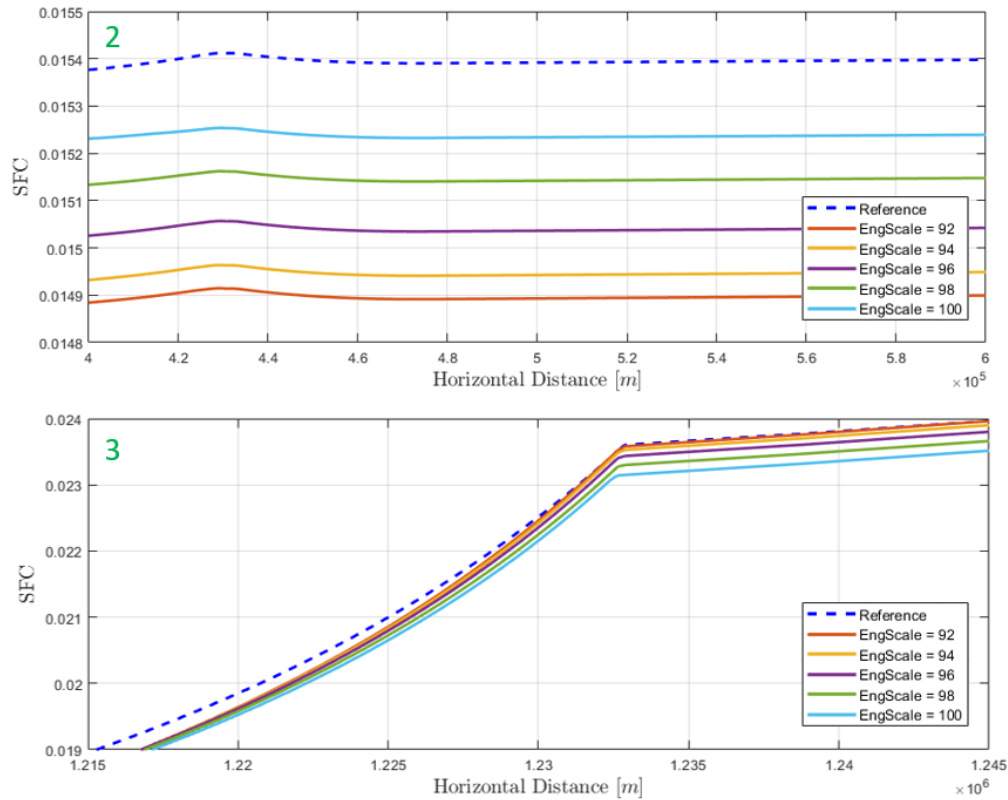


Figure 4.5: Engine scaling effect on the SFC. (2) Closeup of the beginning of the cruise phase. (3) Closeup of the beginning of the descent phase.

### Correcting for Turbine Inlet Temperature

In order to decrease the turbine inlet temperature at the peak value during take-off, this phase needs electric assistance. In this section there will be an analysis of the electric assistance that is needed in order to decrease the  $T_{t4}$  to meet the reference peak temperature of  $1851K$  for an engine scale of 92%. From analysis it was found that only assisting the take-off phase was not sufficient to decrease the peak. While the take-off peak temperature decreased, the added battery mass caused the temperatures of the initial climb phase to increase beyond the value of  $1851K$ . Therefore also the initial climb phase needed to be assisted.

Figure 4.6 shows the  $T_{t4}$  peak of take-off and the initial climb phases. The engine scale is kept at a constant value of 92%. The constant hybridization factor lines show the  $\phi_{TO}$  and the  $\phi_{IC}$ . The figure shows that a  $\phi_{TO} = \phi_{IC} = 0.04$  is sufficient to keep the peak temperature from exceeding the reference peak of  $1851K$ . The corresponding change in take-off and initial climb Specific Fuel Consumption (SFC) decreases slightly over these two electrically assisted phases, but in terms of fuel burn this small

section does not have an effect on the total fuel burn of the mission.

An important note is that this analysis was done without hybridizing any of the other flight phases. When this will be the case in the next sections, the battery mass will increase and therefore this also increases the  $T_{t4,max}$ . This means that the electrical assist of the take-off phase needs to be increased as well.

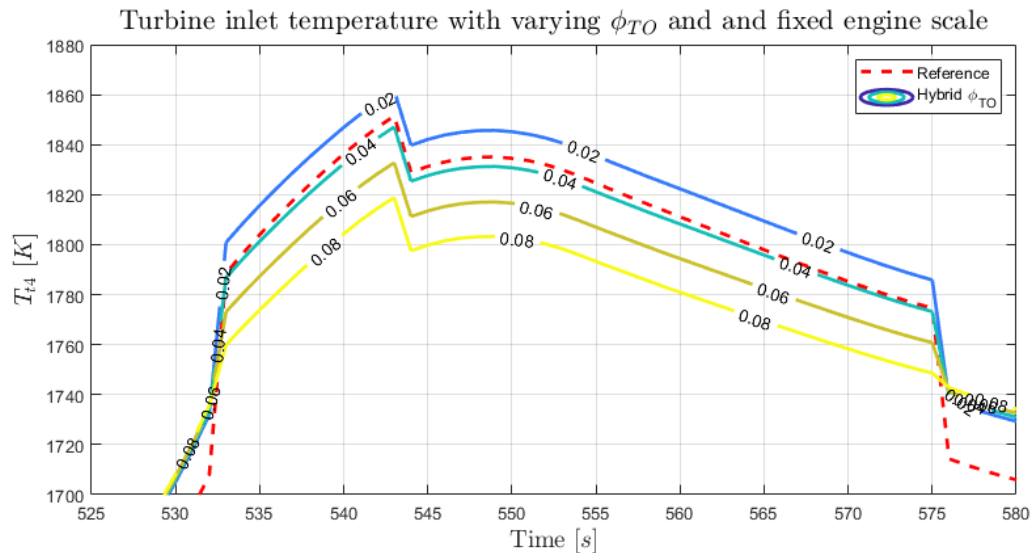


Figure 4.6: The effect of electrically assisting the take-off phase with  $V_{TO} = 85m/s$  in order to decrease the turbine inlet temperature  $T_{t4}$  of the scaled engine (92%).

## 4.2. Electric component masses

When the aircraft is electrically assisted, the electric components add mass to the original Operational Empty Weight (OEW). As previously mentioned in Section 3.2.5, this will be at the expense of the Payload if the MLW is exceeded during a hybrid-electric mission.

Figure 4.7 depicts the mass distribution of the electric equipment with increasing take-off hybridization  $\phi_{TO}$ . The figure shows that the power inverter mass, the electric motor mass and the battery mass are correlated linearly with the increase in hybridization. One should note that this figure only shows the masses for varying  $\phi_{TO}$ , which is a small portion of the mission. This means that when other parts of the flight are also electrically assisted, the hybridization portion of the battery mass can be significantly greater than the power off-takes part of the battery mass. This leads to the battery mass becoming a constraint at high  $\phi$  when the total mass of the aircraft at landing exceeds the MLW.

The following observations can be made:

- The total electric system mass increases linearly with  $1455kg$ , for every increase in  $\phi_{TO}$  of  $0.1$ .
- The total battery mass increases linearly with  $134.5kg$ , for every increase in  $\phi_{TO}$  of  $0.1$ .

Figure 4.8 shows the mass breakdown of the A320neo. The MLW is not depicted in this figure, which is  $67400kg$ . For every step of  $\phi_{TO} = 0.1$ , the original OEW of the aircraft increases by  $3.43\%$ .

Simultaneously the fuel load will decrease. This means that even for  $\phi_{TO} = 1$ , the MLW will not be exceeded. However, there will be almost no Payload left. This of course is a very drastic example. For the remainder of the results, the hybridization values will be much lower and the MLW will always be monitored to prevent losing too much Payload or assessing infeasible flight results.

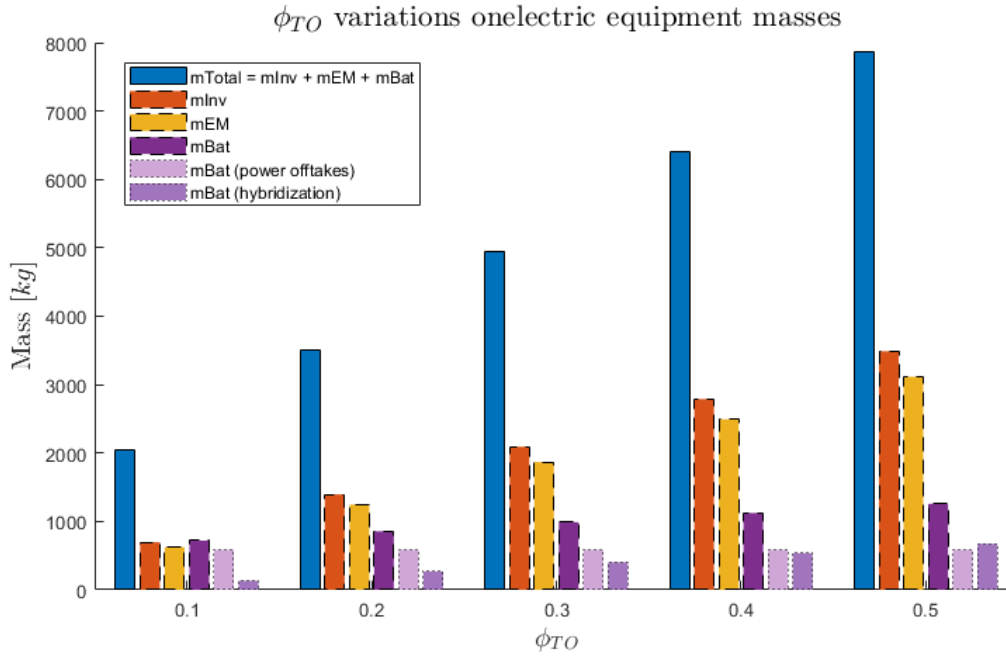


Figure 4.7: The effect of hybridization on the electric equipment masses: the inverter, the electric motor and the battery mass. The battery mass is divided into the fixed offtakes part and the varying hybridization part.

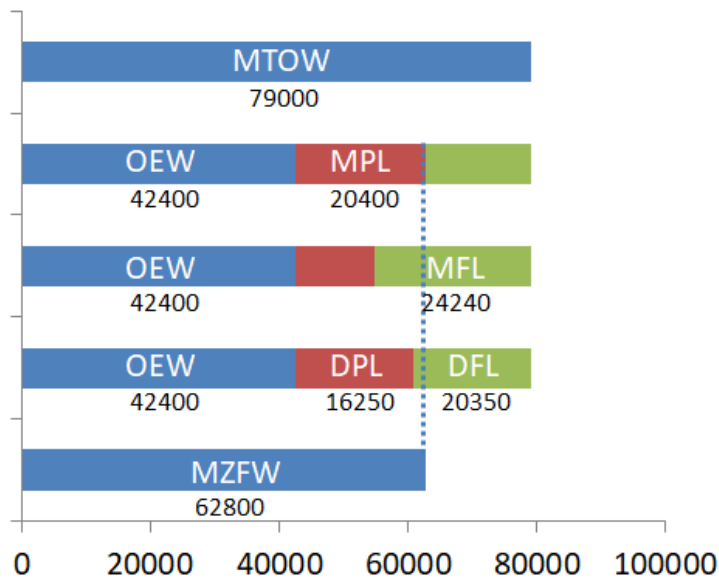


Figure 4.8: Mass breakdown of the A320neo. The horizontal axis depicts the mass in kg. Legend: Max. Take-Off Weight (MTOW), Operational Empty Weight (OEW), Max. Zero-Fuel Weight (MZFW), Max. Payload (MPL), Max. Fuel Load (MFL), Design Payload (DPL), Design Fuel Load (DFL). Data retrieved from: [7] [32] [35]. Repetition of Figure 2.14

### 4.3. Sensitivity analysis of the flight phases

The previous sections showed that the turbine inlet temperature  $T_{t4}$  and the MLW are two constraining factors for the analysis performed in this study. This section shows the results of the sensitivity analysis of varying the mission parameters during the different flight phases. The take-off phase analysis was focused on lowering the peak  $T_{t4}$  to meet the requirements for a down-sized engine. The focus of the analysis of the climb and the cruise phase will be to decrease the fuel and energy consumption and emissions by varying the mission velocities, altitudes and power split. As mentioned earlier, the descent phase will not be included in this report due to it mostly being operated at idle. It is expected that there is not much space for improvements during this phase, because safety regulations do not allow for turning off the engines.

#### 4.3.1. Take-off phase analysis

In Section 4.1 it was determined that an engine scale of 92% yields the highest overall fuel efficiency for the whole reference flight. However, this also caused an increase in the turbine inlet temperature  $T_{t4}$  which is not desired during the peak power requirement phase.

##### Sensitivity of Velocity and Hybridization factor

Figure 4.9 shows the effect of changing the take-off velocity and the take-off hybridization factor on the block fuel of the entire mission. The take-off velocity itself does not seem to have an impact on the total fuel consumption due to the very short phase and the very slight changes in velocity. Furthermore, the figure shows that increasing the  $\phi_{TO}$  also increases the block fuel due to the increasing battery mass. This shows that it is necessary to only assist the take-off phase to match the reference  $T_{t4}$  and

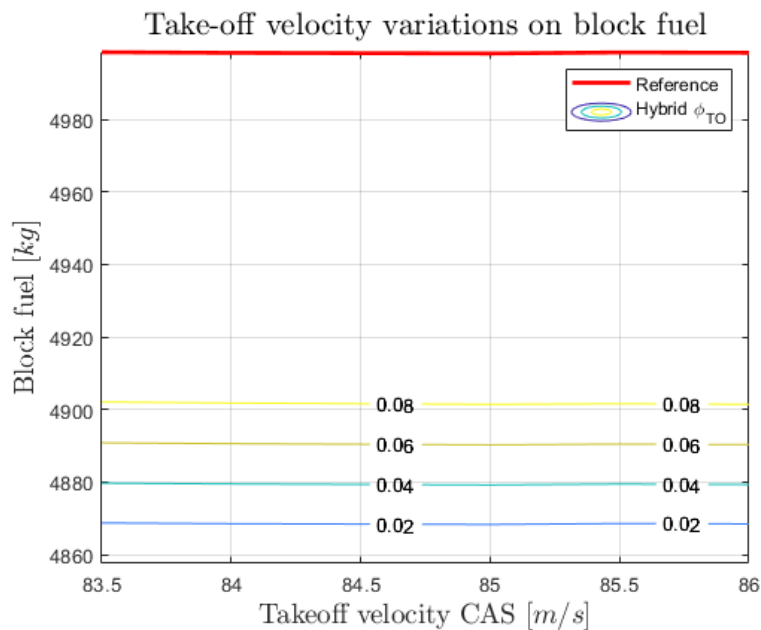


Figure 4.9: Effect of the take-off velocity and  $\phi_{TO}$  variations on the total block fuel of the entire mission.



to not increase the  $\phi_{TO}$  beyond that value. For this reference mission,  $\phi_{TO} = 0.04$  is sufficient, which leads to an overall fuel saving of 2.38%. This is lower than the 2.8% achieved with engine scaling only. However, engine scaling without electrically assisting the take-off phase where the peak  $T_{t4}$  exceeds the reference maximum  $T_{t4}$  value is not considered feasible. Solely assisting the take-off phase to decrease the peak temperature of a scaled engine therefore has a positive impact on the total fuel efficiency of the mission.

### 4.3.2. Climb phase analysis

After the take-off and initial climb phase, there are two climb phases. The first is the constant CAS-climb phase and the second is the constant mach-climb phase. In this section these phases will be referred to as 'climb 1' and 'climb 2'. Figure 4.10 shows the two climb phases for the reference flight, where climb 1 starts at an altitude of 1500ft (457.2m) and climb 2 starts at 29314ft (8934.9m) and ends at cruise 35827ft (10920m). For both phases the hybridization  $\phi_{CL}$  and the climb velocity  $V_{CL}$  will be assessed separately. Also the peak turbine inlet temperature will be monitored in order to find feasible results.

In this section the hybridization and the climb velocity of the specified climb phase are varied. For the figures in this section the climb hybridization has been varied between  $\phi = 0.02$  and  $\phi = 0.2$ . For both phases the block fuel, total energy consumption and the emissions will be analysed in order to assess the mission performance. The emissions that will be analysed in this section are the  $NO_x$ , the unburnt hydrocarbons  $UHC$  and the carbon monoxide  $CO$ .

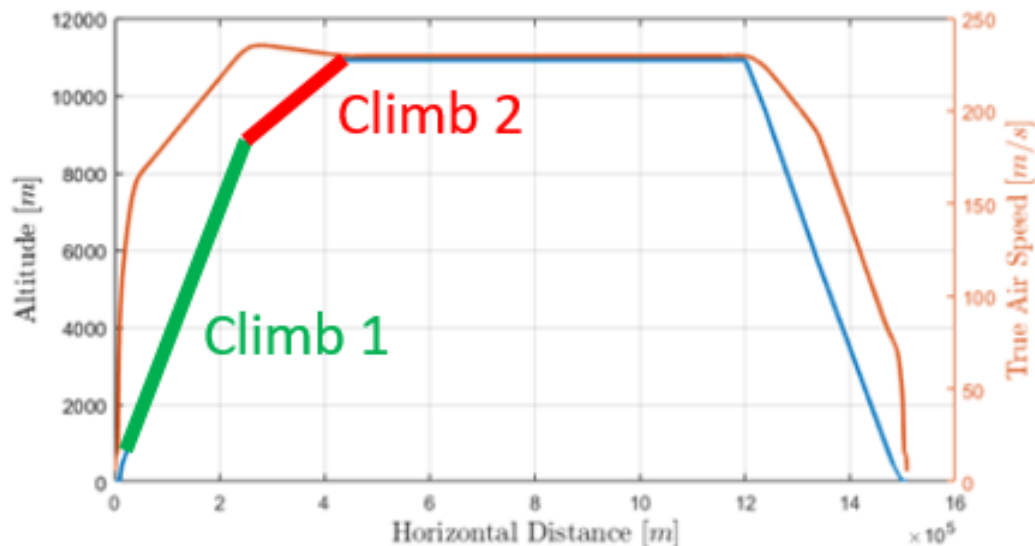


Figure 4.10: Climb 1 and climb 2 phases.

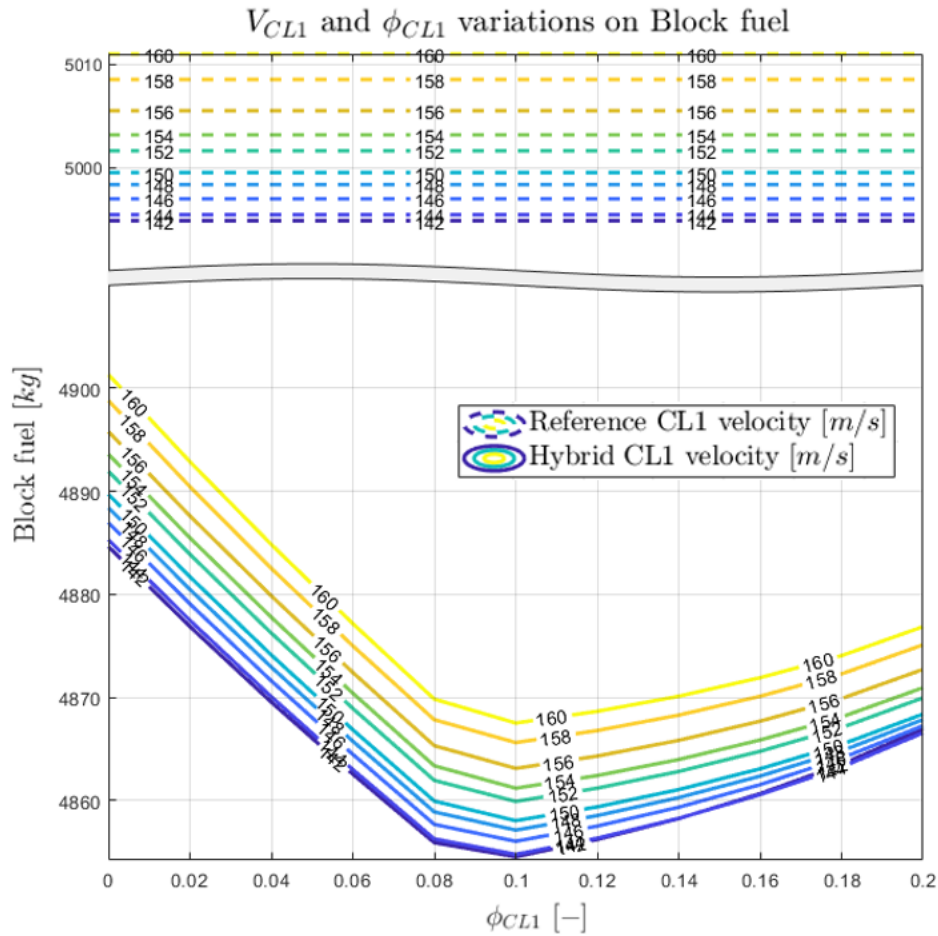


Figure 4.11: Effect of the climb1 velocity (CAS) and  $\phi_{CL1}$  variations on the block fuel. With take-off hybridization  $\phi_{TO} = 0.06$  and Engine Scale is 92%.

### Climb 1: Sensitivity of Velocity and Hybridization factor

In the previous sections it was determined that the  $\phi_{TO} = 0.04$  was sufficient for the reference mission with a scaled engine. However, this is not the case when an additional flight phase is electrically assisted due to the added battery weight. With  $\phi_{CL1} = 0.10$  and  $\phi_{TO} = 0.04$  a fuel reduction of 2.80% can be achieved but this leads to a turbine inlet temperature of 1858K which is higher than the reference. From the analysis of these missions it was found that a  $\phi_{TO} = 0.06$  leads to the highest gain without exceeding the  $T_{t4}$ . This leads to a block fuel reduction of 2.80% at  $\phi_{CL1} = 0.1$ . This is 0.42% higher than the reference aircraft with only a scaled engine.

$V_{CL1}$  is the first climb phase that will be analysed. The mission performance for varying this climb 1 velocity will be shown in the next figures. Figure 4.11 shows the block fuel for different climb velocities. In terms of block fuel consumption  $\phi_{CL1} = 0.1$  yields the highest difference between the reference and the hybrid-electric aircraft. When the hybridization is increased further, the weight of the battery starts to make the overall aircraft less fuel efficient. This is due to the increased mass than has to be carried during the cruise phase. Reducing the climb 1 velocity further than 142m/s does not yield a higher fuel saving.

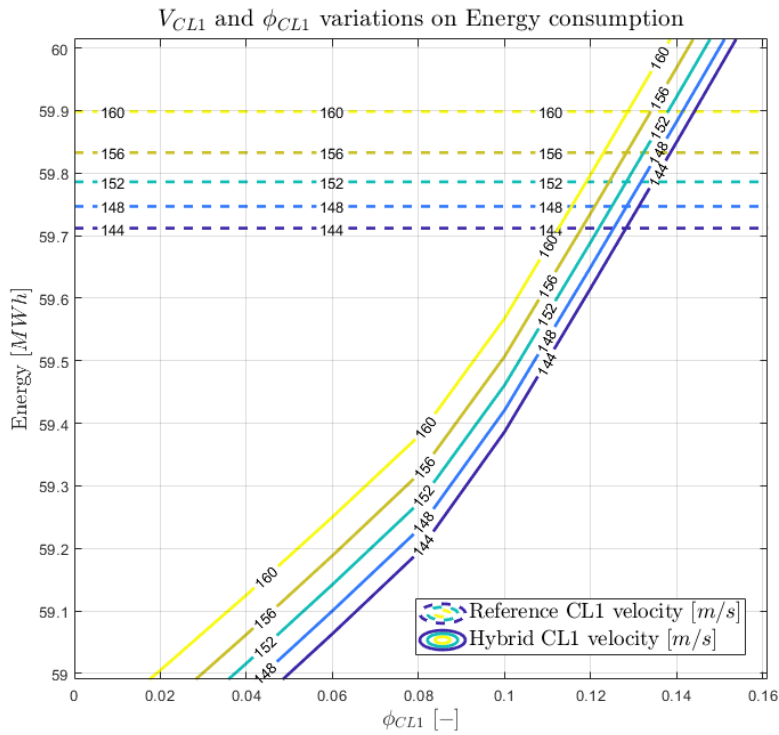


Figure 4.12: Effect of the climb1 velocity and  $\phi_{CL1}$  variations on the total energy consumption. With take-off hybridization  $\phi_{TO} = 0.06$  and Engine Scale is 92%.

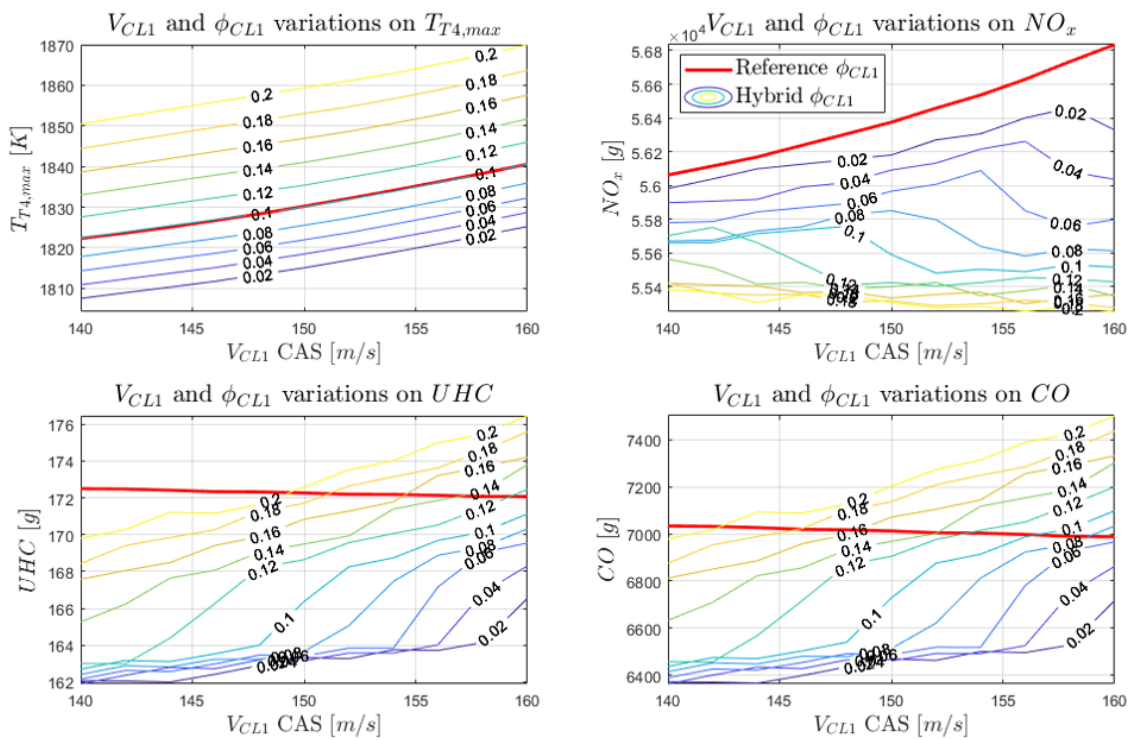


Figure 4.13: Effect of the climb1 velocity and  $\phi_{CL1}$  variations on the  $T_{t4}$  peak and the emissions. With take-off hybridization  $\phi_{TO} = 0.06$  and Engine Scale is 92%.

Figure 4.12 shows the energy consumption for the entire mission. The coloured lines in the graph depict the changing climb 1 velocity. The dotted lines correspond to the reference mission. The figure shows that for the  $\phi_{CL1} = 0.1$ , the energy consumption for all the velocities is lower than the reference. This corresponds to an energy reduction of 0.55% at climb 1 velocity  $V_{CL1} = 142m/s$ .

Figure 4.13 consists out of four plots. Please note that these graphs depict  $\phi$  in the contour plot instead of the velocity, which was the case in the previous figures. For these figures this was done to increase the readability. The first plot shows the  $T_{t4,max}$  where the reference aircraft's maximum turbine inlet temperature is depicted with a red line. At the previously mentioned hybridization  $\phi_{CL1} = 0.1$  where the block fuel was at its minimum, the figure shows that the  $T_{t4,max}$  is the same as the reference aircraft. This temperature increases with increased climb 1 velocity and increased  $\phi_{CL1}$  due to the added battery weight.

The second plot shows that the  $NO_x$  production increases for the reference aircraft with increased climb 1 velocity. For the hybrid-electric aircraft, this trend is also visible, although for higher  $\phi_{CL1}$  values than 0.1 it looks like there is an optimum and the  $NO_x$  does not decrease further. The increased battery weight causes the  $NO_x$  to increase its production during the cruise phase, which eliminates the decrease in  $NO_x$  during the assisted climb 1 phase. For  $\phi_{CL1} = 0.1$  and  $V_{CL1} = 142m/s$  the  $NO_x$  production decreases with 0.8% for the whole mission.

The third and the fourth plots show the unburnt hydrocarbons  $UHC$  and the carbon monoxide  $CO$  production for the entire mission. These variables show an opposite trend to the  $NO_x$ . These emissions are increasing when the hybridization is increased. This effect was explained in Section 2.1.

### **Climb 2: Sensitivity of Velocity and Hybridization factor**

The second climb phase  $V_{CL2}$  that will be analysed is the Mach climb phase, which will be called climb 2 in this section. Like in the previous climb phase, also this phase is assisted electrically during take-off with  $\phi_{TO} = 0.06$ . Figure 4.14 depicts the block fuel consumption over the mission for varying  $V_{CL2}$  and  $\phi_{CL2}$ . The minimum block fuel is found at  $V_{CL2} = 124m/s$ . Decreasing the Mach climb velocity beyond this value does not lead to an improvement in the fuel consumption. The corresponding hybridization is  $\phi_{CL2} = 0.14$ . At this point the block fuel is decreased by 2.49% compared to the reference aircraft. This phase has a lower impact on the total block fuel compared to the first climb phase due to it being a shorter phase.

Figure 4.15 shows the energy consumption which also is at its minimum for a climb 2 velocity of  $V_{CL2} = 124m/s$ . For the previously found hybridization  $\phi_{CL2} = 0.14$  where the block fuel was at its lowest, the energy savings are 0.98%. In terms of energy consumption, the highest gains can be found when only the take-off phase is assisted while scaling down the engine. When another phase is hybridized in addition to engine scaling, this difference will always become lower until the point where the total energy becomes greater than the total energy of the reference aircraft. In Figure 4.6 the corresponding  $T_{t4,max}$  is shown where  $\phi_{CL2} = 0.14$  stays below the reference value.

Figure 4.17 shows the  $NO_x$  production for this climb 2 assessment. At  $V_{CL2} = 124m/s$  and  $\phi_{CL2} =$

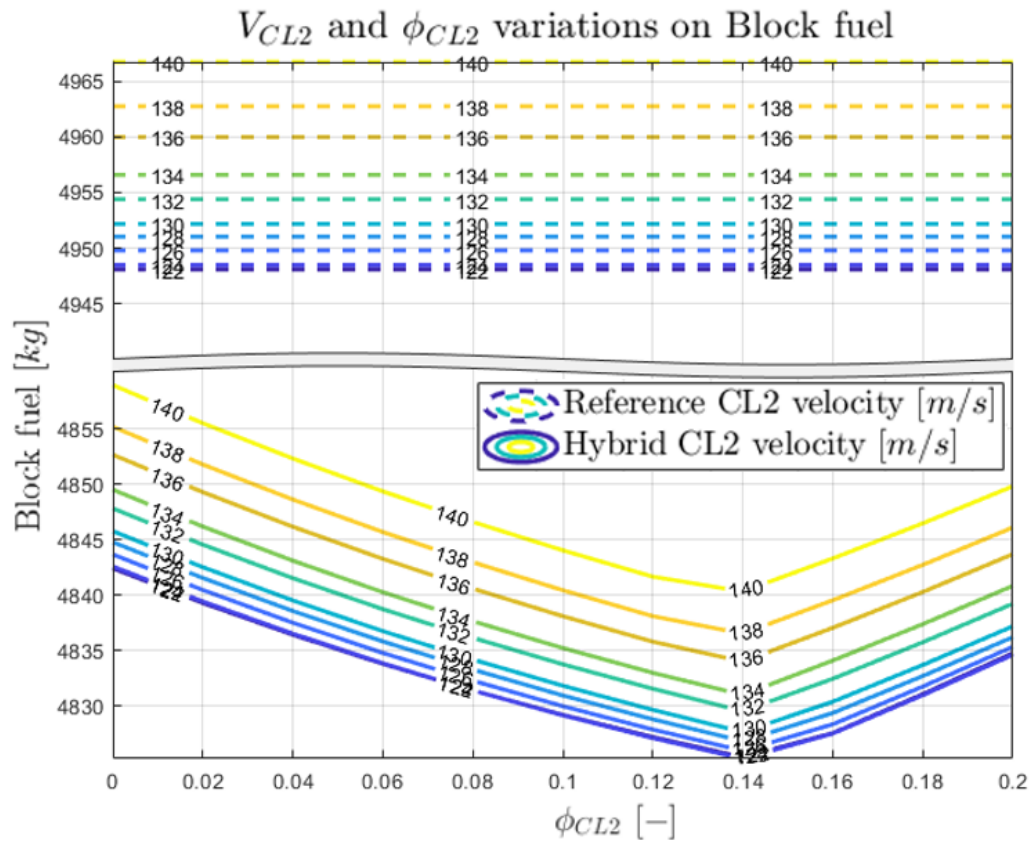


Figure 4.14: Effect of the climb2 velocity and  $\phi_{CL2}$  variations on the block fuel. With take-off hybridization  $\phi_{TO} = 0.06$  and Engine Scale is 92%.

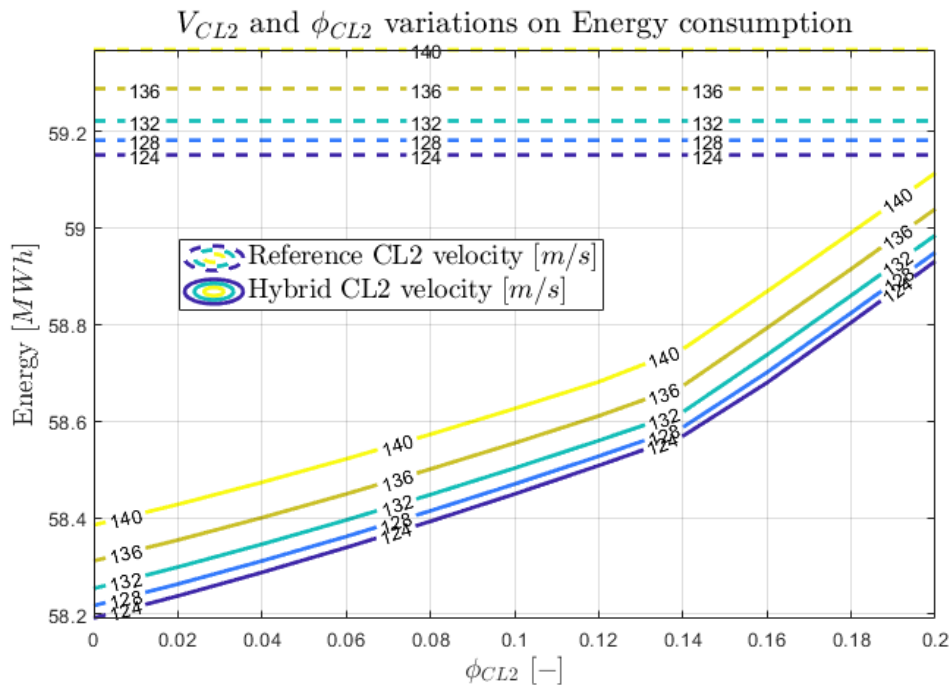


Figure 4.15: Effect of the climb2 velocity and  $\phi_{CL2}$  variations on the total energy consumption. With take-off hybridization  $\phi_{TO} = 0.06$  and Engine Scale is 92%.

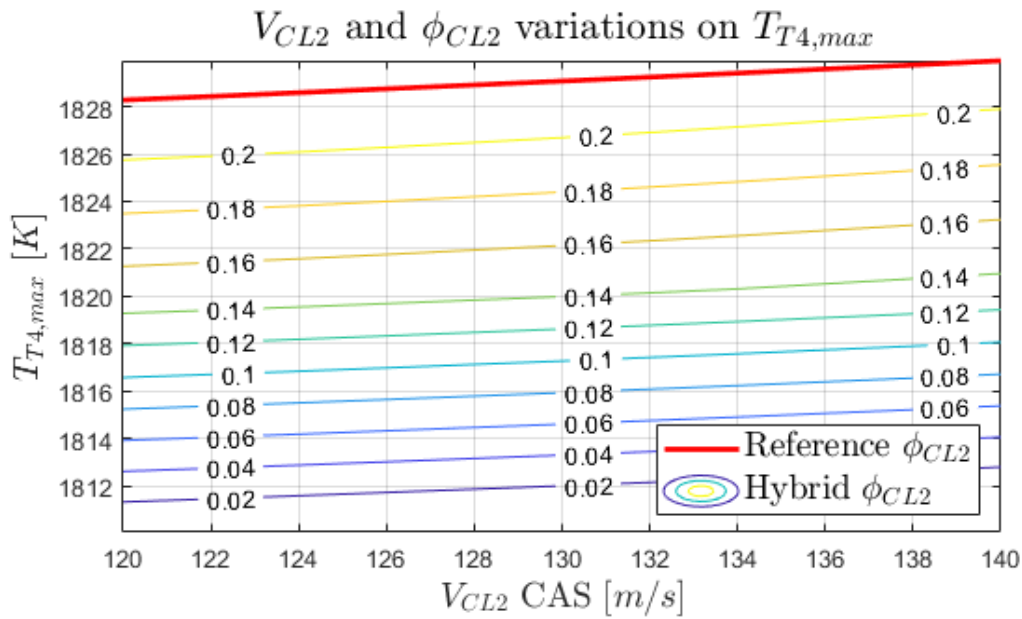


Figure 4.16: Effect of the climb2 velocity and  $\phi_{CL2}$  variations on the  $T_{T4}$  peak. With take-off hybridization  $\phi_{TO} = 0.06$  and Engine Scale is 92%.

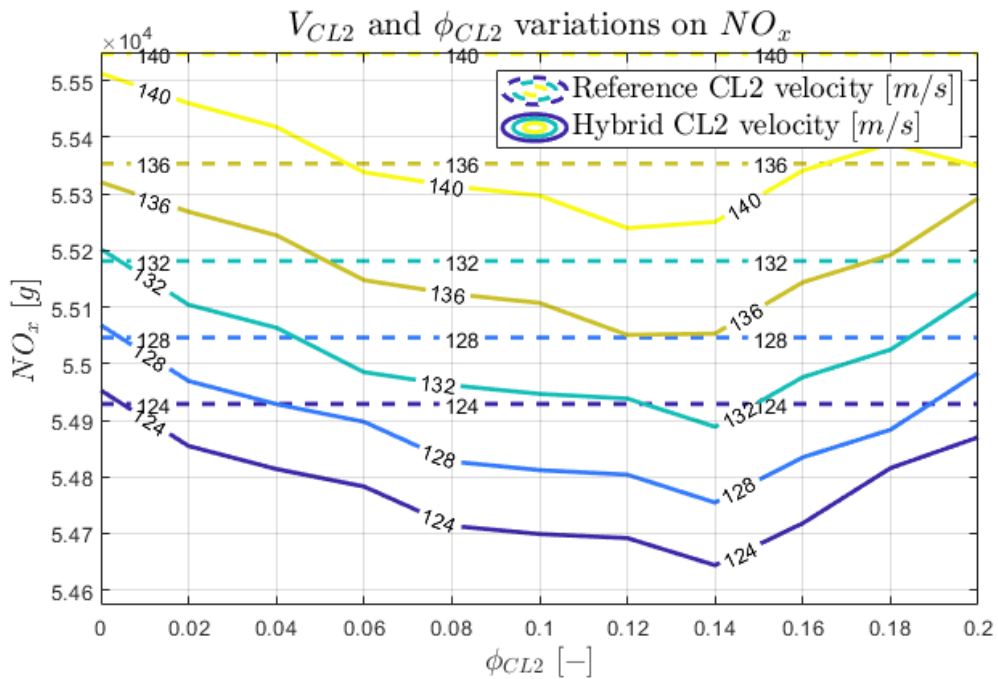


Figure 4.17: Effect of the climb2 velocity and  $\phi_{CL2}$  variations on the  $NO_x$  emissions. With take-off hybridization  $\phi_{TO} = 0.06$  and Engine Scale is 92%.

0.14 we find a total reduction of the  $NO_x$  of 0.53%. This figure shows the relation between the fuel consumption and the  $NO_x$  emissions. However, the highest reduction in  $NO_x$  between the reference aircraft and the hybrid-electric aircraft can be found at higher velocities. So even though the total  $NO_x$  production is higher at a higher speed, the difference to the reference increases too. For the  $UHC$  and the  $CO$  there were no noteworthy differences for this relatively short flight phase.

### 4.3.3. Cruise phase analysis

For the cruise phase the cruise altitude has been varied between 32000ft and 42000ft together with the cruise hybridization between  $\phi_{CR} = 0.02$  and  $\phi_{CR} = 0.2$ . This section also includes a range variation study. For this phase the  $\phi_{TO} = 0.07$  in order to account for the  $T_{t4,max}$  increase due to engine scaling. The engine scale is 92%. No other phases are hybridized except for the take-off and cruise phases. The figures in this section are plotted with the altitude on the x-axis for improvement of interpretation.

#### Sensitivity of Altitude and Hybridization factor

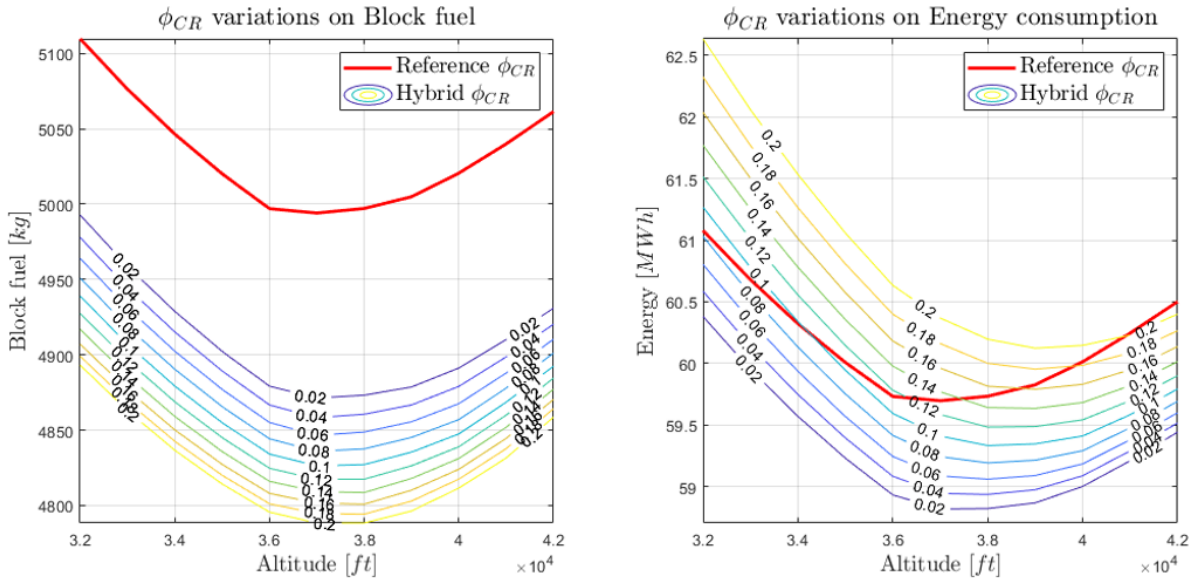


Figure 4.18: Effect of the cruise altitude and  $\phi_{CR}$  variations on the total block fuel and energy consumption. With take-off hybridization  $\phi_{TO} = 0.07$  and Engine Scale is 92%.

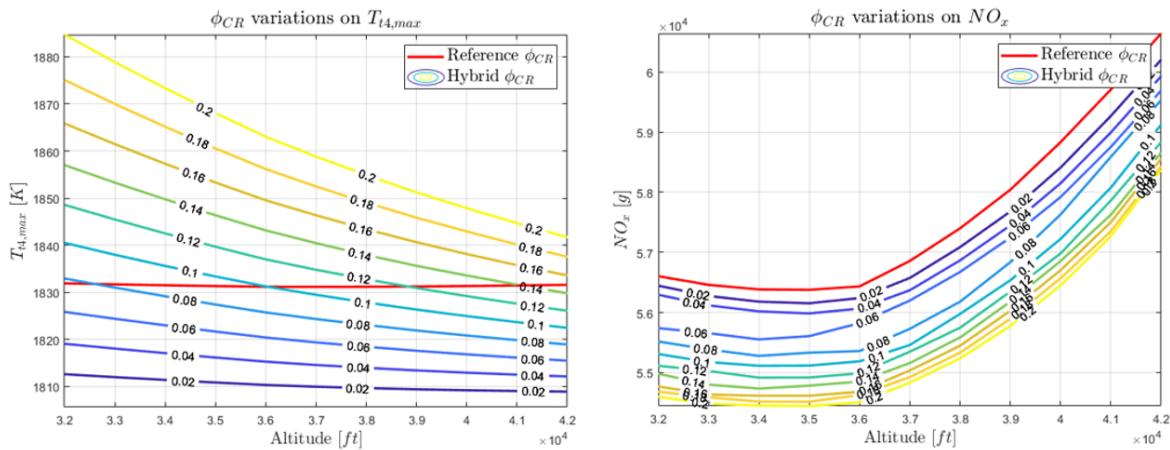


Figure 4.19: Effect of the cruise altitude and  $\phi_{CR}$  variations on the  $T_{t4}$  and the  $NO_x$  emissions. With take-off hybridization  $\phi_{TO} = 0.07$  and Engine Scale is 92%.

Figure 4.18 shows the effect of the cruise altitude and cruise hybridization on the block fuel and energy consumption of the flight. The lowest block fuel is achieved at an altitude of 37000ft. The corresponding lowest block fuel can be achieved for  $\phi_{CR} = 0.1$ . At this point in the design space the

turbine inlet temperature stays below the reference, which can be seen in Figure 4.19. The  $T_{t4,max}$  shows a decreasing trend for higher altitudes. This decreasing temperature is because of the lower drag at higher altitudes which in turn requires less battery power for the same amount of hybridization. Less battery power translates in less battery weight during take-off, which lowers the take-off mass and therefore also the  $T_{t4,max}$ . The  $T_{t4,max}$  figure also shows why the take-off hybridization  $\phi_{TO}$  needed to be increased compared to the climb phases.

At the cruise phase the  $NO_x$  emission becomes an important factor too. This is because the emitted  $NO_x$  has a higher impact on the environment when it's emitted directly into high altitudes. The  $NO_x$  increases for higher altitudes and has an optimum at an altitude of  $35000ft$ . The  $NO_x$  increases due to the overall combustion temperature increasing when the engine has less air mass flow at higher altitudes. The combustion moves from lean (excess air) to richer burn which in turn increases the temperature and therefore the  $NO_x$  emissions.

For  $\phi_{CR} = 0.1$  the difference between the optimal altitude for the block fuel ( $37000ft$ ) and the optimal altitude for  $NO_x$  ( $35000ft$ ) is 1.47%, which is a small increase in  $NO_x$ . However, the difference in block fuel consumption between the two altitudes is only 0.52%. The rate at which the  $NO_x$  increases beyond  $35000ft$  is therefore much higher than the block fuel decreases at higher altitudes. Therefore it is a better mission design choice to match the optimal altitude for  $NO_x$  instead of the block fuel.

In Figure 4.18 also the energy consumption can be found. Like for the climb phase in the previous section, the same can be observed here. In terms of energy consumption the best option is to size the engine and only electrically assist the take-off phase. Therefore, hybridization of all phases other than the take-off phase is only beneficial for the block fuel and the  $NO_x$  emissions. For  $\phi_{CR} = 0.1$  and a cruise altitude of  $37000ft$ , there is only an energy saving of 0.49%. CO and UHC show a decreasing trend with increasing altitude and  $\phi_{CR}$ .

### Sensitivity of Range and Hybridization factor

In order to assess the effect of the range, the cruise altitude of  $37000ft$  was used. The range was varied between  $1000km$  and  $3000km$  and  $\phi_{CR}$  between 0.02 and 0.2.

Figure 4.20 shows the effect of range variations on the total fuel consumption for  $\phi_{TO} = 0.07$ . The reference block fuel is depicted with the dashed lines and the hybrid-electric block fuel is depicted by the continuous lines. The first thing to note is that for very high hybridization factors the graph seems to show that it is still feasible to accomplish a fuel consumption for low ranges ( $1000km$  to  $1500km$ ). This is however not the case. At these high hybridization factors the maximum turbine inlet temperature is much higher than the reference. This can also be seen in Figure 4.20. The feasible flights with the higher gain are the short haul missions. The highest gain for all missions that satisfy the temperature constraint can be found at  $\phi_{CR} = 0.1$  and a range of  $R = 1500km$ .

At  $\phi_{TO} = 0.07$  and  $\phi_{CR} = 0.1$ , the highest fuel reduction can be achieved at a range of  $1500km$ . At this configuration the turbine inlet temperature stays below the reference. This point also satisfies the MTOW and MLW requirements.



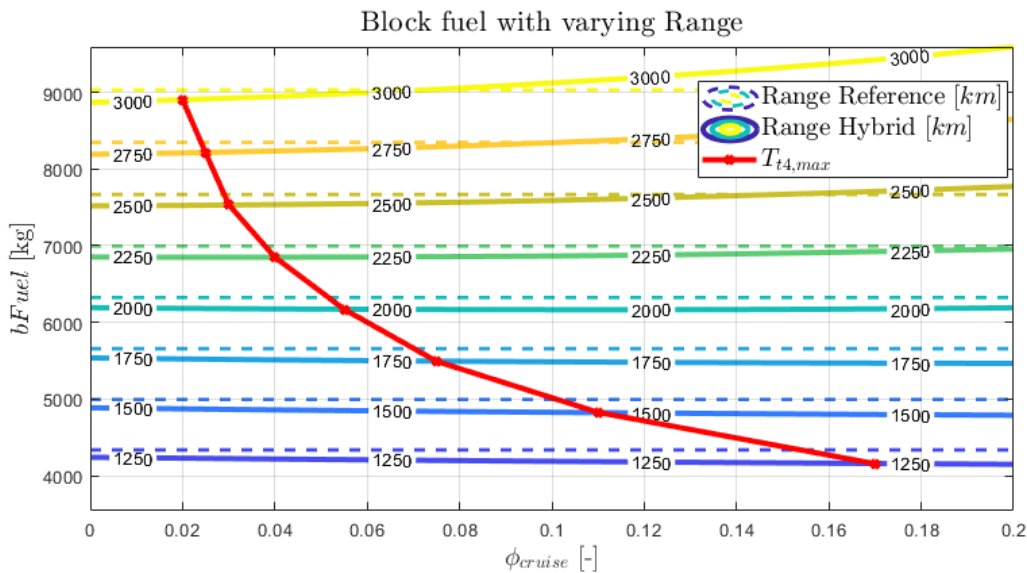


Figure 4.20: Effect of the range and  $\phi_{cruise}$  variations on the total block fuel. With take-off hybridization  $\phi_{TO} = 0.07$  and Engine Scale is 92%.

### 4.3.4. Combined hybridization of different phases

The information gathered in the previous sections has been used as a starting point to find the best combination. The outcomes have been summarized in Figure 4.21. The energy and  $NO_x$  reductions are with respect to the location at which the lowest block fuel occurs. All data points have been verified with respect to turbine inlet temperature, MTOW and MLW. The best combination did not involve applying hybridization to the climb phases. This is due to the cruise phase being the longest phase and therefore it has the greatest impact on the flight performance. The biggest reduction in block fuel was 3.10% at an altitude of  $h = 37000ft$ , climb 1 velocity of  $V_{CL1} = 142m/s$ , climb 2 velocity of  $V_{CL2} = 124m/s$ , cruise velocity of  $V_{CR} = 133m/s$  and range  $R = 1500km$ . Electrically assisting the climb and cruise phases at the same time did not yield a fuel reduction higher than when only the cruise phase was assisted.

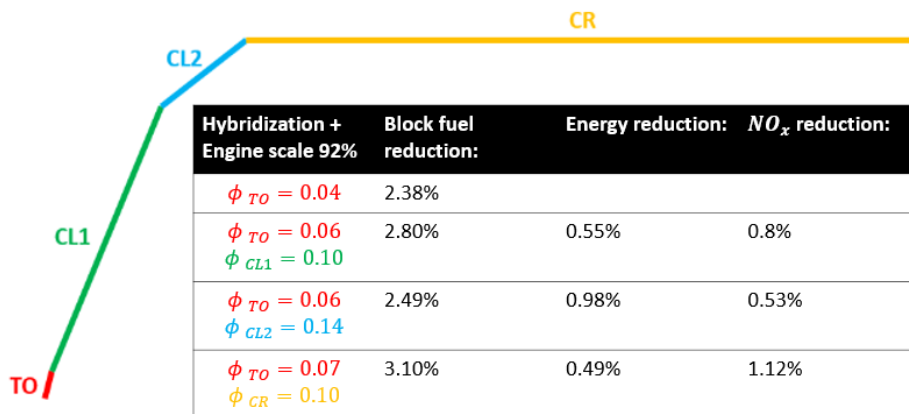


Figure 4.21: Sensitivity analysis summary.



# 5

## Conclusion and recommendations

All-electric aircraft are a long way off. The current battery technology level is still insufficient to propel larger aircraft like the A320neo. Hybrid-electric propulsion has the potential to be a stepping stone towards all-electric aircraft. With the knowledge that the majority of aircraft emissions stem from passenger operations [20], more researchers are shifting their focus towards hybrid-electric propulsion systems. Hybrid-electric aircraft have the potential to decrease emissions due to lower fuel burn. However, there are some challenges out of which down-scaling of the gas turbine is one of the main concerns. When a gas turbine is being supported by a battery, the core flow of the gas turbine can be scaled down due to the lower power requirements. This also leads to a higher combustion temperatures which in turn can drastically increase  $NO_x$  production [9, 40].

The objective of this study was to add to the scientific knowledge about the performance of hybrid-electric aircraft by assessing changes in the mission of a hybrid-electric A320neo. For this purpose the aircraft performance tool MASS has been used, which has been developed at NLR. This tool assesses parallel hybrid-electric aircraft for a given mission. The parallel hybrid-electric power train typically consists out of a gas turbine, an electric motor and an energy carrier such as a battery.

Next the mission model had to be redesigned to be more efficient at automating the mission variation process. The main mission variables that this study focuses on are:

- Cruise altitude
- Take-off and climb velocities
- Range
- Hybridization factor

Figure 4.21 shows a table with a brief summary of the findings of this study. The last row depicts the overall best performing combination of hybridization factors for a cruise altitude  $h_{cr} = 37000ft$ . The hybridization factor of the take-off and the initial climb phase  $\phi_{TO} = 0.07$ . This is necessary in order to lower the turbine inlet temperature of the down-scaled engines to match the reference aircraft's temperature.

**Cruise altitude:**

The hypothesis was that the optimum altitude would be lower for the heavier hybrid-electric aircraft due to the optimum  $L/D$  being at a lower altitude. This however does not show from this study. In terms of block fuel consumption the optimum altitude is the same at around  $37000ft$ . However, there is a difference between  $NO_x$  and block fuel. The minimum  $NO_x$  altitude is lower than the minimum block fuel altitude. This is due to the air density becoming lower and the engine having to provide the same thrust, which leads to higher combustion temperatures.

**Flight velocities:**

The flight velocities do have an impact on the fuel consumption but not very much on the  $NO_x$ . A slightly lower velocity during climb will decrease the overall block fuel. However, when the range of velocities were examined, it was found that even though the block fuel decreases, the difference between the reference aircraft and the hybrid-electric aircraft stays the same. Hence, the delta gain is the same for these changes in velocity. Overall, almost all flight velocities of the end point of this research appeared to be lower than the velocities of the reference.

**Range:**

The range was the most straightforward mission variable. The main conclusion is that the higher the range, the less feasible the mission and the lower the hybridization can be. Ranges up to  $1750km$  were saving fuel at low hybridization factors. This leads to the conclusion that the battery technology level is far from being sufficient to propel larger aircraft.

**Hybridization factor:**

For the hybridization factor it was determined that only hybridizing the take-off and climb phases did not yield the highest fuel gain. This is due to the fact that these phases are relatively short in time, so overall they make a lesser impact on the entire mission. The cruise phase has the greatest impact on the fuel consumption, which led to an overall fuel consumption of 3.10% at an altitude of  $37000ft$ ,  $\phi_{CR} = 0.1$ , a range of  $R = 1500km$  and 92% scaled engines.

The study shows that designing a new mission for hybrid-electric aircraft does have an impact on the overall fuel consumption and emissions. However, the gains are very small for EIS2030 battery technology forecasts. Mission assessment is therefore a tool that has the potential to increase the

performance of hybrid-electric aircraft, but it needs to work alongside other measures, such as hydrogen technology.

Recommendations for further research include but are not limited to:

- Researching future mission characteristics such as cruise climb.
- Assessing the effects of hybrid-electric performance on the production of noise during taxi, take-off and landing.
- Assessing the effects of hybrid-electric performance on local air pollution during taxi, take-off and landing.
- Assessing the effect of aircraft aerodynamic and geometry sizing.
- Assessing other types of hybrid-electric architectures such as the series or turbo-electric architectures.
- Assessing the performance of hydrogen fuel cells of which the energy density is much higher than batteries, in combination with optimizing the mission.



# Bibliography

- [1] Flightpath 2050 - Europe's Vision for Aviation. Luxembourg, 2011. Publications Office of the European Union. doi:10.2777/50266. URL <https://ec.europa.eu/transport/sites/transport/files/modes/air/doc/flightpath2050.pdf>. OCLC: 930887434.
- [2] European Aviation Safety Agency, European Environment Agency, and Eurocontrol. European Aviation Environmental Report 2019. 2019. doi:10.2822/309946. URL <https://op.europa.eu/en/publication-detail/-/publication/615da9d1-713e-11e9-9f05-01aa75ed71a1/language-en>.
- [3] European Environment Agency. Transport and Environment Reporting Mechanism - mixed progress for Europe's transport sector in meeting environment, climate goals, 2017. URL <https://www.eea.europa.eu/highlights/term-2017-mixed-progress-for>.
- [4] Airbus. *Getting to grips with aircraft performance*. Blagnac Cedex, France, January 2002. URL <https://www.skybrary.aero/bookshelf/books/2263.pdf>.
- [5] Airbus. *Global Market Forecast - Mapping Demand 2016/2035*. Art and Caractère, Blagnac Cedex, France, 2016. ISBN 978-2-9554382-1-6.
- [6] Airbus. *Airbus: A320 aircraft characteristics*. Revision no. 34 - feb 01/18 edition, February 2018. URL [https://web.archive.org/web/20180618204221/http://www.airbus.com/content/dam/corporate-topics/publications/backgrounders/techdata/aircraft\\_characteristics/Airbus-Commercial-Aircraft-AC-A320-Feb18.pdf](https://web.archive.org/web/20180618204221/http://www.airbus.com/content/dam/corporate-topics/publications/backgrounders/techdata/aircraft_characteristics/Airbus-Commercial-Aircraft-AC-A320-Feb18.pdf).
- [7] Airbus. *A320neo characteristics*, 2019. URL <https://www.airbus.com/aircraft/passenger-aircraft/a320-family/a320neo.html>.
- [8] A. W. X. Ang. Hybrid Electric Propulsion Systems: Integrated performance analysis applied on short-range aircraft. Master's thesis, 2016. URL <https://repository.tudelft.nl/islandora/object/uuid%3A5148aafa-91ed-485d-ac7a-2883394ec0a4>.
- [9] A. W. X. Ang, A. Gangoli Rao, T. T. Kanakis, and W. Lammen. Performance analysis of an electrically assisted propulsion system for a shortrange civil aircraft. *Proceedings of the Institution of Mechanical Engineers, Part G: Journal of Aerospace Engineering*, 233, 2018. ISSN 0954-4100. doi:10.1177/0954410017754146. URL <https://repository.tudelft.nl/islandora/object/uuid%3A803a8f11-0f0c-4752-88de-2bfc42f20477>.

- [10] The World Bank. CO2 emissions (metric tons per capita), 2014. URL [https://data.worldbank.org/indicator/EN.ATM.CO2E.PC?locations=TZ&most\\_recent\\_value\\_desc=false](https://data.worldbank.org/indicator/EN.ATM.CO2E.PC?locations=TZ&most_recent_value_desc=false).
- [11] Benjamin J. Brelje and Joaquim R. R. A. Martins. Electric, hybrid, and turboelectric fixed-wing aircraft: A review of concepts, models, and design approaches. *Progress in Aerospace Sciences*, 104:1–19, January 2019. ISSN 0376-0421. doi:10.1016/j.paerosci.2018.06.004. URL <http://www.sciencedirect.com/science/article/pii/S0376042118300356>.
- [12] Ulrike Burkhardt and Bernd Kärcher. Global radiative forcing from contrail cirrus. *Nature Climate Change*, 1(1):54–58, April 2011. ISSN 1758-678X, 1758-6798. doi:10.1038/nclimate1068. URL <http://www.nature.com/articles/nclimate1068>.
- [13] CeRAS. Central reference aircraft data system (ceras). URL <http://ceras.ilr.rwth-aachen.de/trac>.
- [14] Lee Chapman. Transport and climate change: a review. *Journal of Transport Geography*, 15(5): 354–367, September 2007. ISSN 0966-6923. doi:10.1016/j.jtrangeo.2006.11.008. URL <http://www.sciencedirect.com/science/article/pii/S0966692306001207>.
- [15] R. de Vries, M. T. H. Brown, and R. Vos. A preliminary sizing method for hybrid-electric aircraft including aero-propulsive interaction effects. *2018 Aviation Technology, Integration, and Operations Conference*, 2018. doi:10.2514/6.2018-4228. URL <https://repository.tudelft.nl/islandora/object/uuid%3Aaced04c8-2e08-49e9-b488-aaf5731f420e>.
- [16] Reynard de Vries, Maurice Hoogreef, and Roelof Vos. Preliminary Sizing of a Hybrid-Electric Passenger Aircraft Featuring Over-the-Wing Distributed-Propulsion. 2019. doi:10.2514/6.2019-1811. URL <https://arc.aiaa.org/doi/abs/10.2514/6.2019-1811>.
- [17] Tyler S. Dean, Gabrielle E. Wroblewski, and Phillip J. Ansell. Mission Analysis and Component-Level Sensitivity Study of Hybrid-Electric General-Aviation Propulsion Systems. *Journal of Aircraft*, 55(6):2454–2465, September 2018. doi:10.2514/1.C034635. URL <https://arc.aiaa.org/doi/10.2514/1.C034635>.
- [18] Timothy P Dever, Kirsten P Duffy, Andrew J Provenza, Patricia L Loyselle, Benjamin B Choi, Carlos R Morrison, and Angela M Lowe. Assessment of Technologies for Noncryogenic Hybrid Electric Propulsion. *NASA*, page 54, 2015. URL <https://ntrs.nasa.gov/search.jsp?R=20150000747>.
- [19] EASA. Type-Certificate Data Sheet No. E.110: LEAP-1A & LEAP-1C Series Engine. Technical Report, May 2019. URL <https://www.easa.europa.eu/documents/type-certificates/engine-cs-e/easae110>.



- [20] Brandon Graver, Kevin Zhang, and Dan Rutherford. CO2 emissions from commercial aviation, 2018. Technical Report 2019-16, The International Council on Clean Transportation ICCT, September 2019.
- [21] Air Transport Action Group. Stakeholder map: the global air transport system. Technical report, Air Transport Action Group, February 2018. URL <https://www.atag.org/our-publications/latest-publications.html>.
- [22] Assia Haddou. Literature survey: Mission assessment for hybrid-electric single aisle aircraft. Technical report, TU Delft, 2020.
- [23] Frederick G. Harmon, Andrew A. Frank, and Jean-Jacques Chattot. Conceptual Design and Simulation of a Small Hybrid-Electric Unmanned Aerial Vehicle. *Journal of Aircraft*, 43(5): 1490–1498, September 2006. doi:10.2514/1.15816. URL <https://arc.aiaa.org/doi/10.2514/1.15816>.
- [24] Martin Hepperle. Electric Flight – Potential and Limitations. *German Aerospace Center*, page 30, 2012.
- [25] Ryan Hiserote and Frederick Harmon. Analysis of Hybrid-Electric Propulsion System Designs for Small Unmanned Aircraft Systems. In *8th Annual International Energy Conversion Engineering Conference*, Nashville, TN, July 2010. American Institute of Aeronautics and Astronautics. ISBN 978-1-62410-156-4. doi:10.2514/6.2010-6687. URL <http://arc.aiaa.org/doi/10.2514/6.2010-6687>.
- [26] Maurice Hoogreef, Roelof Vos, Reynard de Vries, and Leo L. Veldhuis. Conceptual Assessment of Hybrid Electric Aircraft with Distributed Propulsion and Boosted Turbofans. In *AIAA Scitech 2019 Forum*, San Diego, California, January 2019. American Institute of Aeronautics and Astronautics. ISBN 978-1-62410-578-4. doi:10.2514/6.2019-1807. URL <https://arc.aiaa.org/doi/10.2514/6.2019-1807>.
- [27] J. Y. Hung and L. F. Gonzalez. On parallel hybrid-electric propulsion system for unmanned aerial vehicles. *Progress in Aerospace Sciences*, 51:1–17, May 2012. ISSN 0376-0421. doi:10.1016/j.paerosci.2011.12.001. URL <http://www.sciencedirect.com/science/article/pii/S0376042112000097>.
- [28] IATA. *IATA Annual review 2019*. International Air Transport Association, 2019. URL <https://www.iata.org/publications/Documents/iata-annual-review-2019.pdf>.
- [29] ICAO. ICAO Carbon Emissions Calculator, 2016. URL <https://www.icao.int/environmental-protection/CarbonOffset/Pages/default.aspx>.

- [30] ICAO. ICAO Environmental Report 2019: Aviation and environment. Technical report, ICAO, 2019. URL <https://www.icao.int/environmental-protection/Documents/ICAO-ENV-Report2019-F1-WEB%20%281%29.pdf>.
- [31] ICAO. Icao aircraft engine emissions databank, 2020. URL <https://www.easa.europa.eu/domains/environment/icao-aircraft-engine-emissions-databank>.
- [32] IHS. *Jane's all the world's aircraft: Airbus A320*. Aircraft - Fixed-Wing - Civil. IHS Markit, 2019. URL <https://janes.ihs.com/Janes/DisplayFile/JAWA0416#A320neo>.
- [33] Ralph H Jansen, Dr Cheryl Bowman, Amy Jankovsky, and Rodger Dyson. Overview of NASA Electrified Aircraft Propulsion Research for Large Subsonic Transports. NASA, page 27, November 2017. URL <https://ntrs.nasa.gov/search.jsp?R=20170012222>.
- [34] Shankar Jayaraman. Dynamic cutback optimization. November 2020.
- [35] L. Jenkinson, P. Simpkin, and D. Rhodes. *Civil Jet Aircraft Design - Aircraft Data File - Airbus Aircraft*. Butterworth-Heinemann, 2001. URL <https://booksite.elsevier.com/9780340741528/appendices/data-a/table-1/table.htm>.
- [36] Homi Kharas. The unprecedented expansion of the global middle class: An update. Technical report, Brookings Institution, United Nations, February 2017. URL [https://www.brookings.edu/wp-content/uploads/2017/02/global\\_20170228\\_global-middle-class.pdf](https://www.brookings.edu/wp-content/uploads/2017/02/global_20170228_global-middle-class.pdf).
- [37] Wim Lammen and Jos Vankan. Energy Optimization of Single Aisle Aircraft with Hybrid Electric Propulsion. In *AIAA Scitech 2020 Forum*, Orlando, FL, January 2020. American Institute of Aeronautics and Astronautics. ISBN 978-1-62410-595-1. doi:10.2514/6.2020-0505. URL <https://arc.aiaa.org/doi/10.2514/6.2020-0505>.
- [38] David S. Lee, David W. Fahey, Piers M. Forster, Peter J. Newton, Ron C. N. Wit, Ling L. Lim, Bethan Owen, and Robert Sausen. Aviation and global climate change in the 21st century. *Atmospheric Environment*, 43(22):3520–3537, July 2009. ISSN 1352-2310. doi:10.1016/j.atmosenv.2009.04.024. URL <http://www.sciencedirect.com/science/article/pii/S1352231009003574>.
- [39] Leeham. Fundamentals of airliner performance part 6: the engine. URL <https://leehamnews.com/2015/01/19/fundamentals-of-airliner-performance-part-6-the-engine/>.
- [40] A.H. Lefebvre and R.B. Dilip. *Gas Turbine Combustion: Alternative Fuels and Emissions*. Taylor and Francis Group, United States, third edition, 2010. ISBN 978-1-4200-8605-8.
- [41] L. Lorenz, Arne Seitz, and Holger Kuhn. Hybrid Power Trains for Future Mobility. September 2013. doi:10.13140/2.1.2741.7925.

- [42] Ajay Misra. Summary of 2017 NASA Workshop on Assessment of Advanced Battery Technologies for Aerospace Applications, January 2018. URL <https://ntrs.nasa.gov/search.jsp?R=20180001539>.
- [43] Mark D. Moore. Misconceptions of Electric Aircraft and their Emerging Aviation Markets. In *52nd Aerospace Sciences Meeting*, AIAA SciTech Forum. American Institute of Aeronautics and Astronautics, January 2014. doi:10.2514/6.2014-0535. URL <https://arc.aiaa.org/doi/10.2514/6.2014-0535>.
- [44] NASA. Openvsp, nasa open source parametric geometry. URL <http://openvsp.org/>.
- [45] J. E. Penner, D.H. Lister, D.J. Griggs, D.J. Dokken, and M. McFarland. Aviation and the Global Atmosphere. Technical Report pp 373, Cambridge University Press, 1999. URL <https://archive.ipcc.ch/ipccreports/sres/aviation/index.php?idp=0>.
- [46] M Prather, A S Grossman, R Sausen, B H Subbaraya, A Jain, M Ponater, U Schumann, and D J Wuebbles. Potential Climate Change from Aviation. page 32, 1999.
- [47] Junzi Sun, Joost Ellerbroek, and Jacco Hoekstra. *OpenAP: An open-source aircraft performance model for air transportation studies and simulations*. May 2020.
- [48] Sheng Chien Tan. Electrically Assisted Propulsion and Power Systems for Short-Range Missions: Electrification of a Conventional Airbus A320neo. Master's thesis, 2018. URL <https://repository.tudelft.nl/islandora/object/uuid%3A12ff33e4-78ce-43f0-893f-43e0b15b8e1e>.
- [49] E. Torenbeek. Synthesis of subsonic airplane design (student version). 1982. URL <https://repository.tudelft.nl/islandora/object/uuid%3A229f2817-9be9-49b6-959a-d653b5bac054>.
- [50] Egbert Torenbeek. *Advanced Aircraft Design: Conceptual Design, Technology and Optimization of Subsonic Civil Airplanes*. John Wiley & Sons, Incorporated, New York, UNITED KINGDOM, 2013. ISBN 978-1-118-56808-8. URL <http://ebookcentral.proquest.com/lib/delft/detail.action?docID=1184219>.
- [51] H Tran. Efficient Modeling of Hybrid-Electric Aircraft for Design and Performance Optimization Studies. Technical report, 2021.
- [52] Roelof Vos, Alexander Wortmann, and Reno Elmendorp. The optimal cruise altitude of LNG-fuelled turbofan aircraft. *Journal of Aerospace Operations*, 4(4):207–222, December 2017. ISSN 2211002X, 22110038. doi:10.3233/AOP-160063. URL <https://www.medra.org/servlet/aliasResolver?alias=iospress&doi=10.3233/AOP-160063>.

- [53] Graham Warwick. Electric lineup: Who are the new players in electrified aircraft propulsion? *Aviation Week*, (October 2019), October 2019.
- [54] Victoria Williams, Robert B. Noland, and Ralf Toumi. Reducing the climate change impacts of aviation by restricting cruise altitudes. *Transportation Research Part D: Transport and Environment*, 7(6), November 2002. ISSN 1361-9209. doi:10.1016/S1361-9209(02)00013-5. URL <http://www.sciencedirect.com/science/article/pii/S1361920902000135>.
- [55] Gabrielle E. Wroblewski and Phillip J. Ansell. Mission Analysis and Emissions for Conventional and Hybrid-Electric Commercial Transport Aircraft. *Journal of Aircraft*, 56(3):1200–1213, January 2019. doi:10.2514/1.C035070. URL <https://arc.aiaa.org/doi/10.2514/1.C035070>.
- [56] Don Wuebbles, Mohan Gupta, and Malcolm Ko. Evaluating the Impacts of Aviation on Climate Change. *Eos, Transactions American Geophysical Union*, 88(14):157, April 2007. ISSN 0096-3941. doi:10.1029/2007EO140001. URL <http://doi.wiley.com/10.1029/2007EO140001>.
- [57] Jacopo Zamboni, Roelof Vos, Mathias Emeneth, and Alexander Schneegans. A Method for the Conceptual Design of Hybrid Electric Aircraft. In *AIAA Scitech 2019 Forum*, San Diego, California, January 2019. American Institute of Aeronautics and Astronautics. ISBN 978-1-62410-578-4. doi:10.2514/6.2019-1587. URL <https://arc.aiaa.org/doi/10.2514/6.2019-1587>.